2023

Measuring and modeling how plant-microbe interactions control soil carbon and nitrogen cycling in managed and unmanaged ecosystems

Joanna Ridgeway
West Virginia University, jrridgeway@mix.wvu.edu

Measuring and modeling how plant-microbe interactions control soil carbon and nitrogen cycling in managed and unmanaged ecosystems

Joanna Ridgeway

Dissertation submitted to
the Eberly College of Arts and Sciences
at West Virginia University

in partial fulfillment of the requirements for the degree of

Doctor of Philosophy in
Biology

Edward Brzostek, Ph.D., chair
Jonathan Cumming, Ph.D.
Charlene Kelly, Ph.D.
Ember Morrissey, Ph.D.
William Peterjohn, Ph.D.

Department of Biology

Morgantown, West Virginia

2023

Keywords: carbon cycling; soil organic matter; plant-microbe interactions; ecosystem modeling

Abstract

Measuring and modeling how plant-microbe interactions control soil carbon and nitrogen cycling in managed and unmanaged ecosystems

Joanna Ridgeway

Our understanding of how plant-microbe interactions regulate carbon (C) and nitrogen (N) retention in soil organic matter (SOM) remains uncertain. Conflicting evidence suggests that microbial decomposition can lead to the loss of unprotected particulate SOM, but also that microbial decomposition produces simpler compounds that preferentially form more persistent aggregate- or mineral-protected SOM pools. Further, uncertainty remains in how plant-microbe interactions alter SOM retention in these different pools through litter chemistry controls on microbial decomposition traits and rhizosphere priming. As a result, this uncertainty limits our ability to sustainably manage ecosystems and understand future feedbacks between terrestrial ecosystems and the global climate. In this dissertation, I address these uncertainties to answer the following research questions: 1) How do plant-microbe interactions between plant litter and microbial decomposition traits influence the formation of new soil C for different bioenergy crop litters in the lab?; 2) How do rhizosphere plant-microbe interactions influence soil organic matter stabilization and destabilization depending on nutrient levels in-situ?; and 3) Can empirical measurements help constrain, parameterize, and validate modeled plant-microbe interactions to improve representations of forest ecosystem responses to global change?

For question 1, I examined differences between two bioenergy feedstocks, corn and miscanthus, in the ability of their litter to form new unprotected SOM vs. mineral-protected SOM. I traced the fate of isotopically enriched litter C into microbial respiration and SOM pools in the lab and found that corn litter promoted higher microbial uptake and carbon use efficiency, forming less unprotected SOM and more mineral-protected SOM than miscanthus litters. I also demonstrated the potential for our measurements to parameterize a microbial SOM model and improve predictions of soil C formation. This link between litter quality, microbial efficiency, and SOM formation bridges empirical uncertainty in how bioenergy crops build soil C. For question 2, I investigated whether living roots and their associated fungi increase or decrease new SOM formation from litter. I traced isotopically enriched litter C and N into SOM pools in root ingrowth cores incubated in a miscanthus field. I found that roots stimulated litter decomposition but balanced this loss by transferring carbon into aggregate-protected SOM. Further, roots selectively mobilized N from litter without additional C release, suggesting that roots efficiently mine N and build persistent soil C. This work expands our mechanistic understanding of how living roots shape agricultural ecosystem processes. For question 3, I investigated if modelling plant-microbe interactions and microbially-explicit N cycling could improve representations of forest soil C and N retention under changes in anthropogenic N deposition. I leveraged decades of C and N cycling data from a whole-watershed N fertilization experiment to run a microbially-explicit plant-microbe interactions model. The model accurately represented key ecosystem C responses to enhanced N availability, including a decline in plant C cost for N acquisition and an increase in soil C. By incorporating new, microbially-explicit N cycling, the model could also capture how enhanced N availability altered N cycling and streamwater N losses. When we ran the model forward under declining N deposition, the model predicted that N losses recovered faster than soil C pools. However, the C sequestered due to N deposition may be vulnerable to future loss, particularly in a warming climate. Collectively, my research shows that vital ecosystem services like soil C and N retention depend on microbially-mediated processes that are regulated by plant-microbe interactions.

Acknowledgements

My graduate research could not have been accomplished without the help and support of my many colleagues. First, I am sincerely grateful for my mentor, Dr. Eddie Brzostek, for your support and guidance in my graduate research. You have challenged me to think critically, encouraged me to pursue my interests, and helped me discover and develop a love for research. I have learned more from you than I could have imagined was possible and I would not be where I am today without you. I am also grateful to my other mentors and committee members. I thank Dr. Bill Peterjohn for his excellent teaching, helpful advice, and invaluable problem-solving suggestions. I thank Dr. Ben Sulman for his mentorship, professional support, and guidance tackling a new modelling project. I thank Dr. Ember Morrissey for her ideas to improve my research plans and her thoughtful feedback on manuscript writing. I thank Dr. Charlene Kelly for helping me talk through ideas and figure out problems. I thank Dr. Jonathan Cumming for helping me learn more about biology and saving my plants from near-certain death when I was a new graduate student. I thank Dr. Beth Thomas for teaching me to love teaching environmental biology and care for my students.

This research could not have been accomplished without the help and hard work of many other collaborators, especially Dr. Jen Kane who set up my favorite field site and helped teach me new lab skills, Hayden Starcher who worked incredibly hard on our research in the field and in the lab, Dr. Stephanie Juice who helped me tackle model projects and solve infuriating problems, and Dr. Brooke Eastman who I cited over a dozen times in my fourth chapter of this dissertation. I would also like to thank my wonderful and brilliant labmates: Joe, Nan, Emel, Zoe, Hannah, and Dom and I'd like to thank other grad students who have helped with my work or served on the BGSA board with me: Molli, Kristin, Justin, Sam, Cam, Ollie, Mason, Hana, Jess, Brooke, Roshan, Jenni, Greg, Chanso, Amber, and Brin (among many, many others). I have learned so much from you all and navigating grad school together is one of my greatest honors. In particular, I am so grateful to Emel Kangi for coming up with the best puns, working countless hours with me, giving invaluable advice, and for officiating my wedding. I am grateful to Zoe Pagliaro for your excellent insight planning experiments together and for inspiring me to be more correct. I am grateful to Hannah DeHetre for letting me play PI and mentor you in your first PhD chapter.

This work would not have been possible without the love and support of my family. First, I am grateful to my partner Robert who celebrates my wins, helps me talk through problems, co-parents our recalcitrant dogs, and makes my morning coffee. I thank my sister Elizabeth, who always makes me laugh and has been my partner in crime since day 550. Finally, I also could not have reached this point without my parents, who have always supported me and who raised me to have a boundless curiosity and desire to learn more about the world.

Table of Contents

List of Figures:

List of Tables:

Chapter 1: Introduction

Soils play a critical role in global biogeochemistry, providing essential ecosystem services such as carbon (C) sequestration and nitrogen (N) retention (Schmidt et al., 2011). A long history of environmental research has characterized the role of environmental and anthropogenic drivers (e.g.,, climate, elevated CO_2, agricultural management) on global C and N cycling in soils (Davidson & Janssens, 2006; Vitousek et al., 1997). By contrast, we have only recently begun to understand how plant-microbe interactions modulate C sequestration and N retention (Van Der Heijden et al., 2008; Zak et al., 2003). Plant-microbe interactions between litter chemistry and microbial physiology drive soil C and N cycling through litter decomposition and transformation into new soil organic matter (SOM) (Talbot & Treseder, 2012). Further, plants also allocate C belowground to soil microbes to enhance nutrient acquisition, driving both SOM decomposition and formation (Bais et al., 2006; Dijkstra et al., 2013). However, uncertainty remains in the magnitude and direction of the impacts of plant-microbe interactions on soil C storage and N retention. This uncertainty is amplified in predictive models, ultimately limiting the ability to manage ecosystems for increased sustainability and to understand future feedbacks between terrestrial ecosystems and the global climate (Berardi et al., 2020; Saifuddin et al., 2021; Soong et al., 2020). As such, the overarching goals of my Ph.D. research are to investigate how plant-microbe interactions can lead to a net retention or loss of SOM C and N and to use empirical data on plant-microbial interactions to improve model predictions of coupled C and N cycling in both managed and unmanaged ecosystems.

Recent theories have evolved to highlight the role of plant-microbe interactions in driving soil C and N storage (Cotrufo, 2013; Lehmann & Kleber, 2015; Phillips et al., 2013). Plant litter traits can control microbial decomposition and the subsequent storage or loss of C

and N in SOM. For example, chemically complex litter can both increase SOM by decomposing slowly and accumulating as undecomposed fragments in particulate SOM or decrease SOM by reducing the efficiency of microbial decomposition and enhancing respired C losses (Mueller et al., 2015; Stewart et al., 2015). For chemically simple litters, rapid decomposition that leads to respiratory losses or enhanced nitrification may be counterbalanced by the increased production of microbial necromass that preferentially sorbs to soil mineral surfaces as mineral associated SOM (Cotrufo, 2013; Creamer et al., 2019; Lehmann & Kleber, 2015). Further, living roots directly interact with microbes in the rhizosphere, or zone of soil surrounding plant roots, and these active plant-microbe interactions can both increase and decrease SOM pools. On one hand, root exudation of labile C can prime microbial activity, leading to the loss of soil C (Cheng et al., 2014; Jilling et al., 2021; Keiluweit et al., 2015). On the other hand, root C inputs can also promote the protection of SOM in soil aggregates (Six, Elliott, et al., 2000) and increase the production of microbial necromass and microbially-derived mineral associated SOM (Kallenbach et al., 2016; Liang et al., 2017). Thus, there is clear empirical uncertainty in the magnitude and direction of plant-microbial interactions on SOM storage. Moreover, plant-microbe interactions appear to drive the form of SOM protection (i.e.,physically protected mineral associated SOM vs. chemically protected particulate SOM) and as a result they may alter the future vulnerability of SOM (Benbi et al., 2014; Lugato et al., 2021; Williams et al., 2018).

Improving our understanding of plant-microbe interactions is critical in both managed andunmanaged ecosystems. In managed ecosystems, increasing soil C retention could be particularly advantageous for bioenergy systems to help achieve C neutrality and displace fossil fuel emissions (Adler et al., 2007). In particular, perennial grass crops like *Miscanthus x giganteus* (herein, miscanthus) have been proposed as alternative bioenergy feedstocks to

traditional *Zea mays* (herein corn) agriculture, which consistently depletes soil C (Carvalho et al., 2017). Miscanthus differs from corn in traits like greater litter complexity, deeper rooting depth, more biomass, and more efficient N utilization (Dohleman & Long, 2009; Heaton et al., 2008; Studt et al., 2021). However, uncertainty remains in how these plant traits interact with microbial traits that control SOM decomposition and formation and influence observations of soil C sequestration in miscanthus (Davis et al., 2010; Ledo et al., 2020). By contrast, both theory and empirical evidence provide a more robust understanding of how plant-microbial interactions drive C and N cycling in unmanaged ecosystems like temperate forests (Brzostek et al., 2015; Chen et al., 2016; Phillips et al., 2013; Terrer et al., 2016). It remains an open question whether temperate forests will continue to serve as a C sink in the face of global change (Pan et al., 2011), and this potential appears to rely on how differences in plant-microbe interactions allow forests to maintain productivity with increasing nutrient limitation (Phillips et al., 2013). Predictive modelling is a necessary tool to answer this question and guide efforts to address climate change, but model predictions of terrestrial C and N cycling lag behind our empirical understanding (Saifuddin et al., 2021; Sulman et al., 2018).

Empirical uncertainties in how plant-microbe interactions influence SOM and ecosystem C and N cycling are amplified in predictive models. Models that explicitly represent microbial decomposers and enzymatic decomposition vary widely in assumptions of microbial traits and physiology (Robertson et al., 2019; Sulman et al., 2014, 2017; Wieder et al., 2014). As such, uncertainty arises not only from structural differences in models (Myrgiotis et al., 2018; Shi et al., 2018) but also from empirically unconstrained microbial parameters and processes (Luo & Schuur, 2020; Sulman et al., 2018). For example, the CORPSE model (Carbon, Organisms, and Rhizosphere Processes in the Soil Environment, Sulman et al., 2014) simulates how microbial

decomposers uptake and respire or transform SOM, but this process is directly scaled by a single carbon use efficiency parameter that is loosely based on empirical estimates. In addition, the microbially-explicit decomposition (C) models which do simulate N cycling often implicitly represent microbially driven N losses and use microbial C:N stoichiometry to drive N transformations (Kyker-Snowman et al., 2020; Saifuddin et al., 2021; Sulman et al., 2017). This simplification reduces model complexity but also limits our predictive understanding of how soils retain N and how soil N availability constrains ecosystem productivity and C sequestration.

1.1 Research Questions:

To investigate how plant-microbe interactions drive soil C and N cycling, my three main research questions are:

1) **How do plant-microbe interactions between plant litter and microbial decomposition traits influence the formation of new soil C for different bioenergy crops litters in the lab?**
2) **How do active rhizosphere plant-microbe interactions influence soil organic matter stabilization and destabilization depending on nutrient levels in-situ?**
3) **Can empirical measurements constrain, parameterize, and validate model representations of microbial C and N cycling?**

1.2 Research Approach:

To meet my experimental objectives, my research utilizes stable isotope tracing to follow the fate of ^{13}C and ^{15}N enriched plant litter through microbial decomposition and into SOM. First, I investigate how different crop litters drive soil microbial decomposition traits and SOM formation using lab soil incubations. Here, we hypothesize that lower C:N, chemically simple litters promote more efficient microbial decomposition and lead to greater litter incorporation into mineral associated SOM. Next, I investigate the role of living roots and fungi on litter and SOM C and N transformations *in situ*. Here, we present competing hypotheses that living roots either lead to a net loss or retention of litter C and N in SOM pools.

To meet my modelling objectives, my research incorporates empirical measurements of microbial C and N cycling traits into the microbially-explicit CORPSE (Carbon, Organisms, Rhizosphere, and Protection in the Soil Environment, Sulman et al., 2014) and FUN-CORPSE (Fixation and Uptake of Nitrogen-CORPSE, Sulman et al., 2017) models. First, I use data from my lab incubation experiment to constrain modeled microbial traits and predict litter transformations into SOM in the CORPSE model as part of my first chapter. Next, I leverage decades of C and N cycling data from the Fernow Experimental Forest in Parsons, WV (Eastman et al., 2021) to build and incorporate microbially-explicit N cycling in the FUN-CORPSE model.

Labelled Litter generation: I constructed a plant growth chamber with automated ^{13}C-CO_2 and ^{12}C-CO_2 inputs and ^{15}N-ammonium nitrate fertilizer to grow ^{13}C and ^{15}N isotopically labelled corn and miscanthus plants. Corn was grown hydroponically and miscanthus was grown in soil from rhizomes. Both crops grew in the chamber for 8 weeks, and then were drought-senesced before harvest. Aboveground and belowground plant material was separated, dried, and finely

ground. Litter characteristics for each are shown in table 1.1.

Site Descriptions: For the lab experiment (objective 1), soils were collected from the University of Illinois Energy Farm (40°3′46″N, 88°11′46″W) located in Urbana, IL on October 10, 2019. Four replicate plots of corn-corn-soy rotations and perennial miscanthus crops were established in 2008. These are managed in standard agricultural practices for each crop, including inorganic N fertilization, yearly tillage, and leaving crop residues in the field for corn plots, and no fertilization, no tillage, and aboveground biomass removal for miscanthus. Prior to this establishment the land had been in row crops, primarily corn and soybean rotations, for over a century. Soils were collected from the top 20 cm, brought back to the lab in Morgantown where roots and stones were removed, and sieved to 2 mm. Soils were processed within one week and stored at 5°C until the beginning of the soil incubation. Soils from replicate plots were mixed within crop type, and combined soil characteristics for each are shown in table 1.1.

For the *in situ* experiment (objective 2), ingrowth cores were installed at the West Virginia University Animal Sciences Farm (39°40'10.2"N, 79°55'53.6"W) located in Morgantown, WV from April-September 2021. Miscanthus plots were established in 2019 from rhizomes in 8 replicate blocks of 4 fertilization treatments: no fertilizer added, low inorganic NPK (19 kg NPK/ha), high inorganic NPK (57 kg NPK/ha), and organic fertilizer (57 kg N/ha) for a total of 32 plots. The plots are 5 m by 5 m square with miscanthus plants established on a 1 m grid for a total of 25 plants per plot. Of the plots with successful miscanthus establishment in year 1, 5 plots were randomly selected for each of the three nutrient treatments used in this experiment (control, high inorganic NPK, and organic fertilizer) for a total of 15 plots. Soil characteristics for miscanthus plots by treatment are shown in table 1.1.

For the unmanaged forest model experiment (objective 3), I leveraged decades of C and N cycling data from the Fernow Experimental Forest in Parsons, WV (herein, the Fernow) to build, constrain, and

validate N cycling in the FUN-CORPSE model. The Fernow is home to a N deposition experiment where an entire watershed was fertilized with ammonium sulfate at a rate of 35.4 kg N/ha/yr for 30 years, from 1989-2019. An adjacent, similar watershed serves as a reference. A wealth of C and N cycling data is available from this site (e.g., streamwater nitrate leaching, soil and vegetation C and N pools, soil nitrification and N mineralization rate measurements) to build, parameterize, and validate model representations of ecosystem responses to N deposition.

Table 1.1- Litter and soil traits: Values shown are mean(SE). Letters denote $p<0.05$ differences within each category (i.e., litter C:N). Litters for each crop are denoted by aboveground (AG) or belowground (BG).

	%C	C:N	$\delta^{13}C$	$\delta^{15}N$
Energy Farm Soil				
Corn	1.4(0.20)[a]	11.4(0.32)[a]	-14.8(0.3)[a]	88(13)[a]
Miscanthus	1.7(0.15)[a]	12.2(0.37)[a]	-14.5(0.2)[a]	120(42)[a]
WV Miscanthus Soil				
Control	2.7(0.05)[ab]	10.3(0.12)[a]	-24.1(0.08)[a]	8.6(0.09)[a]
High NPK	2.5(0.03)[a]	10.2(0.15)[a]	-24.0(0.08)[a]	8.4(0.2)[a]
Organic	2.8(0.12)[b]	10.5(0.23)[a]	-24.0(0.1)[a]	8.6(0.2)[a]
Litter				
Corn AG	41.7(0.17)[a]	18.8(0.64)[a]	7,018(49)[a]	34,796(306)[a]
Corn BG	42.1(0.30)[a]	18.6(0.30)[a]	5,631(131)[b]	38,871(120)[b]
Miscanthus AG	42.1(0.06)[a]	31.7(0.83)[b]	5,941(76)[b]	6,585(48)[c]
Miscanthus BG	43.1(0.10)[b]	27.0(1.30)[c]	3,005(43)[c]	3,909(143)[d]

Model Descriptions:

The CORPSE model (Sulman et al., 2014) predicts microbially-controlled decomposition of unprotected SOC and formation of physically protected SOC. Here, unprotected SOC is analogous to our particulate SOC, and protected SOC is analogous to mineral associated SOC. SOC is split between chemical types that represent recalcitrant, labile, and microbial necromass compounds, with preferential microbial uptake of labile compounds and the fastest protection rate for microbial necromass. The CORPSE model traditionally has 3 compartments for bulk soil, rhizosphere soil, and

litter. We adapted this to simulate lab microcosms with a single bulk soil compartment and added litter C compartment.

The FUN-CORPSE model (Fixation and Uptake of Nitrogen-CORPSE, Sulman et al., 2017) simulates plant-microbe interactions and coupled C and N cycles in terrestrial ecosystems. To meet plant N demand, the FUN model (Brzostek et al., 2014) uses a resistance framework to optimally allocate C belowground to the rhizosphere where the microbes represented in the CORPSE model can use it to prime decomposition and enhance N availability. N cycling is simplistic in FUN-CORPSE, with N mineralization driven by substrate and microbial stoichiometry. This process results in one inorganic N pool that can be accessed by plants and microbes to meet N demand. Losses of N are modeled as a first order flux that is assumed to capture both denitrification and leaching.

1.3 Literature Cited

Adler, Paul, Del Grosso, Stephen, & Parton, William. (2007). Life-cycle assessment of net greenhouse gas flux for bioenergy cropping systems. *Ecological Applications*. https://esajournals.onlinelibrary.wiley.com/doi/full/10.1890/05-2018

Bais, H. P., Weir, T. L., Perry, L. G., Gilroy, S., & Vivanco, J. M. (2006). The role of root exudates in rhizosphere interactions with plants and other organisms. *Annual Review of Plant Biology*, *57*(1), 233–266. https://doi.org/10.1146/annurev.arplant.57.032905.105159

Benbi, D. K., Boparai, A. K., & Brar, K. (2014). Decomposition of particulate organic matter is more sensitive to temperature than the mineral associated organic matter. *Soil Biology and Biochemistry*, *70*, 183–192. https://doi.org/10.1016/j.soilbio.2013.12.032

Berardi, D., Brzostek, E., Blanc-Betes, E., Davison, B., DeLucia, E. H., Hartman, M. D., Kent, J., Parton, W. J., Saha, D., & Hudiburg, T. W. (2020). 21st-century biogeochemical modeling: Challenges for Century-based models and where do we go from here? *GCB Bioenergy*, *12*(10), 774–788. https://doi.org/10.1111/gcbb.12730

Brzostek, E. R., Dragoni, D., Brown, Z. A., & Phillips, R. P. (2015). Mycorrhizal type determines the magnitude and direction of root-induced changes in decomposition in a temperate forest. *New Phytologist*, *206*(4), 1274–1282. https://doi.org/10.1111/nph.13303

Brzostek, E. R., Fisher, J. B., & Phillips, R. P. (2014). Modeling the carbon cost of plant nitrogen acquisition: Mycorrhizal trade-offs and multipath resistance uptake improve predictions of retranslocation. *Journal of Geophysical Research: Biogeosciences*, *119*(8), 1684–1697. https://doi.org/10.1002/2014JG002660

Carvalho, J. L. N., Hudiburg, T. W., Franco, H. C. J., & DeLucia, E. H. (2017). Contribution of above- and belowground bioenergy crop residues to soil carbon. *GCB Bioenergy*, *9*(8), 1333–1343. https://doi.org/10.1111/gcbb.12411

Chen, W., Koide, R. T., Adams, T. S., DeForest, J. L., Cheng, L., & Eissenstat, D. M. (2016). Root morphology and mycorrhizal symbioses together shape nutrient foraging strategies of temperate trees. *Proceedings of the National Academy of Sciences*, *113*(31), 8741–8746. https://doi.org/10.1073/pnas.1601006113

Cheng, W., Parton, W. J., Gonzalez-Meler, M. A., Phillips, R., Asao, S., McNickle, G. G., Brzostek, E., & Jastrow, J. D. (2014). Synthesis and modeling perspectives of rhizosphere priming. *New Phytologist*, *201*(1), 31–44. https://doi.org/10.1111/nph.12440

Cotrufo, M. F., Wallenstein, M. D., Boot, C. M., Denef, K., & Paul, E. (2013). The Microbial Efficiency-Matrix Stabilization (MEMS) framework integrates plant litter decomposition with soil organic matter stabilization: Do labile plant inputs form stable soil organic matter? *Global Change Biology*, *19*(4), 988–995. https://doi.org/10.1111/gcb.12113

Creamer, C. A., Foster, A. L., Lawrence, C., McFarland, J., Schulz, M., & Waldrop, M. P. (2019). Mineralogy dictates the initial mechanism of microbial necromass association. *Geochimica Et Cosmochimica Acta*, *260*, 161–176. https://doi.org/10.1016/j.gca.2019.06.028

Davidson, E. A., & Janssens, I. A. (2006). Temperature sensitivity of soil carbon decomposition and feedbacks to climate change. *Nature*, *440*(7081), Article 7081. https://doi.org/10.1038/nature04514

Davis, S. C., Parton, W. J., Dohleman, F. G., Smith, C. M., Grosso, S. D., Kent, A. D., & DeLucia, E. H. (2010). Comparative biogeochemical cycles of bioenergy crops reveal

nitrogen-fixation and low greenhouse gas emissions in a Miscanthus × giganteus agro-ecosystem. *Ecosystems*, *13*(1), 144–156. https://doi.org/10.1007/s10021-009-9306-9

Dijkstra, F. A., Carrillo, Y., Pendall, E., & Morgan, J. A. (2013). Rhizosphere priming: A nutrient perspective. *Frontiers in Microbiology*, *4*, 216. https://doi.org/10.3389/fmicb.2013.00216

Dohleman, F. G., & Long, S. P. (2009). More productive than maize in the midwest: how does miscanthus do it? *Plant Physiology*, *150*(4), 2104–2115. https://doi.org/10.1104/pp.109.139162

Eastman, B. A., Adams, M. B., Brzostek, E. R., Burnham, M. B., Carrara, J. E., Kelly, C., McNeil, B. E., Walter, C. A., & Peterjohn, W. T. (2021). Altered plant carbon partitioning enhanced forest ecosystem carbon storage after 25 years of nitrogen additions. *New Phytologist*, *230*(4), 1435–1448. https://doi.org/10.1111/nph.17256

Heaton, E. A., Dohleman, F. G., & Long, S. P. (2008). Meeting US biofuel goals with less land: The potential of Miscanthus. *Global Change Biology*, *14*(9), 2000–2014. https://doi.org/10.1111/j.1365-2486.2008.01662.x

Jilling, A., Keiluweit, M., Gutknecht, J. L., & Grandy, A. S. (2021). Priming mechanisms providing plants and microbes access to mineral-associated organic matter. *Soil Biology and Biochemistry*, *158*, 108265.

Kallenbach, C. M., Frey, S. D., & Grandy, A. S. (2016). Direct evidence for microbial-derived soil organic matter formation and its ecophysiological controls. *Nature Communications*, *7*(1), Article 1. https://doi.org/10.1038/ncomms13630

Keiluweit, M., Bougoure, J. J., Nico, P. S., Pett-Ridge, J., Weber, P. K., & Kleber, M. (2015). Mineral protection of soil carbon counteracted by root exudates. *Nature Climate Change*, *5*(6), 588–595. https://doi.org/10.1038/nclimate2580

Kyker-Snowman, E., Wieder, W. R., Frey, S. D., & Grandy, A. S. (2020). Stoichiometrically coupled carbon and nitrogen cycling in the MIcrobial-MIneral Carbon Stabilization model version 1.0 (MIMICS-CN v1.0). *Geoscientific Model Development*, *13*(9), 4413–4434. https://doi.org/10.5194/gmd-13-4413-2020

Ledo, A., Smith, P., Zerihun, A., Whitaker, J., Vicente-Vicente, J. L., Qin, Z., McNamara, N. P., Zinn, Y. L., Llorente, M., Liebig, M., Kuhnert, M., Dondini, M., Don, A., Diaz-Pines, E., Datta, A., Bakka, H., Aguilera, E., & Hillier, J. (2020). Changes in soil organic carbon under perennial crops. *Global Change Biology*, *26*(7), 4158–4168. https://doi.org/10.1111/gcb.15120

Lehmann, J., & Kleber, M. (2015). The contentious nature of soil organic matter. *Nature*, *528*(7580), Article 7580. https://doi.org/10.1038/nature16069

Liang, C., Schimel, J. P., & Jastrow, J. D. (2017). The importance of anabolism in microbial control over soil carbon storage. *Nature Microbiology*, *2*(8), Article 8. https://doi.org/10.1038/nmicrobiol.2017.105

Lugato, E., Lavallee, J. M., Haddix, M. L., Panagos, P., & Cotrufo, M. F. (2021). Different climate sensitivity of particulate and mineral-associated soil organic matter. *Nature Geoscience*, *14*(5), Article 5. https://doi.org/10.1038/s41561-021-00744-x

Luo, Y., & Schuur, E. A. G. (2020). Model parameterization to represent processes at unresolved scales and changing properties of evolving systems. *Global Change Biology*, *26*(3), 1109–1117. https://doi.org/10.1111/gcb.14939

Mueller, K. E., Hobbie, S. E., Chorover, J., Reich, P. B., Eisenhauer, N., Castellano, M. J., Chadwick, O. A., Dobies, T., Hale, C. M., Jagodzinski, A. M., Kalucka, I., Kieliszewska-Rokicka, B., Modrzynski, J., Rozen, A., Skorupski, M., Sobczyk, L., Stasinska, M., Trocha, L. K., Weiner, J., … Oleksyn, J. (2015). Effects of litter traits, soil biota, and soil chemistry on soil carbon stocks at a common garden with 14 tree species. *Biogeochemistry*, *123*(3), 313–327. https://doi.org/10.1007/s10533-015-0083-6

Myrgiotis, V., Rees, R. M., Topp, C. F. E., & Williams, M. (2018). A systematic approach to identifying key parameters and processes in agroecosystem models. *Ecological Modelling*, *368*, 344–356. https://doi.org/10.1016/j.ecolmodel.2017.12.009

Pan, Y., Birdsey, R. A., Fang, J., Houghton, R., Kauppi, P. E., Kurz, W. A., Phillips, O. L., Shvidenko, A., Lewis, S. L., Canadell, J. G., Ciais, P., Jackson, R. B., Pacala, S. W., McGuire, A. D., Piao, S., Rautiainen, A., Sitch, S., & Hayes, D. (2011). A Large and Persistent Carbon Sink in the World's Forests. *Science*, *333*(6045), 988–993. https://doi.org/10.1126/science.1201609

Phillips, R. P., Brzostek, E., & Midgley, M. G. (2013). The mycorrhizal-associated nutrient economy: A new framework for predicting carbon–nutrient couplings in temperate forests. *New Phytologist*, *199*(1), 41–51. https://doi.org/10.1111/nph.12221

Robertson, A. D., Paustian, K., Ogle, S., Wallenstein, M. D., Lugato, E., & Cotrufo, M. F. (2019). Unifying soil organic matter formation and persistence frameworks: The MEMS model. *Biogeosciences*, *16*(6), 1225–1248. https://doi.org/10.5194/bg-16-1225-2019

Saifuddin, M., Abramoff, R. Z., Davidson, E. A., Dietze, M. C., & Finzi, A. C. (2021). Identifying Data Needed to Reduce Parameter Uncertainty in a Coupled Microbial Soil C

and N Decomposition Model. *Journal of Geophysical Research: Biogeosciences*, *126*(12), e2021JG006593. https://doi.org/10.1029/2021JG006593

Schmidt, M. W. I., Torn, M. S., Abiven, S., Dittmar, T., Guggenberger, G., Janssens, I. A., Kleber, M., Kögel-Knabner, I., Lehmann, J., Manning, D. A. C., Nannipieri, P., Rasse, D. P., Weiner, S., & Trumbore, S. E. (2011). Persistence of soil organic matter as an ecosystem property. *Nature*, *478*(7367), Article 7367. https://doi.org/10.1038/nature10386

Shi, Z., Crowell, S., Luo, Y., & Moore, B. (2018). Model structures amplify uncertainty in predicted soil carbon responses to climate change. *Nature Communications*, *9*(1), Article 1. https://doi.org/10.1038/s41467-018-04526-9

Six, J., Elliott, E. T., & Paustian, K. (2000). Soil macroaggregate turnover and microaggregate formation: A mechanism for C sequestration under no-tillage agriculture. *Soil Biology and Biochemistry*, *32*(14), 2099–2103. https://doi.org/10.1016/S0038-0717(00)00179-6

Soong, J. L., Fuchslueger, L., Maranon-Jimenez, S., Torn, M. S., Janssens, I. A., Penuelas, J., & Richter, A. (2020). Microbial carbon limitation: The need for integrating microorganisms into our understanding of ecosystem carbon cycling. *Global Change Biology*, *26*(4), 1953–1961. https://doi.org/10.1111/gcb.14962

Stewart, C. E., Moturi, P., Follett, R. F., & Halvorson, A. D. (2015). Lignin biochemistry and soil N determine crop residue decomposition and soil priming. *Biogeochemistry*, *124*(1–3), 335–351. https://doi.org/10.1007/s10533-015-0101-8

Studt, J. E., McDaniel, M. D., Tejera, M. D., VanLoocke, A., Howe, A., & Heaton, E. A. (2021). Soil net nitrogen mineralization and leaching under Miscanthus × giganteus and Zea mays. *GCB Bioenergy*, *13*(9), 1545–1560. https://doi.org/10.1111/gcbb.12875

Sulman, B. N., Brzostek, E. R., Medici, C., Shevliakova, E., Menge, D. N. L., & Phillips, R. P. (2017). Feedbacks between plant N demand and rhizosphere priming depend on type of mycorrhizal association. *Ecology Letters*, *20*(8), 1043–1053. https://doi.org/10.1111/ele.12802

Sulman, B. N., Moore, J. A., Abramoff, R., Averill, C., Kivlin, S., Georgiou, K., Sridhar, B., Hartman, M. D., Wang, G., & Wieder, W. R. (2018). Multiple models and experiments underscore large uncertainty in soil carbon dynamics. *Biogeochemistry*, *141*(2), 109–123.

Sulman, B. N., Phillips, R. P., Oishi, A. C., Shevliakova, E., & Pacala, S. W. (2014). Microbe-driven turnover offsets mineral-mediated storage of soil carbon under elevated CO2. *Nature Climate Change*, *4*(12), Article 12. https://doi.org/10.1038/nclimate2436

Talbot, J. M., & Treseder, K. K. (2012). Interactions among lignin, cellulose, and nitrogen drive litter chemistry-decay relationships. *Ecology*, *93*(2), 345–354. https://doi.org/10.1890/11-0843.1

Terrer, C., Vicca, S., Hungate, B. A., Phillips, R. P., & Prentice, I. C. (2016). Mycorrhizal association as a primary control of the CO2 fertilization effect. *Science*, *353*(6294), 72–74. https://doi.org/10.1126/science.aaf4610

Van Der Heijden, M. G. A., Bardgett, R. D., & Van Straalen, N. M. (2008). The unseen majority: Soil microbes as drivers of plant diversity and productivity in terrestrial ecosystems. *Ecology Letters*, *11*(3), 296–310. https://doi.org/10.1111/j.1461-0248.2007.01139.x

Vitousek, P. M., Mooney, H. A., Lubchenco, J., & Melillo, J. M. (1997). Human Domination of Earth's Ecosystems. *Science*, *277*(5325), 494–499. https://doi.org/10.1126/science.277.5325.494

Wieder, W. R., Grandy, A. S., Kallenbach, C. M., & Bonan, G. B. (2014). Integrating microbial physiology and physio-chemical principles in soils with the MIcrobial-MIneral Carbon Stabilization (MIMICS) model. *Biogeosciences*, *11*(14), 3899–3917. https://doi.org/10.5194/bg-11-3899-2014

Williams, E. K., Fogel, M. L., Berhe, A. A., & Plante, A. F. (2018). Distinct bioenergetic signatures in particulate versus mineral-associated soil organic matter. *Geoderma*, *330*, 107–116. https://doi.org/10.1016/j.geoderma.2018.05.024

Zak, D. R., Holmes, W. E., White, D. C., Peacock, A. D., & Tilman, D. (2003). Plant diversity, soil microbial communities, and ecosystem function: Are there any links? *Ecology*, *84*(8), 2042–2050. https://doi.org/10.1890/02-0433

Chapter 2: Plant litter traits control microbial decomposition and drive soil carbon stabilization

Reprinted from: ***J. Ridgeway****, E.M. Morrissey, and E.R. Brzostek, 2022. Plant litter traits control microbial decomposition and drive soil carbon stabilization. Soil Biology and Biochemistry doi.org/10.1016/j.soilbio.2022.108857*

2.1 Abstract:

Efforts to manage soils for carbon (C) sequestration remain limited by our understanding of how differences in plant traits and microbial traits mechanistically drive soil organic C (SOC) storage. Addressing this uncertainty is particularly critical in bioenergy agriculture, due to its potential to enhance soil C and provide a C neutral fuel. As such, we examined differences between two contrasting feedstocks, *Zea mays* (corn) and *Miscanthus x giganteus* (miscanthus), in the ability of their litter to form new chemically resistant particulate SOC vs. protected mineral associated SOC and used this data to improve the parameterization of a microbial SOC model. We tested a hypothesized conceptual model whereby easy to decompose corn litters drive greater microbial carbon use efficiency (CUE) and the formation of more mineral associated SOC over particulate SOC than more complex miscanthus litters. To do this, we performed a soil microcosm experiment where we added ^{13}C enriched aboveground and belowground litters to soils and traced the fate of the ^{13}C into microbial respiration and SOC pools. We found that corn litters promoted higher microbial CUE (0.37) than miscanthus litters (0.24). In turn, corn litter formed approximately 50% more mineral associated SOC than miscanthus litters. Similarly, structurally complex root litters promoted a lower CUE and formed less mineral associated SOC than leaf and shoot litters for both crops. When we used our data to parameterize the SOC model, we found that modelling microbial trait differences uniquely allowed the model to capture the fate of litter C in SOC. Collectively, we found a robust link between litter quality, microbial efficiency, and the formation of SOC. This link bridges the empirical uncertainty in how different crops can form new soil C and provides an empirical basis for modelling SOC transformations.

2.2 Introduction:

Soil carbon (C) sequestration has emerged as a potential strategy to combat climate change, but our predictive understanding of soil organic C (SOC) stabilization remains uncertain. Addressing this uncertainty is especially imperative for the bioenergy industry, as policy and management strategies aimed at improving the sustainability and C neutrality of bioenergy focus on enhancing SOC. The long-term sustainability of using *Zea mays* (herein, corn) as the dominant bioenergy crop is limited by the broadly observed pattern of SOC depletion (Carvalho et al., 2017) in conjunction with extensive land use (Sands et al., 2017) and energy demands (Cherubini et al., 2009). Given the urgent need to drastically reduce emissions (Sixth Assessment Report of the IPCC, 2021), perennial grasses like *Miscanthus x giganteus* (herein miscanthus) and switchgrass have emerged as a more sustainable alternative to corn owing to plant traits and management practices that enhance productivity and reduce SOC losses (Heaton et al., 2008; Anderson-Teixeira et al., 2013). However, our mechanistic understanding of how these perennial grasses build new SOC remains limited. In particular, the extent to which SOC persists due to chemical recalcitrance vs. physical protection remains a critical uncertainty in assessing the potential for both SOC accumulation and vulnerability. This uncertainty also impacts the accuracy of models used to project the impacts of bioenergy production on the soil carbon sink.

The extent to which bioenergy crops can build new SOC depends not only on chemical complexity of litter inputs but also on physical protection of decomposable organic matter from microbial decomposers through associations with soil mineral surfaces (Cotrufo et al., 2013; Lehmann & Kleber, 2015; and others). Thus, SOC can be split into two main categories that differ in composition and characteristics: particulate SOC and mineral associated SOC. Particulate SOC primarily consists of undecomposed litter fragments or partially decomposed

organic matter that unless occluded in aggregates remains physically accessible to microbial decomposers (Witzgall et al., 2021). Particulate SOC may be slow to decompose due to chemical complexity, making this pool more vulnerable to environmental changes like warming that ameliorate energetic decomposition constraints (Davidson & Janssens, 2006). Mineral associated SOC primarily consists of chemically simple compounds (Sanderman et al., 2014; Williams et al., 2018), much of which is thought to be microbially-derived (Liang et al., 2017). These labile compounds become physically protected from microbial decomposers through sorption to clay and mineral surfaces in the soil, potentially allowing this C to persist over longer timescales. Mineral associated SOC accumulation may be limited by mineral saturation, high nitrogen (N) stoichiometric demand, or rhizosphere mobilization, constraining the potential for C accumulation in this pool (Stewart et al., 2009; Jilling et al., 2018; Schlesinger & Amundson, 2019). Given that particulate and mineral associated SOC differ in their ability to accumulate and susceptibility to climate change (Lugato et al., 2021), comparing how different bioenergy crop litters form soil C is critical, particularly with controlled experiments where the impact of plant litter differences on microbial decomposers can be mechanistically determined.

We tested a conceptual framework (Figure 2.1) for how plant-microbe interactions may drive differences in C accumulation between particulate vs. mineral associated SOC for corn and a model perennial crop, miscanthus. Here, we link distinct differences in litter chemistry like higher C to N or lignin to N ratios for miscanthus than corn (Meineke et al., 2014; Brancourt-Hulmel et al., 2022) with our current understanding of SOC formation that emphasizes the contribution of microbially-derived products to mineral associated SOC (Cotrufo et al., 2013; Lehmann and Kleber, 2015; and others). While this conceptual framework is broadly accepted, inconsistent empirical evidence highlights the need for testing if microbial decomposition and

efficiency can be linked with mineral associated SOC protection in bioenergy soils. In our conceptual framework (Figure 2.1), corn plants produce relatively labile (easily decomposable) litter to the particulate SOC pool. We expect soil microbes to decompose this SOC rapidly and efficiently, respiring CO_2 and producing simpler compounds that can preferentially sorb to clay and mineral surfaces (Figure 2.1a). Miscanthus is a perennial grass that produces larger quantities of more recalcitrant (difficult to decompose) litter to the particulate SOC pool (Heaton et al., 2010; Meineke et al., 2014). Microbes may slowly and less efficiently decompose this litter, leading to a slower flux of litter C into mineral associated SOC. As belowground litters have been found to decompose more slowly than aboveground litters (Rasse et al., 2005; Fulton-Smith & Cotrufo, 2019; and others), we also expect that belowground litter C will preferentially remain as particulate SOC and aboveground litter C will form more mineral associated SOC. Importantly, this framework provides a linked theoretical and empirical foundation that could explain how these crops currently differ in SOC.

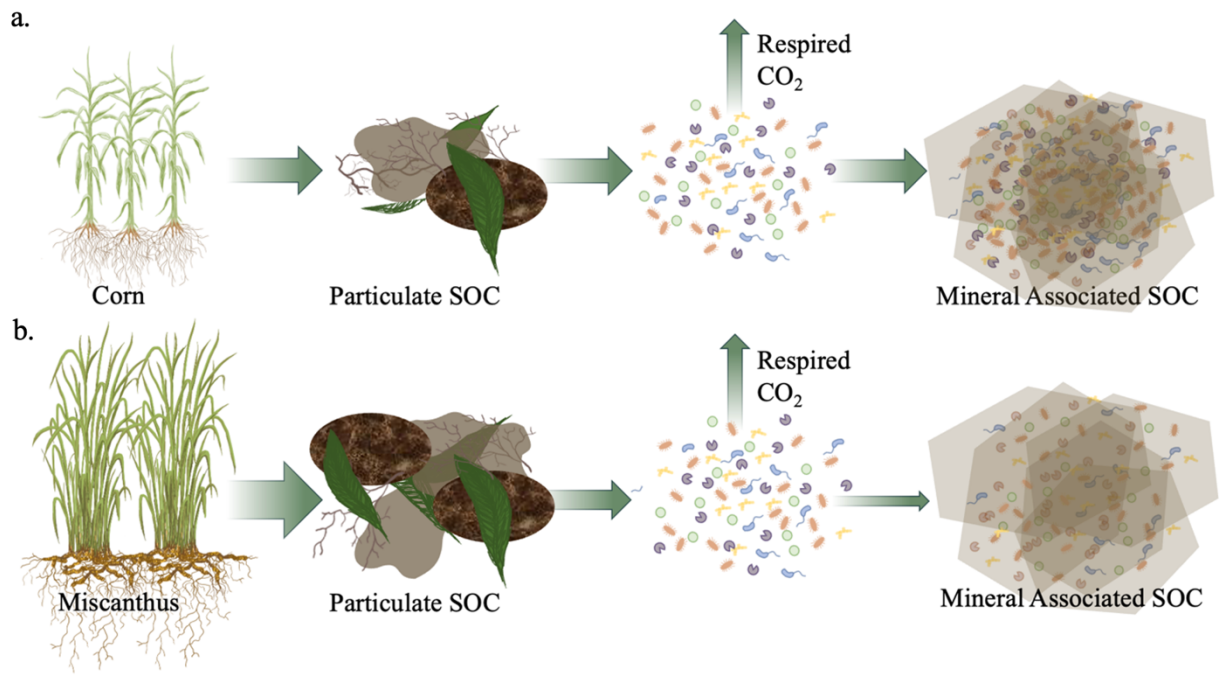

Fig. 2.1: Corn and miscanthus differ in the fate of litter C between SOC fractions. Corn (a) produces relatively labile litter that microbes can decompose rapidly and efficiently, producing compounds that can preferentially sorb to clay and mineral surfaces as mineral associated SOC. Miscanthus (b) produces greater quantities of more recalcitrant litter that enters the particulate SOC pool. Here, microbial uptake is slower and less efficient which leads to a reduced flux of litter C into mineral associated SOC.

Testing this conceptual model also provides an empirical basis for improving model projections of the potential for bioenergy crops to deplete or build SOC. However, traditional soil models implicitly represent microbes through first-order decomposition processes and broadly lack the ability to represent the processes of microbially-driven transformations of plant C between the particulate vs. mineral SOC pools (Berardi et al., 2020). This omission limits their ability to capture how microbial processes impacting net C cycling respond to climate change drivers beyond the range of historical conditions. Emerging models incorporate explicit representations of the microbial decomposers that drive belowground C fluxes (e.g., CORPSE, Sulman et al., 2014; MIMICS, Wieder et al., 2014; MEMS, Robertson et al., 2019; FUN Bio-CROP, Juice et al., 2022). While these models include formulations of the role of microbes in

controlling the decomposition and stabilization of particulate and mineral SOC pools, many of the parameters in these formulations are poorly constrained by experimental data or are only grounded by theoretical constraints. Specifically, the empirical uncertainty in microbial control over mineral protection is amplified in predictive models that use tuned parameters to drive microbial decomposition, production, turnover, and protection. Thus, empirical data is necessary to constrain decomposition parameters and validate predictions of modeled SOC pools.

We tested our conceptual framework by tracking the fate of ^{13}C labelled litters of corn and miscanthus into microbial respiration, microbial biomass, and particulate and mineral SOC pools in an incubation experiment. We focused on the fate of each litter in soils that had a long history of corn or miscanthus cultivation (i.e., corn litter in corn soils, miscanthus litter in miscanthus soils) to improve our mechanistic understanding of how these crops and their corresponding microbial communities differ in SOC formation. We also measured how corn and miscanthus litter differed in their impacts on the efficiency of microbial decomposition. Based on our conceptual model, we hypothesized that (1) more easily decomposed corn litters will form more mineral associated SOC and less particulate SOC than miscanthus litters, (2) more easily decomposed leaf and shoot litters will form more mineral associated SOC and less particulate SOC than root litters, and (3) that microbial carbon use efficiency is linked to the formation of mineral associated SOC. Using the data generated by testing these hypotheses, we investigated the degree to which measured differences in microbial carbon use efficiency can inform model predictions of litter decomposition and mineral associated SOC formation with the CORPSE model.

2.3 Methods

To investigate our hypotheses, we performed a lab experiment comparing litter decomposition and SOC formation for corn and miscanthus bioenergy crops. We incubated soils from each crop with corresponding ^{13}C and ^{15}N enriched aboveground and belowground litters. We traced litter C transfers through microbial decomposition and into mineral associated and particulate pools of SOC.

Experimental design

Our experimental design was 2 crops (corn, miscanthus) x 3 litter treatments (aboveground (AG) litter, belowground (BG) litter, no (NO) litter) x 8 reps for a total of 48 microcosms. We measured soil and litter characteristics, total and litter-derived microbial respiration, total and litter-derived microbial biomass, and litter C incorporation into SOC fractions.

Site description and soil sampling

Soils for this experiment were collected from the University of Illinois Energy Farm (40°3′46″N, 88°11′46″W) located in Urbana, IL on October 10, 2019. A more detailed site description is published by Anderson-Teixeira, 2013. Briefly, 4 replicate plots of corn-corn-soy rotations and perennial miscanthus crops were established in 2008. These are managed in standard agricultural practices for each crop. Notable management differences between the crop systems include inorganic N fertilization, yearly tillage, and leaving crop residues in the field for corn plots, and no fertilization, no tillage, and aboveground biomass removal for miscanthus (Kantola et al., 2022). Prior to this establishment the land had been in row crops, primarily corn and soybean rotations, for over a century. Soils were collected from the top 20 cm using a soil

auger from each replicate block for each crop (4 locations within plot transects). Soils were brought back to the lab in Morgantown where roots and stones were removed, and soils were sieved to 2 mm. Soils were processed within one week and stored at 5°C before beginning the soil incubation. Soils from replicate plots were mixed within crop type, and combined soil characteristics for each are shown in table 2.1.

Isotopically enriched litter generation

To meet our experimental objectives of tracing the fate of litter decomposition into soil organic matter fractions, ^{13}C enriched litter was generated for corn and miscanthus. A plant growth chamber was constructed with automated CO_2 inputs set at 8 atom percent $^{13}CO_2$ to grow isotopically enriched corn and miscanthus plants.

Rhizomatous miscanthus was grown in the chamber using standard potting soil mixed with vermiculite. Rhizomes were collected from established, 5 year old plots while still dormant in April 2019 from the University of Illinois Energy Farm, shipped to West Virginia, and planted in large tubs. Of the viable plants, a subset was re-planted and moved into the isotope labelling chamber when the average shoot height was 6-8". Miscanthus was watered as needed with ^{15}N enriched Johnson's nutrient solution.

Corn was grown hydroponically in the chamber in dilute, ^{15}N enriched Johnson's nutrient solution. Corn seedlings were started in the greenhouse from seeds sent from the University of Illinois Energy Farm. Seedlings were moved into the chamber when roots were long enough (~2-3") for the hydroponic setup, at which point the average shoot height was around 2".

Both crops grew in the chamber for 8 weeks, and then were drought-senesced before harvest. Aboveground and belowground plant material was separated, dried, and finely ground.

Litter characteristics for each are shown in table 2.1. Differences in isotopic enrichment of litters were accounted for in data analysis.

Table 2. 1- Litter and soil traits

	%C	C:N	Atom % ^{13}C
Corn Soil	1.43(0.20)[a]	11.4(0.32)[a]	1.10(4.1E-4)[a]
Miscanthus Soil	1.72(0.15)[a]	12.2(0.37)[a]	1.10(2.2E-4)[a]
Corn AG Litter	41.7(0.17)[a]	18.8(0.64)[a]	8.26(0.05)[a]
Corn BG Litter	42.1(0.30)[a]	18.6(0.30)[a]	6.93(0.13)[b]
Miscanthus AG Litter	42.1(0.06)[a]	31.7(0.83)[b]	7.24(0.07)[b]
Miscanthus BG Litter	43.1(0.10)[b]	27.0(1.30)[c]	4.31(0.04)[c]

Values shown are mean(SE). Letters denote $p<0.05$ differences within each category (i.e., litter C:N or soil atom % ^{13}C)

Incubations and soil respiration sampling

Microcosm incubations were set up in wide mouth glass mason jars (930mL volume) fitted with rubber septa. Each microcosm had 50.0 ± 0.05g of dry soil from each crop adjusted to 50% water-holding capacity (30% gravimetric water content) with deionized water and 250 ±1.5 mg litter C from each litter type gently mixed throughout the soil. Microcosms were incubated at lab room temperature (~22 °C) in the dark until microbial respiration levelled off to less than 10% of the initial respiration rates at 12 weeks.

Microcosm headspace was sampled on days 1,3, and 7 and then weekly afterwards for 12 weeks. Total headspace CO_2 concentration was measured with an infrared gas analyzer (LI-6400, LI-Cor Biosciences Inc.) and $\delta^{13}CO_2$ was measured with a Picarro G2201 (Picarro Inc.). The respiration data was partitioned to calculate the proportion of microbial respiration from added litter (Morrissey et al., 2017). At the end of each sampling, all jars were equilibrated with

ambient lab air using a vacuum line to facilitate complete gas exchange. Jars were weighed and any mass change was compensated for by adding deionized water to maintain soil moisture.

Soil fractionation, isotope analysis, and litter C fate recovery

At the end of the incubations, microcosms were destructively harvested and a subsample of soil was fractionated into the particulate SOC (light and heavy particulate SOC) and mineral associated SOC fractions as described in Lavallee et al., 2020. Briefly, the light fraction of particulate SOC is first separated through density floatation. Soil particles less dense than 1.85g/mL form light particulate SOC. Soil denser than 1.85g/mL is then separated into the heavy fraction of particulate SOC and the silt or clay sized mineral associated SOC fraction by wet sieving. Soil particles greater than 53 um diameter form heavy particulate SOC. Soil particles that pass through the 53 um sieve form the mineral associated SOC fraction. Mass recovery is calculated as:

eq.2.1: $$Recovery = \frac{light\ particulate\ SOC(g) + heavy\ particulate\ SOC(g) + mineral\ associated\ SOC(g)}{Initial\ soil\ mass\ (g)} * 100$$

Samples with 100±5% mass recovery were accepted for further analysis.

To trace the fate of the ^{13}C enriched litter, soil fractions were analyzed for %C and $\delta\ ^{13}C$ using a Thermo Fisher Delta V+ isotope ratio mass spectrometer interfaced with a Carlo Erba NC2500 Elemental Analyzer. This data was scaled up by the dry mass of soil in the microcosms to determine total litter C incorporation into each SOC pool. Due to incomplete recovery datasets during fractionation and elemental analyzer detector saturation for some samples, sample sizes vary for litter C recovery in soil pools (Table 2).

We recovered litter C in respiration, particulate SOC, and mineral associated SOC and report total particulate SOC as the sum of light and heavy particulate SOC components. Litter C in microbial biomass is omitted from calculations of litter C recovery because it cannot be separated from the soil organic matter pools. With the exception of miscanthus root treatments, there was good recovery of the enriched litter in microbial respiration, particulate C, and mineral associated C pools. Table 2.2 shows the total litter C recovered in each pool using endmember mixing models based on the measured isotopic signatures of the litter and the unincubated soil. To limit the effect of inaccurate initial litter ^{13}C characterization, particularly for miscanthus belowground litters, all subsequent data is reported as the percentage of labelled litter C recovered in respiration and SOC pools.

Table 2. 2- Added litter C recovered in respiration and SOC pools

Crop	Litter	Sample Size	Respired	Particulate SOC	Mineral associated SOC	Total
Corn	AG	5	58.9(2.5) [a]	16.9(3.2) [a]	29.3(3.9) [a]	105.0(1.5) [a]
Corn	BG	4	56.3(0.84) [a]	32.5(1.5) [b]	19.7(2.7) [b]	108.5(4.3) [a]
Miscanthus	AG	5	55.9(1.3) [a]	26.2(1.8) [c]	22.0(3.1) [b]	104.1(2.0) [a]
Miscanthus	BG	5	72.6(3.1) [b]	70.5(3.6) [d]	14.6(2.2) [c]	157.8(6.0) [b]

Data shown is % Litter C recovered of added litter C mean(se) for crops corn and miscanthus and litter types aboveground (AG) and belowground (BG)

Microbial biomass extractions and carbon use efficiency

At the end of the incubations, a subsample of soil was used to extract microbial biomass C in chloroform slurry fumigations (Witt et al., 2000) followed by persulfate digestion (Doyle et al., 2004). Briefly, soils were extracted in potassium sulfate salt solutions with and without chloroform for 4hrs, decanted, and filtered through a Whatman #3 filter. Next, filtered solutions underwent persulfate digestions where dissolved C was oxidized to CO_2 and the headspace CO_2

and $\delta\ ^{13}CO_2$ was measured on a Picarro G2201. Microbial biomass C and ^{13}C was calculated as the difference between chloroform-fumigated and non-fumigated samples scaled by 2.64 to correct for extraction efficiency (Vance et al., 1987).

A proxy for Carbon Use Efficiency (CUE) was measured using stable isotope tracing as the proportion of ^{13}C incorporated into microbial biomass out of what is taken up, or the ^{13}C in biomass and in respiration. Here, endpoint measurements of microbial biomass and endpoint respiration measurements from the last week of data were used. Thus, CUE was calculated as:

eq.2.2: $$CUE = \frac{litter\ C\ in\ microbial\ biomass}{litter\ C\ in\ microbial\ biomass + litter\ C\ in\ last\ week\ of\ respiration}$$

Using endpoint (1 week) instead of cumulative (12 week) respiration reflects a more rapid average microbial turnover rate, which we believe is supported for two main reasons. The first of these is that estimates of microbial turnover vary widely, from 333 days to 21 hours (Koch et al., 2018), with estimated averages on the scale of 1-2 weeks. CUE is known to decrease with long term incubations because of turnover, although we acknowledge this may not reflect the entire biomass pool (Geyer et al., 2019). Secondly, although evidence suggests that some plant-derived C can directly sorb to soil minerals (Kramer et al., 2012; Sanderman et al., 2014; Angst et al., 2021), much of the organic matter in this fraction is thought to preferentially form from microbial necromass and products (Bradford et al., 2013; Kallenbach et al., 2016), particularly in zones of high microbial activity (Sokol & Bradford, 2019). As such, we expect turnover rates to be much more rapid than 12 weeks in our microcosms due to the observed accumulation of litter C in mineral associated SOC pools.

Statistical analyses

To determine the extent to which treatments differed in microbial decomposition traits and the fate of litter C in each pool, we performed a two-way analysis of variance (ANOVA) in R version 3.5.1 (Copyright © 2018 The R Foundation for Statistical Computing). We used crop (corn, miscanthus) and litter treatment (aboveground, belowground, no litter) as factors. Post-hoc comparisons were also made across treatments using the Tukey HSD test.

Microbial modelling: incorporating measured microbial traits as parameters

The aim of this exercise was to investigate the degree to which data-based microbial traits could facilitate model predictions of total decomposition and the fate of litter C in SOC pools. We simulated our microcosm experiment with the CORPSE model (Sulman et al., 2014). CORPSE (Carbon, Organisms, Rhizosphere, and Protection in the Soil Environment) predicts microbially-controlled decomposition of unprotected SOC and formation of physically protected SOC. Here, unprotected SOC is analogous to our particulate SOC, and protected SOC is analogous to mineral associated SOC. SOC is split between chemical types that represent recalcitrant, labile, and microbial necromass compounds, with preferential microbial uptake of labile compounds and the fastest protection rate for microbial necromass.

We adapted the CORPSE model to simulate lab microcosms with a bulk soil pool and added litter C pool. We initialized the bulk soil pool using data simulated by FUN-BioCROP (Juice et al., 2022) from the same experimental plots and soil collection date. The model was not spun up to equilibrium, as the microcosms did not have any continuing C inputs to balance soil respiration so equilibrium conditions would only exist for C-depleted soil. Litter addition pools were constructed using both our measured litter chemistry and published lignin:N ratios for corn and miscanthus litters (Abiven et al., 2011; Meineke et al., 2014). We then performed a nested suite of model experiments where we (1) modeled plant trait differences, (2) increased protection

and turnover to capture magnitude of treatment responses, and (3) incorporated our CUE data to capture differences between treatments.

First, we tested the ability of CORPSE to represent measured litter incorporation into SOC pools by only modelling plant trait differences and using the original microbial decomposition parameters. These parameters reflect in-situ conditions parameterized for temperate forest ecosystems and were kept the same across all treatments. The parameter inputs for this model run are listed in SI table 1 as Baseline CORPSE.

Then, we adapted the model to capture the magnitude of the average response of the incubation experiments. Protection rates for fast and necro pools of litter C were increased to reflect the greater potential for mixed-in litter C derived compounds to sorb to exposed clay and mineral surfaces in sieved soil. Turnover rates for microbial biomass were increased to better reflect a 1-2 week turnover in soil incubations (Koch et al., 2018; Wang et al., 2021). In addition, we removed microbial N limitation to reflect the lack of competition with plant uptake. These parameters were kept the same across all treatments. The parameter inputs for this model run are listed in SI table 1 as Microcosm CORPSE.

Finally, we used our experimental data to constrain the CUE parameter in CORPSE. Here, we tested the ability of CORPSE to represent measured SOC pools when CUE differed across the treatments. Our CUE data best represents relative differences across treatments and as such we used it scale the CUE in the model for each treatment. To do this, treatment specific CUE parameters were generated by scaling the baseline CUE parameter by the relative differences across treatments so that the average CUE of all the treatments remained at the baseline value (equation in SI). The parameter inputs for this model run are listed in SI table 1 as CUE CORPSE.

Model performance for each run was assessed by comparing the percent error of total litter C fluxes out of the soil (modeled CO2 vs. measured respiration) and the percent error of litter C transfers into mineral associated SOC pools.

2.4 RESULTS

Litter C decomposition: balance of litter C lost to respiration and remaining in SOC

The proportion of litter C lost to respiration or remaining in soil organic matter varied by crop and litter treatment. Belowground (BG) litters exhibited less respiration loss and greater SOC remaining than aboveground (AG) litters (Figure 2.2a; p=0.013), with the lowest average percent of recovered litter C respired for miscanthus BG litter (46.1%), followed by corn BG litter (52.1%), miscanthus AG litter (53.9%), and corn AG litter (56.1%) (Figure 2.2b).

Microbial respiration of litter C was lower for miscanthus than corn litters, especially at earlier stages of decomposition. Towards the end of the incubation, respiration from corn litters levelled off to a greater degree while miscanthus litter respiration continued such that total litter C lost to respiration or remaining in SOC was similar across the crops and only marginally significant (Figure 2.2b; p=0.059).

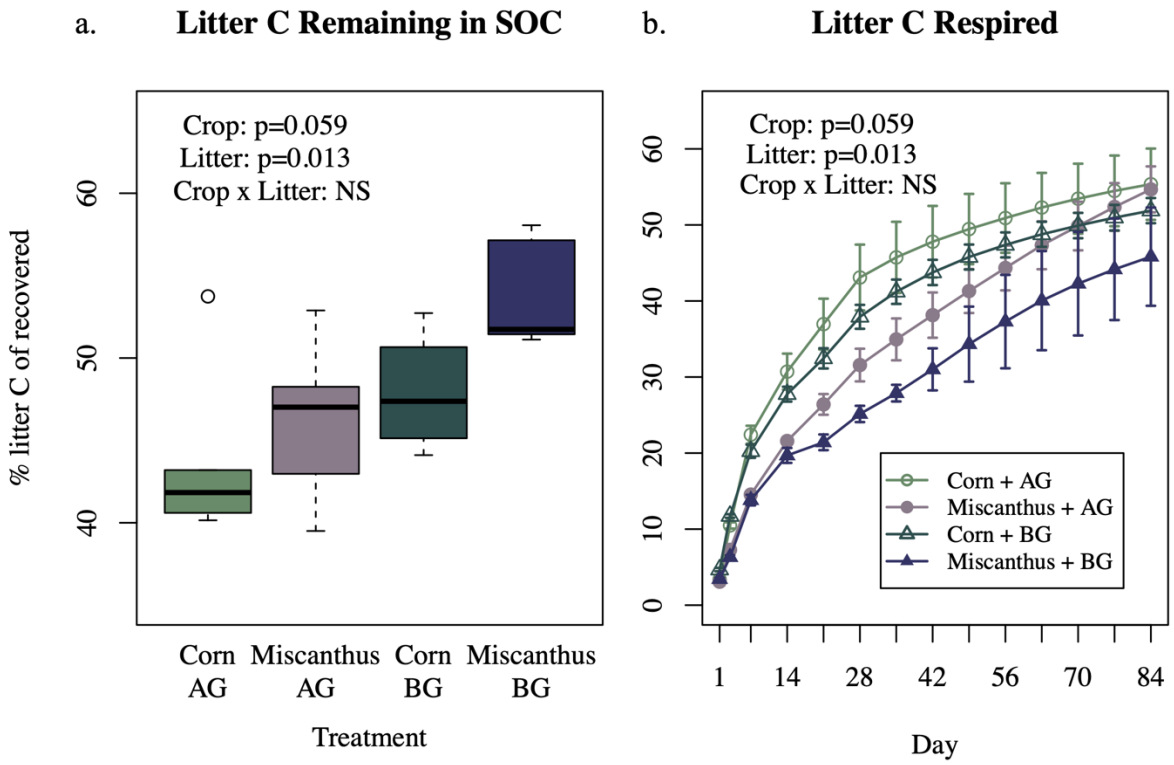

Fig. 2.2: Litter C lost as respiration varied by crop and litter type, with **(a)** litter C remaining in SOC shown as the inverse of final timepoint respiration and **(b)** cumulative litter respired over the course of the incubation

Litter C transformation into particulate and mineral associated SOC pools

Overall, our results show that the transfer of litter C into particulate and mineral associated pools of SOC depended on crop type with more corn litter recovered in mineral associated SOC and less in particulate SOC than miscanthus litters.

More enriched litter C from miscanthus remained in particulate SOC compared to corn litter C (Figure 2.3a, $p<0.001$). Enriched BG litter also remained in particulate SOC to a greater extent than AG litters (Figure 2.3a, $p<0.001$). Miscanthus BG litter had the highest recovery in particulate SOC at 44.6%, followed by corn BG litter (30.0%), miscanthus AG litter (25.2%), and corn AG litter (16.0%) (Figure 2.3a).

Similarly, more enriched litter C from corn formed mineral associated SOC than miscanthus litter C (Figure 2.3b, $p<0.01$). There was also greater recovery of enriched AG litter C in mineral associated SOC than BG litter C (Figure 2.3b, $p<0.001$). Corn AG litter had the highest recovery in mineral associated SOC at 28.0%, followed by miscanthus AG litter at 21.0%, corn BG litter at 18.0%, and miscanthus BG litter at 9.3% (Figure 2.3b).

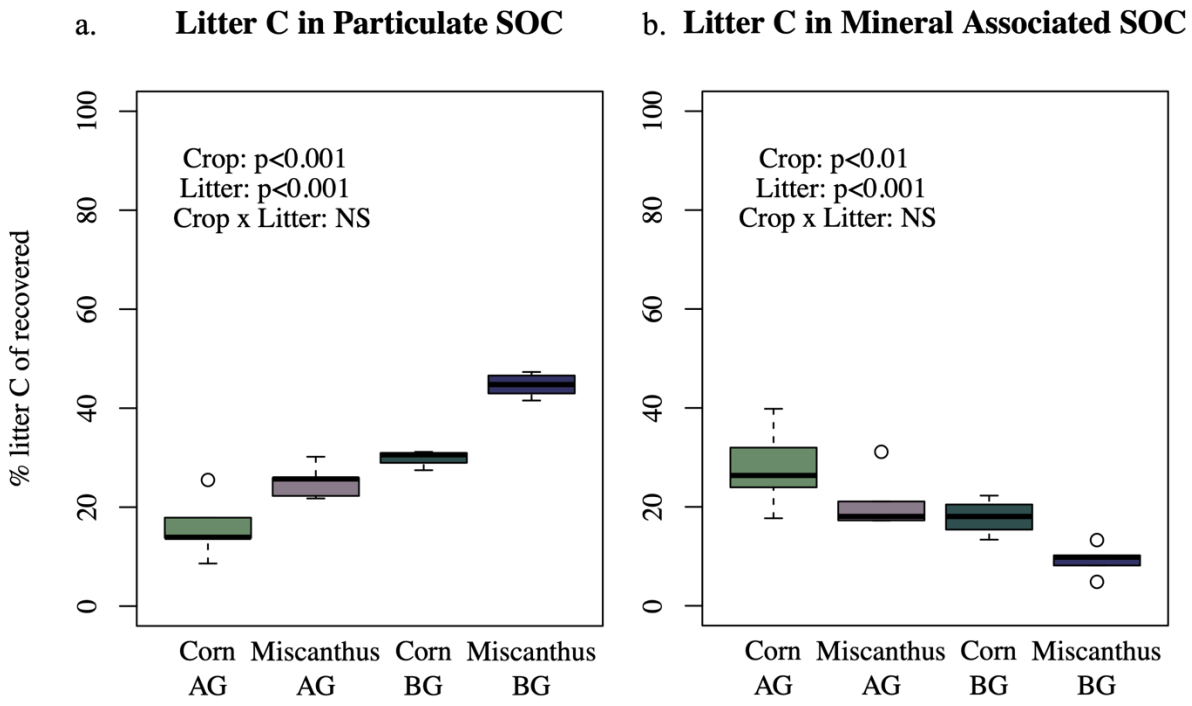

Fig. 2. 3: Litter C incorporated into **(a)** particulate SOC and **(b)** mineral associated SOC pools

Crop and litter type influence microbial carbon use efficiency

Microbial carbon use efficiency (CUE, equation 1) also differed by crop community and by added litter type. CUE was significantly higher for corn than miscanthus crops (p<0.001) and for AG than BG litters (p<0.001). Corn AG litter promoted the highest average CUE values at 0.41, followed by corn BG litter (0.33), miscanthus AG litter (0.31), and miscanthus BG litter (0.17) (Figure 2.4).

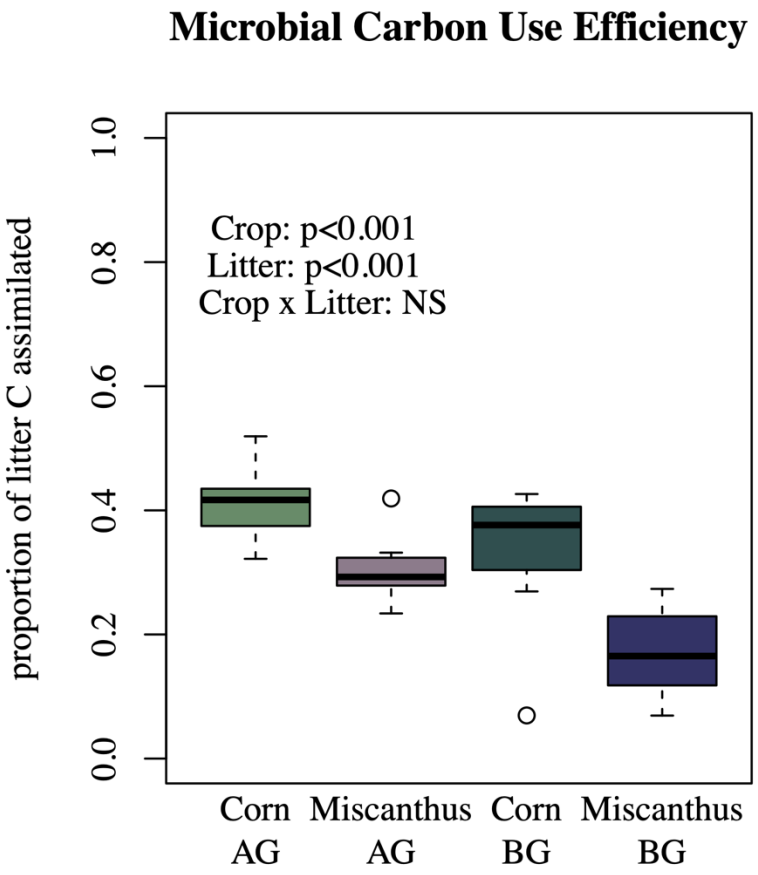

Fig. 2.4: Microbial CUE measured at the final timepoint

Modeled litter C fate is sensitive to microbial traits

When we simulated litter decomposition in the microcosms, we found that the CORPSE model approximately captured the balance of total C remaining in SOC vs. C lost to respiration (Figure 2.5a). However, the model could not represent the observed distribution between mineral associated and particulate SOC and underpredicted SOC protection in the lab (Figure 2.5b). In

the model, constrained microbial turnover and mineral protection are more representative of field processes and couldn't capture accelerated lab incubation processes.

To better represent processes in the lab, we modified model parameters influencing microbial turnover and protection rate of simple compounds and microbial necromass. Increasing turnover rates better reflected observations of more rapid microbial turnover in the lab and increasing protection better reflected the ability of simple carbon compounds to sorb to available mineral surfaces of sieved and homogenized soil. With these adjustments, the average modeled litter C protection for all treatments aligned with the average observations of litter C in mineral associated SOC. However, the model could not represent differences across the treatments and modeled predictions of litter C protection fell within a narrow range from 18.9-20.2%. Although these differences were minor, the model predicted the opposite trend as observed with highest litter C in mineral associated SOC for miscanthus belowground litters.

Finally, we incorporated our measurements of microbial differences in carbon use efficiency across the treatments. In the simulations with data-based parameters, model representations of litter C in microbial respiration slightly improved (Figure 2.5a) and modeled litter C protection became more representative of observations across the treatments. (Figure 2.5b).

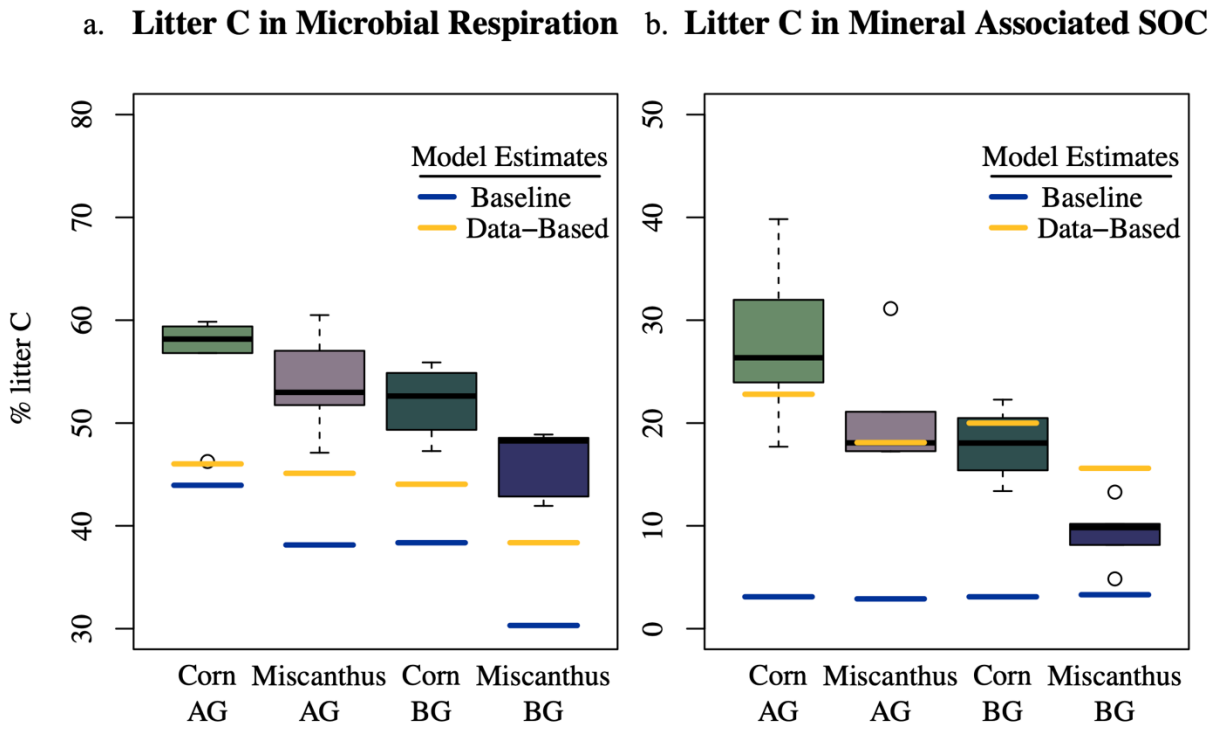

Fig. 2.5: Litter C that is **(a)** respired or **(b)** incorporated into mineral associated SOC in the lab (boxplots) vs. CORPSE model estimates using baseline parameters (blue) or data-based parameters (gold).

2.5 DISCUSSION:

Understanding how crops differ in particulate and mineral associated SOC is necessary to evaluate the potential for soils to serve as a C sink or source in bioenergy systems. Here, we quantified differences between bioenergy crops in the fate of their litters in soil. We demonstrate that crops differ significantly in the distribution of this C between SOC pools (Figure 2.3) with corn litter C forming more mineral associated SOC and less particulate SOC than miscanthus litter C. We also found that microbial carbon use efficiency mirrored these differences in the fate of corn and miscanthus litters (Figure 2.4). Finally, when we used our data to parameterize CORPSE, we found that the empirically constrained microbial decomposition parameters enable the model to better represent the observed differences in SOC pools (Figure 2.5). Overall, these results suggest that differences in litter chemistry between corn and miscanthus shape microbial decomposition traits. Importantly, this interaction appears to control the extent to which the litter of different bioenergy crops enters the particulate vs. mineral associated SOC pools and whether this new soil C is stable or vulnerable to future loss.

Our results indicate that the balance of litter C in the particulate vs. mineral associated SOC pools depends on crop type. Lower C:N corn litter inputs to particulate SOC had more recovery in mineral associated SOC at the end of the incubation compared to miscanthus litter C (Figure 2.3). By contrast, our results show that higher C:N litter from miscanthus preferentially remains in particulate SOC as undecomposed or partially decomposed litter fragments (Figure 2.3). This pattern supports our first hypothesis and aligns with recent theory (Lehmann & Kleber, 2015; Cotrufo et al., 2013) as well as our conceptual model (Figure 2.1). In addition, these differences in the fate of the litters are consequential because mineral associated SOC is

generally understood to persist longer than particulate SOC (Six et al., 2002; Kögel-Knabner et al., 2008; many others) while particulate SOC is potentially vulnerable to future loss with soil warming lowering activation energy barriers and enhancing enzyme activity (Conant et al., 2011; Benbi et al., 2014 but see Robinson et al., 2020). However, particulate SOC can accumulate with no apparent upper limit, while mineral associated SOC has been observed to saturate (Stewart et al., 2009; Cotrufo et al., 2019). With the advent of new feedstocks, particularly genetically modified versions, these results highlight the need to characterize the impact of new feedstocks on total soil C as well as the balance of particulate vs. mineral associated SOC.

Supporting hypothesis 2, we found that root litters formed less mineral associated SOC and more particulate SOC than leaf and shoot litters for both crops in our experiment. This pattern aligns with similar findings of greater mineral associated SOC formation from shoots vs. roots (Lavallee et al., 2018; Almeida et al., 2021) and likely reflects differences in the chemical composition and structure of roots vs. aboveground tissues. Root tissues tend to exhibit chemical characteristics that correlate with recalcitrance and the formation of particulate SOC (Kögel-Knabner, 2002; Geldner et al., 2013), including the presence of a casparian strip and higher concentrations of suberin or lignin (Hose et al., 2001; Rasse et al., 2005). In the field, this pattern may be enhanced due to feedstocks that promote root aggregation and the production of deep roots that enter soils with low microbial activity (Six et al., 2000; Hicks Pries et al., 2018). Opposingly, leaf and shoot litters in our incubation preferentially entered the mineral associated SOC pool (Figure 2.3b) owing to faster decomposition and higher microbial CUE relative to roots (Figure 2.4). In the field, leaving more aboveground residues and switching to no-till or reduced till may enhance the accumulation of mineral associated SOC in bioenergy systems. Overall, these results showing different fates for root and aboveground litters highlight the need

for models to have representations of root litter decomposition that are distinct from aboveground litters.

The correlation between CUE and mineral-associated SOC observed here (SI Figure 3) supports hypothesis 3 and may reflect important characteristics of our soils, including microbial communities, soil texture, and a history of C depletion. On the microbial side, functional differences in microbial communities between corn and miscanthus may have strengthened this link. Soil microbial communities have been observed to differ between corn and miscanthus agriculture (Mao et al., 2013; Cattaneo et al., 2014; Zhu et al., 2018; McGowan et al., 2019), but limited data exists that links microbial community structure with functional differences in how microbes alter soil C in bioenergy systems. Thus, directly investigating the function of different bioenergy soil microbial communities is a critical future research need. On the soil side, the availability of soil mineral surfaces controls the extent to which microbially-derived compounds can be protected from continuing uptake and recycling in mineral associated SOC (Castellano et al., 2015). The corn and miscanthus soils we used likely have a high capacity to form mineral associated SOC owing to a high clay content (~22%; Smith et al., 2013) and a history of intensive tillage. Our observations of rapid C accumulation in mineral associated SOC indicate that our soils remain below the maximum C saturation threshold. Given the prevalence of regions with similar land use history, there may remain considerable potential to enhance SOC using perennial bioenergy crops (Hudiburg et al., 2016; Bell et al., 2020; Ledo et al., 2020 but see Schlesinger & Amundson, 2019; Anderson et al., 2019 for contrasting opinions).

Collectively, our results indicate that miscanthus forms soil C differently than corn. Although we observe that corn has the potential in the lab to form more mineral associated SOC per gram litter C input, differences in the management and biology of these feedstocks in the

field likely limit the ability of corn to sequester soil C. By contrast, there are multiple plausible mechanisms for the potential we observed for miscanthus to form particulate and mineral associated SOC in the lab to be realized in the field. First, management differences between corn and miscanthus play a significant role in SOC formation and retention. For example, perennial miscanthus systems benefit from reduced disturbance compared with yearly planting and tillage regimes that destabilize SOC (Six et al., 1999). Thus, our lab observations of litter C incorporation into mineral associated SOC may not be realized over longer timespans in the field for corn systems. Second, miscanthus production leads to more plant inputs to soils each year (Heaton et al., 2010). More miscanthus C inputs not only could enhance particulate SOC but also could compensate for lower microbial efficiency or even promote mineral associated SOC formation (Witzgall et al., 2021). Third, miscanthus produces more extensive root systems than corn (Dohleman & Long, 2009), which may further drive SOC retention through a myriad of mechanisms (Poirier et al., 2018). Deeper and more extensive root systems lead to the deposition of root-derived C into soils with slower microbial processing and SOC turnover (Hicks Pries et al., 2018). Roots can also facilitate SOC retention through protection from decomposers within aggregates (Six et al., 2000) and through root exudation which promotes efficient microbial growth and mineral associated SOC formation (Sokol & Bradford, 2019). Although only measured at a single timepoint, our field observations of SOC demonstrate the potential of miscanthus to maintain mineral associated SOC and build particulate SOC stocks (SI Figure 1). Importantly, transitioning to crops that can more effectively build particulate and mineral associated SOC could help meet the critical need to rapidly accumulate SOC, even in less persistent forms (Matthews et al., 2022).

While there are some artifacts associated with our use of soil incubations, these incubation experiments are still useful for identifying mechanisms that can inform our predictive understanding of how bioenergy crops impact SOC stabilization. The duration of an incubation experiment can affect the magnitude of litter that remains in soil or is respired. We acknowledge that there is the potential for processes like abiotic sorption or microbial recycling to alter the fate of litter C in long-term incubations. Moreover, we acknowledge that our 12-week incubation does not reflect soil C cycling processes that operate over decades or centuries. Given the stabilization of respiration (Figure 2.2b), our incubation is likely more indicative of intermediate litter decay. However, our recovery of added litter C in mineral associated SOC ranged from 5% to 40%, which suggests that our incubation was long enough to test the mechanisms in our conceptual model and supports recent empirical evidence that mineral associated SOC is more dynamic than previously thought (e.g., Keiluweit et al., 2015; Jilling et al., 2018, 2021; Fossum et al., 2022). We also note that there is the potential for differences we observed between our treatments in the ratio of particulate to mineral associated SOC formation (Figure 2.3) could change over time. A shift in these ratios is unlikely though because it would require a dramatic shift in microbial carbon use efficiency and in the proportion of mineral associated SOC formed vs CO_2 respired from the litter inputs (SI Figure 2). In support, observational evidence shows that litters that initially decompose rapidly lead to a higher mineral associated to particulate SOC ratio over ~100 years of ecosystem development than those that decompose slowly (Craig et al., 2018).

In addition to the length of the incubation, we also acknowledge that how we measured and modeled CUE could influence the interpretation of our results and our modeling efforts. On the measurements side, using the endpoint and not cumulative measurements of microbial

biomass and respiration to calculate a proxy for CUE relies on assumptions of rapid microbial turnover (~ 1 week vs. 3 months) that we were unable to directly measure. However, we emphasize the utility of this trait as a comparative rather than absolute value. The significant correlation between microbial CUE and mineral associated SOC (SI Figure 3) supports the theory that microbial efficiency drives mineral stabilization (Cotrufo et al., 2013). On the modeling side, we acknowledge that measurements of microbial decomposition, microbial CUE, and mineral associated SOC formation likely reflect optimal or potential rates rather than realistic processes in the field. Rather than reducing the applicability of our work, potential rates are often easier to integrate into microbial models. For example, in the COPRSE model, microbial parameters (e.g.,, maximum enzymatic decomposition rates, CUE) generally represent theoretical maximums which are scaled down by influential factors like temperature, soil moisture, and soil porosity (Sulman et al., 2014). Despite these limitations, our work lays the foundation for future empirical and modelling efforts to investigate how fluctuations in microclimate and living roots and mycorrhizal fungi impact the formation of new SOC in situ for bioenergy cultivation.

Soil biogeochemical models represent plant traits, but often lack similar detail on how plant traits influence microbial traits that control soil organic matter dynamics (Kallenbach et al., 2016; Domeignoz-Horta et al., 2021). Even models that explicitly represent microbial traits often rely on tuned or poorly constrained microbial parameters (Craig et al., 2021). Here, our model exercise shows that lab measurements of microbial carbon use efficiency have the potential to constrain model parameters and improve representations of the distribution of new C inputs between particulate and mineral associated SOC. When we attempted to capture our incubation results with only plant litter chemistry differences, the model failed to capture the distribution of

litter C that entered particulate vs. mineral associated SOC (Figure 2.5b, baseline parameters). By contrast, when we updated parameters that are directly or indirectly controlled by microbial traits (i.e., CUE, turnover, protection rate), the model better captured the entire fate of the litter (Figure 2.5b, data-based parameters). However, we note that only CUE was constrained by direct measurements. The finding that we also needed to adjust parameters that controlled the protection rate and microbial turnover highlight important avenues for future empirical research to inform models. For example, our assumption that microbial turnover was the same across treatments shows a clear need for empirical efforts to examine how turnover varies across gradients in soil chemistry, microbial communities, and plant communities due to the relative importance of this trait (Sokol et al., 2022). While limited, our modeling exercise indicates that linking measurements of microbial traits with SOC formation in the lab and in the field is critical to improving our predictive understanding of the potential for bioenergy soils to sequester C.

Collectively, our results suggest that bioenergy crops differ in the mechanisms by which their litters form new SOC, which can inform ecosystem model projections of how, why, and to what extent bioenergy crops can slow climate change. Importantly, we show a mechanistic link between plant litter quality (i.e., C:N ratio, lignin content), microbial carbon use efficiency, and mineral associated SOC formation. Corn litters decomposed faster, led to higher microbial CUE, and formed more mineral associated SOC than miscanthus litters. While this result may suggest that corn cultivation leads to more stable mineral associated SOC than miscanthus cultivation; the lack of tillage, high root C inputs, and the ability of miscanthus inputs to form substantial particulate SOC (Figure 2.3a), suggest that miscanthus cultivation can be an effective way to build overall soil C stocks. As such, efforts that focus solely on building mineral associated SOC

neglect the ability of perennial bioenergy grasses to rapidly build particulate SOC and slow climate change.

2.6 Literature Cited

Abiven, S., Heim, A., & Schmidt, M. W. I. (2011). Lignin content and chemical characteristics in maize and wheat vary between plant organs and growth stages: Consequences for assessing lignin dynamics in soil. *Plant and Soil*, *343*(1), 369–378. https://doi.org/10.1007/s11104-011-0725-y

Almeida, L. F. J., Souza, I. F., Hurtarte, L. C. C., Teixeira, P. P. C., Inagaki, T. M., Silva, I. R., & Mueller, C. W. (2021). Forest litter constraints on the pathways controlling soil organic matter formation. *Soil Biology and Biochemistry*, *163*, 108447. https://doi.org/10.1016/j.soilbio.2021.108447

Anderson, C. M., DeFries, R. S., Litterman, R., Matson, P. A., Nepstad, D. C., Pacala, S., Schlesinger, W. H., Shaw, M. R., Smith, P., Weber, C., & Field, C. B. (2019). Natural climate solutions are not enough. *Science*, *363*(6430), 933–934. https://doi.org/10.1126/science.aaw2741

Anderson-Teixeira, K. J., Masters, M. D., Black, C. K., Zeri, M., Hussain, M. Z., Bernacchi, C. J., & DeLucia, E. H. (2013). Altered belowground carbon cycling following land-use change to perennial bioenergy crops. *Ecosystems*, *16*(3), 508–520. https://doi.org/10.1007/s10021-012-9628-x

Angst, G., Mueller, K. E., Nierop, K. G. J., & Simpson, M. J. (2021). Plant- or microbial-derived? A review on the molecular composition of stabilized soil organic matter. *Soil Biology and Biochemistry*, *156*, 108189. https://doi.org/10.1016/j.soilbio.2021.108189

Bell, S. M., Barriocanal, C., Terrer, C., & Rosell-Melé, A. (2020). Management opportunities for soil carbon sequestration following agricultural land abandonment. *Environmental Science & Policy*, *108*, 104–111. https://doi.org/10.1016/j.envsci.2020.03.018

Benbi, D. K., Boparai, A. K., & Brar, K. (2014). Decomposition of particulate organic matter is more sensitive to temperature than the mineral associated organic matter. *Soil Biology and Biochemistry*, *70*, 183–192. https://doi.org/10.1016/j.soilbio.2013.12.032

Berardi, D., Brzostek, E., Blanc-Betes, E., Davison, B., DeLucia, E. H., Hartman, M. D., Kent, J., Parton, W. J., Saha, D., & Hudiburg, T. W. (2020). 21st-century biogeochemical modeling: Challenges for Century-based models and where do we go from here? *GCB Bioenergy*, *12*(10), 774–788. https://doi.org/10.1111/gcbb.12730

Bradford, M. A., Keiser, A. D., Davies, C. A., Mersmann, C. A., & Strickland, M. S. (2013). Empirical evidence that soil carbon formation from plant inputs is positively related to microbial growth. *Biogeochemistry*, *113*(1), 271–281. https://doi.org/10.1007/s10533-012-9822-0

Brancourt-Hulmel, M., Arnoult, S., Cézard, L., El Hage, F., Gineau, E., Girones, J., Griveau, Y., Jacquemont, M.-P., Jaffuel, S., Mignot, E., Mouille, G., Lapierre, C., Legée, F., Méchin, V., Navard, P., Vo, L. T. T., & Reymond, M. (2022). A comparative study of maize and miscanthus regarding cell-wall composition and stem anatomy for conversion into

bioethanol and polymer composites. *BioEnergy Research*, *15*(2), 777–791. https://doi.org/10.1007/s12155-020-10239-z

Carvalho, J. L. N., Hudiburg, T. W., Franco, H. C. J., & DeLucia, E. H. (2017). Contribution of above- and belowground bioenergy crop residues to soil carbon. *GCB Bioenergy*, *9*(8), 1333–1343. https://doi.org/10.1111/gcbb.12411

Castellano, M. J., Mueller, K. E., Olk, D. C., Sawyer, J. E., & Six, J. (2015). Integrating plant litter quality, soil organic matter stabilization, and the carbon saturation concept. *Global Change Biology*, *21*(9), 3200–3209. https://doi.org/10.1111/gcb.12982

Cattaneo, F., Di Gennaro, P., Barbanti, L., Giovannini, C., Labra, M., Moreno, B., Benitez, E., & Marzadori, C. (2014). Perennial energy cropping systems affect soil enzyme activities and bacterial community structure in a South European agricultural area. *Applied Soil Ecology*, *84*, 213–222. https://doi.org/10.1016/j.apsoil.2014.08.003

Cherubini, F., Bird, N. D., Cowie, A., Jungmeier, G., Schlamadinger, B., & Woess-Gallasch, S. (2009). Energy- and greenhouse gas-based LCA of biofuel and bioenergy systems: Key issues, ranges and recommendations. *Resources, Conservation and Recycling*, *53*(8), 434–447. https://doi.org/10.1016/j.resconrec.2009.03.013

Conant, R. T., Ryan, M. G., Ågren, G. I., Birge, H. E., Davidson, E. A., Eliasson, P. E., Evans, S. E., Frey, S. D., Giardina, C. P., Hopkins, F. M., Hyvönen, R., Kirschbaum, M. U. F., Lavallee, J. M., Leifeld, J., Parton, W. J., Megan Steinweg, J., Wallenstein, M. D., Martin Wetterstedt, J. Å., & Bradford, M. A. (2011). Temperature and soil organic matter decomposition rates – synthesis of current knowledge and a way forward. *Global Change Biology*, *17*(11), 3392–3404. https://doi.org/10.1111/j.1365-2486.2011.02496.x

Cotrufo, M. F., Ranalli, M. G., Haddix, M. L., Six, J., & Lugato, E. (2019). Soil carbon storage informed by particulate and mineral-associated organic matter. *Nature Geoscience*, *12*(12), 989–994. https://doi.org/10.1038/s41561-019-0484-6

Cotrufo, M. F., Wallenstein, M. D., Boot, C. M., Denef, K., & Paul, E. (2013). The Microbial Efficiency-Matrix Stabilization (MEMS) framework integrates plant litter decomposition with soil organic matter stabilization: Do labile plant inputs form stable soil organic matter? *Global Change Biology*, *19*(4), 988–995. https://doi.org/10.1111/gcb.12113

Craig, M. E., Mayes, M. A., Sulman, B. N., & Walker, A. P. (2021). Biological mechanisms may contribute to soil carbon saturation patterns. *Global Change Biology*, *27*(12), 2633–2644. https://doi.org/10.1111/gcb.15584

Craig, M. E., Turner, B. L., Liang, C., Clay, K., Johnson, D. J., & Phillips, R. P. (2018). Tree mycorrhizal type predicts within-site variability in the storage and distribution of soil organic matter. *Global Change Biology*, *24*(8), 3317–3330.

Davidson, E. A., & Janssens, I. A. (2006). Temperature sensitivity of soil carbon decomposition and feedbacks to climate change. *Nature*, *440*(7081), 165–173. https://doi.org/10.1038/nature04514

Dohleman, F. G., & Long, S. P. (2009). More productive Than maize in the Midwest: how does miscanthus do it? *Plant Physiology*, *150*(4), 2104–2115. https://doi.org/10.1104/pp.109.139162

Domeignoz-Horta, L. A., Shinfuku, M., Junier, P., Poirier, S., Verrecchia, E., Sebag, D., & DeAngelis, K. M. (2021). Direct evidence for the role of microbial community

composition in the formation of soil organic matter composition and persistence. *ISME Communications*, *1*(1), 1–4. https://doi.org/10.1038/s43705-021-00071-7

Doyle, A., Weintraub, M. N., & Schimel, J. P. (2004). Persulfate digestion and simultaneous colorimetric analysis of carbon and nitrogen in soil extracts. *Soil Science Society of America Journal*, *68*(2), 669–676. https://doi.org/10.2136/sssaj2004.6690

Fossum, C., Estera-Molina, K. Y., Yuan, M., Herman, D. J., Chu-Jacoby, I., Nico, P. S., Morrison, K. D., Pett-Ridge, J., & Firestone, M. K. (2022). Belowground allocation and dynamics of recently fixed plant carbon in a California annual grassland. *Soil Biology and Biochemistry*, *165*, 108519. https://doi.org/10.1016/j.soilbio.2021.108519

Fulton-Smith, S., & Cotrufo, M. F. (2019). Pathways of soil organic matter formation from above and belowground inputs in a *Sorghum bicolor* bioenergy crop. *GCB Bioenergy*, *11*(8), 971–987. https://doi.org/10.1111/gcbb.12598

Geldner, N. (2013). The Endodermis. *Annual Review of Plant Biology*, *64*(1), 531–558. https://doi.org/10.1146/annurev-arplant-050312-120050

Geyer, K. M., Dijkstra, P., Sinsabaugh, R., & Frey, S. D. (2019). Clarifying the interpretation of carbon use efficiency in soil through methods comparison. *Soil Biology and Biochemistry*, *128*, 79–88. https://doi.org/10.1016/j.soilbio.2018.09.036

Heaton, E. A., Dohleman, F. G., & Long, S. P. (2008). Meeting US biofuel goals with less land: The potential of Miscanthus. *Global Change Biology*, *14*(9), 2000–2014. https://doi.org/10.1111/j.1365-2486.2008.01662.x

Heaton, E. A., Dohleman, F. G., Miguez, A. F., Juvik, J. A., Lozovaya, V., Widholm, J., Zabotina, O. A., McIsaac, G. F., David, M. B., Voigt, T. B., Boersma, N. N., & Long, S.

P. (2010). Chapter 3 - Miscanthus: A Promising Biomass Crop. In J.-C. Kader & M. Delseny (Eds.), *Advances in Botanical Research* (Vol. 56, pp. 75–137). Academic Press. https://doi.org/10.1016/B978-0-12-381518-7.00003-0

Hicks Pries, C. E., Sulman, B. N., West, C., O'Neill, C., Poppleton, E., Porras, R. C., Castanha, C., Zhu, B., Wiedemeier, D. B., & Torn, M. S. (2018). Root litter decomposition slows with soil depth. *Soil Biology and Biochemistry*, *125*, 103–114. https://doi.org/10.1016/j.soilbio.2018.07.002

Hose, E., Clarkson, D. T., Steudle, E., Schreiber, L., & Hartung, W. (2001). The exodermis: A variable apoplastic barrier. *Journal of Experimental Botany*, *52*(365), 2245–2264. https://doi.org/10.1093/jexbot/52.365.2245

Hudiburg, T. W., Wang, W., Khanna, M., Long, S. P., Dwivedi, P., Parton, W. J., Hartman, M., & DeLucia, E. H. (2016). Impacts of a 32-billion-gallon bioenergy landscape on land and fossil fuel use in the US. *Nature Energy*, *1*(1), 1–7. https://doi.org/10.1038/nenergy.2015.5

Jilling, A., Keiluweit, M., Contosta, A. R., Frey, S., Schimel, J., Schnecker, J., Smith, R. G., Tiemann, L., & Grandy, A. S. (2018). Minerals in the rhizosphere: Overlooked mediators of soil nitrogen availability to plants and microbes. *Biogeochemistry*, *139*(2), 103–122. https://doi.org/10.1007/s10533-018-0459-5

Jilling, A., Keiluweit, M., Gutknecht, J. L., & Grandy, A. S. (2021). Priming mechanisms providing plants and microbes access to mineral-associated organic matter. *Soil Biology and Biochemistry*, *158*, 108265.

Juice, S. M., Walter, C. A., Allen, K. E., Berardi, D. M., Hudiburg, T. W., Sulman, B. N., & Brzostek, E. R. (2022). A new bioenergy model that simulates the impacts of plant-microbial interactions, soil carbon protection, and mechanistic tillage on soil carbon cycling. *GCB Bioenergy*, *n/a*(n/a). https://doi.org/10.1111/gcbb.12914

Kallenbach, C. M., Frey, S. D., & Grandy, A. S. (2016). Direct evidence for microbial-derived soil organic matter formation and its ecophysiological controls. *Nature Communications*, *7*(1), 13630. https://doi.org/10.1038/ncomms13630

Kantola, I. B., Masters, M. D., Blanc-Betes, E., Gomez-Casanovas, N., & DeLucia, E. H. (2022). Long-term yields in annual and perennial bioenergy crops in the Midwestern United States. *GCB Bioenergy*, *14*(6), 694–706. https://doi.org/10.1111/gcbb.12940

Keiluweit, M., Bougoure, J. J., Nico, P. S., Pett-Ridge, J., Weber, P. K., & Kleber, M. (2015). Mineral protection of soil carbon counteracted by root exudates. *Nature Climate Change*, *5*(6), 588–595. https://doi.org/10.1038/nclimate2580

Koch, B. J., McHugh, T. A., Hayer, M., Schwartz, E., Blazewicz, S. J., Dijkstra, P., van Gestel, N., Marks, J. C., Mau, R. L., Morrissey, E. M., Pett-Ridge, J., & Hungate, B. A. (2018). Estimating taxon-specific population dynamics in diverse microbial communities. *Ecosphere*, *9*(1), e02090. https://doi.org/10.1002/ecs2.2090

Kögel-Knabner, I. (2002). The macromolecular organic composition of plant and microbial residues as inputs to soil organic matter. *Soil Biology and Biochemistry*, *34*(2), 139–162. https://doi.org/10.1016/S0038-0717(01)00158-4

Kögel-Knabner, I., Guggenberger, G., Kleber, M., Kandeler, E., Kalbitz, K., Scheu, S., Eusterhues, K., & Leinweber, P. (2008). Organo-mineral associations in temperate soils:

Integrating biology, mineralogy, and organic matter chemistry. *Journal of Plant Nutrition and Soil Science*, *171*(1), 61–82. https://doi.org/10.1002/jpln.200700048

Kramer, M. G., Sanderman, J., Chadwick, O. A., Chorover, J., & Vitousek, P. M. (2012). Long-term carbon storage through retention of dissolved aromatic acids by reactive particles in soil. *Global Change Biology*, *18*(8), 2594–2605. https://doi.org/10.1111/j.1365-2486.2012.02681.x

Lavallee, J. M., Conant, R. T., Paul, E. A., & Cotrufo, M. F. (2018). Incorporation of shoot versus root-derived 13C and 15N into mineral-associated organic matter fractions: Results of a soil slurry incubation with dual-labelled plant material. *Biogeochemistry*, *137*(3), 379–393. https://doi.org/10.1007/s10533-018-0428-z

Lavallee, J. M., Soong, J. L., & Cotrufo, M. F. (2020). Conceptualizing soil organic matter into particulate and mineral-associated forms to address global change in the 21st century. *Global Change Biology*, *26*(1), 261–273. https://doi.org/10.1111/gcb.14859

Ledo, A., Smith, P., Zerihun, A., Whitaker, J., Vicente-Vicente, J. L., Qin, Z., McNamara, N. P., Zinn, Y. L., Llorente, M., Liebig, M., Kuhnert, M., Dondini, M., Don, A., Diaz-Pines, E., Datta, A., Bakka, H., Aguilera, E., & Hillier, J. (2020). Changes in soil organic carbon under perennial crops. *Global Change Biology*, *26*(7), 4158–4168. https://doi.org/10.1111/gcb.15120

Lehmann, J., & Kleber, M. (2015). The contentious nature of soil organic matter. *Nature*, *528*(7580), 60–68. https://doi.org/10.1038/nature16069

Liang, C., Schimel, J. P., & Jastrow, J. D. (2017). The importance of anabolism in microbial control over soil carbon storage. *Nature Microbiology*, *2*(8), 1–6. https://doi.org/10.1038/nmicrobiol.2017.105

Lugato, Emanuele, Lavallee, Jocelyn, Haddix, Michelle, Panagos, Panos, & Cotrufo, Francesca. (2021). Different climate sensitivity of particulate and mineral-associated soil organic matter. *Nature Geoscience*, *14*, 295–300.

Mao, Y., Yannarell, A. C., Davis, S. C., & Mackie, R. I. (2013). Impact of different bioenergy crops on N-cycling bacterial and archaeal communities in soil. *Environmental Microbiology*, *15*(3), 928–942. https://doi.org/10.1111/j.1462-2920.2012.02844.x

Matthews, H. D., Zickfeld, K., Dickau, M., MacIsaac, A. J., Mathesius, S., Nzotungicimpaye, C.-M., & Luers, A. (2022). Temporary nature-based carbon removal can lower peak warming in a well-below 2°C scenario. *Communications Earth & Environment*, *3*(1), 1–8. https://doi.org/10.1038/s43247-022-00391-z

McGowan, A. R., Nicoloso, R. S., Diop, H. E., Roozeboom, K. L., & Rice, C. W. (2019). Soil Organic Carbon, Aggregation, and Microbial Community Structure in Annual and Perennial Biofuel Crops. *Agronomy Journal*, *111*(1), 128–142. https://doi.org/10.2134/agronj2018.04.0284

Meineke, T., Manisseri, C., & Voigt, C. A. (2014). Phylogeny in Defining Model Plants for Lignocellulosic Ethanol Production: A Comparative Study of *Brachypodium distachyon*, Wheat, Maize, and *Miscanthus x giganteus* Leaf and Stem Biomass. *PLOS ONE*, *9*(8), e103580. https://doi.org/10.1371/journal.pone.0103580

Morrissey, E. M., Mau, R. L., Schwartz, E., McHugh, T. A., Dijkstra, P., Koch, B. J., Marks, J. C., & Hungate, B. A. (2017). Bacterial carbon use plasticity, phylogenetic diversity and the priming of soil organic matter. *The ISME Journal*, *11*(8), 1890–1899.

Poirier, V., Roumet, C., & Munson, A. D. (2018). The root of the matter: Linking root traits and soil organic matter stabilization processes. *Soil Biology and Biochemistry*, *120*, 246–259. https://doi.org/10.1016/j.soilbio.2018.02.016

Rasse, D. P., Rumpel, C., & Dignac, M.-F. (2005). Is soil carbon mostly root carbon? Mechanisms for a specific stabilisation. *Plant and Soil*, *269*(1), 341–356. https://doi.org/10.1007/s11104-004-0907-y

Robertson, A. D., Paustian, K., Ogle, S., Wallenstein, M. D., Lugato, E., & Cotrufo, M. F. (2019). Unifying soil organic matter formation and persistence frameworks: The MEMS model. *Biogeosciences*, *16*(6), 1225–1248. https://doi.org/10.5194/bg-16-1225-2019

Robinson, J. M., Barker, S. L. L., Arcus, V. L., McNally, S. R., & Schipper, L. A. (2020). Contrasting temperature responses of soil respiration derived from soil organic matter and added plant litter. *Biogeochemistry*, *150*(1), 45–59. https://doi.org/10.1007/s10533-020-00686-3

Sanderman, J., Maddern, T., & Baldock, J. (2014). Similar composition but differential stability of mineral retained organic matter across four classes of clay minerals. *Biogeochemistry*, *121*(2), 409–424. https://doi.org/10.1007/s10533-014-0009-8

Sands, R., Malcolm, S., Suttles, S., & Marshall, E. (2009) *Dedicated Energy Crops and Competition for Agricultural Land*. Retrieved March 18, 2022, from http://www.ers.usda.gov/publications/pub-details/?pubid=81902

Schlesinger, W. H., & Amundson, R. (2019). Managing for soil carbon sequestration: Let's get realistic. *Global Change Biology*, *25*(2), 386–389. https://doi.org/10.1111/gcb.14478

Six, J., Conant, R. T., Paul, E. A., & Paustian, K. (2002). Stabilization mechanisms of soil organic matter: Implications for C-saturation of soils. *Plant and Soil*, *241*(2), 155–176. https://doi.org/10.1023/A:1016125726789

Six, J., Elliott, E. T., & Paustian, K. (1999). Aggregate and Soil Organic Matter Dynamics under Conventional and No-Tillage Systems. *Soil Science Society of America Journal*, *63*(5), 1350–1358. https://doi.org/10.2136/sssaj1999.6351350x

Six, J., Elliott, E. T., & Paustian, K. (2000). Soil macroaggregate turnover and microaggregate formation: A mechanism for C sequestration under no-tillage agriculture. *Soil Biology and Biochemistry*, *32*(14), 2099–2103. https://doi.org/10.1016/S0038-0717(00)00179-6

Smith, C. M., David, M. B., Mitchell, C. A., Masters, M. D., Anderson-Teixeira, K. J., Bernacchi, C. J., & DeLucia, E. H. (2013). Reduced Nitrogen Losses after Conversion of Row Crop Agriculture to Perennial Biofuel Crops. *Journal of Environmental Quality*, *42*(1), 219–228. https://doi.org/10.2134/jeq2012.0210

Sokol, N. W., & Bradford, M. A. (2019). Microbial formation of stable soil carbon is more efficient from belowground than aboveground input. *Nature Geoscience*, *12*(1), 46–53. https://doi.org/10.1038/s41561-018-0258-6

Sokol, N. W., Slessarev, E., Marschmann, G. L., Nicolas, A., Blazewicz, S. J., Brodie, E. L., Firestone, M. K., Foley, M. M., Hestrin, R., Hungate, B. A., Koch, B. J., Stone, B. W., Sullivan, M. B., Zablocki, O., & Pett-Ridge, J. (2022). Life and death in the soil

microbiome: How ecological processes influence biogeochemistry. *Nature Reviews Microbiology*, 1–16. https://doi.org/10.1038/s41579-022-00695-z

Stewart, C. E., Paustian, K., Conant, R. T., Plante, A. F., & Six, J. (2009). Soil carbon saturation: Implications for measurable carbon pool dynamics in long-term incubations. *Soil Biology and Biochemistry*, *41*(2), 357–366. https://doi.org/10.1016/j.soilbio.2008.11.011

Sulman, B. N., Phillips, R. P., Oishi, A. C., Shevliakova, E., & Pacala, S. W. (2014). Microbe-driven turnover offsets mineral-mediated storage of soil carbon under elevated CO2. *Nature Climate Change*, *4*(12), 1099–1102. https://doi.org/10.1038/nclimate2436

Vance, E. D., Brookes, P. C., & Jenkinson, D. S. (1987). An extraction method for measuring soil microbial biomass C. *Soil Biology and Biochemistry*, *19*(6), 703–707. https://doi.org/10.1016/0038-0717(87)90052-6

Wang, C., Qu, L., Yang, L., Liu, D., Morrissey, E., Miao, R., Liu, Z., Wang, Q., Fang, Y., & Bai, E. (2021). Large-scale importance of microbial carbon use efficiency and necromass to soil organic carbon. *Global Change Biology*, *27*(10), 2039–2048. https://doi.org/10.1111/gcb.15550

Wieder, W. R., Grandy, A. S., Kallenbach, C. M., & Bonan, G. B. (2014). Integrating microbial physiology and physio-chemical principles in soils with the MIcrobial-MIneral Carbon Stabilization (MIMICS) model. *Biogeosciences*, *11*(14), 3899–3917. https://doi.org/10.5194/bg-11-3899-2014

Williams, E. K., Fogel, M. L., Berhe, A. A., & Plante, A. F. (2018). Distinct bioenergetic signatures in particulate versus mineral-associated soil organic matter. *Geoderma*, *330*, 107–116. https://doi.org/10.1016/j.geoderma.2018.05.024

Witt, C., Gaunt, J. L., Galicia, C. C., Ottow, J. C. G., & Neue, H.-U. (2000). A rapid chloroform-fumigation extraction method for measuring soil microbial biomass carbon and nitrogen in flooded rice soils. *Biology and Fertility of Soils*, *30*(5), 510–519. https://doi.org/10.1007/s003740050030

Witzgall, K., Vidal, A., Schubert, D. I., Höschen, C., Schweizer, S. A., Buegger, F., Pouteau, V., Chenu, C., & Mueller, C. W. (2021). Particulate organic matter as a functional soil component for persistent soil organic carbon. *Nature Communications*, *12*(1), 4115. https://doi.org/10.1038/s41467-021-24192-8

Zhu, X., Liang, C., Masters, M. D., Kantola, I. B., & DeLucia, E. H. (2018). The impacts of four potential bioenergy crops on soil carbon dynamics as shown by biomarker analyses and DRIFT spectroscopy. *Global Change Biology Bioenergy*, *10*(7), 489–500. https://doi.org/10.1111/gcbb.12520

Chapter 3: Roots selectively decompose litter to acquire nitrogen and build new soil carbon

Reprinted from: ***J. Ridgeway****, J. Kane, H. Starcher, E.M. Morrissey, and E.R. Brzostek. Roots selectively decompose litter to acquire nitrogen and build new soil carbon. In press, Ecology Letters*

3.1 Abstract:

Plant-microbe interactions in the rhizosphere shape carbon and nitrogen cycling in soil organic matter (SOM). However, there is conflicting evidence on whether these interactions lead to a net loss or increase of SOM. In part, this conflict is driven by uncertainty in how living roots and microbes alter SOM formation or loss in the field. To address these uncertainties, we traced the fate of isotopically labeled litter into SOM using root and fungal ingrowth cores incubated in a *Miscanthus x giganteus* field. Roots stimulated litter decomposition, but balanced this loss by transferring carbon into more persistent, aggregate associated SOM. Further, roots selectively mobilized nitrogen from litter without additional carbon release. Overall, our fundings suggest that roots can efficiently mine nitrogen and build persistent soil carbon.

3.2 Introduction:

Managing soils in agricultural systems to sequester carbon (C) in soil organic matter (SOM) may be a powerful approach to offset anthropogenic C emissions (Lal, 2004). Soils are the largest terrestrial C pool, and experimental manipulations such as changing vegetation type, increasing organic inputs, or altering management practices demonstrate the potential for significant and rapid SOM accumulation (Minasny et al., 2017; Paustian et al., 2016). However, there is a high degree of uncertainty in understanding, predicting, and optimizing soil C accumulation (Sulman et al., 2018). Much of this uncertainty arises because plant roots and soil microbes, the active drivers of soil biogeochemical cycling, both build and deplete SOM through simultaneously occurring processes. As such, our ability to optimize soil C sequestration relies on improving our understanding of how roots and microbes drive the transfer of new litter C inputs into SOM.

As per the current understanding of SOM formation, litter inputs are decomposed into simpler compounds that can be physically protected from microbial decomposers by occlusion in soil aggregates or sorption to mineral surfaces (Lehmann & Kleber, 2015). As such, SOM is often delineated into three main pools (Fig. 3.1a): undecomposed or partially-decomposed particulate organic matter (here, light POM), aggregate-occluded SOM (here, heavy POM), and mineral associated organic matter (MAOM) (Lavallee et al., 2020). Light POM accumulation depends upon the balance between litter inputs to soil and litter decomposition, and can accumulate with no apparent upper limit but is also vulnerable to factors like warming that enhance decomposition rates (Benbi et al., 2014; Cotrufo et al., 2019). Heavy POM is operationally separated from light POM by density fractionation and is linked with stable soil

aggregates (Lavallee et al., 2020). Accumulation in this pool may saturate and is vulnerable to factors like soil disturbance and land use change (Bronick & Lal, 2005). MAOM is generally considered to be the most persistent or protected form of SOM (Cotrufo et al., 2013; Liang et al., 2017). However, optimizing MAOM accumulation may only be practical in soils like those in degraded agricultural ecosystems that have lost nearly 50% of their C since ploughing the prairie (Stockmann et al., 2015), as MAOM accumulation appears to saturate (Cotrufo et al., 2019; but see Georgiou et al., 2022). To manage ecosystems for soil C sequestration, it is critical to understand what drives the transfer of new litter inputs between these SOM pools to enhance our predictive understanding of how much soil C can accumulate and how persistent this soil C may be in a changing climate.

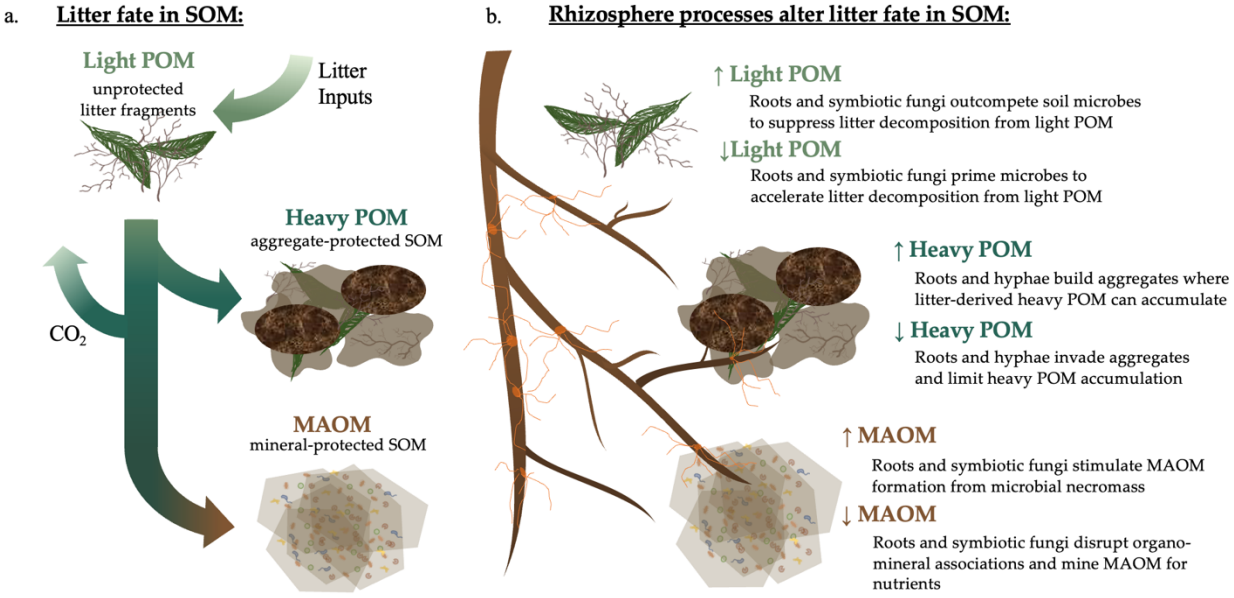

Fig. 3. 1**a:** Litter inputs join SOM as light POM, which is largely composed of undecomposed litter fragments. As decomposition progresses, litter-derived SOM can more easily become incorporated into aggregates in heavy POM or microbial decomposition products and necromass can preferentially sorb to soil mineral surfaces as MAOM. 3.1**b:** Roots and root-associated fungal symbionts can enhance both retention or loss of litter in light POM (top), heavy POM (middle), and MAOM (bottom) pools.

Living roots and their associated fungi alter SOM formation by sending C-rich exudates to the rhizosphere to enhance decomposition and acquire N (Bais et al., 2006; Grayston et al., 1997). However, a high degree of uncertainty remains in whether this increases or decreases soil C accumulation. In Figure 3.1b, we diagram potential hypotheses for how roots could alter litter loss from light POM and the accumulation of new heavy POM and MAOM through distinct mechanisms. First, root stimulation of microbial decomposition to mineralize soil N can increase the loss of unprotected light POM through the rhizosphere priming effect (Cheng et al., 2014). However, there is also evidence that roots and symbiotic fungi can outcompete saprotrophic microbes for resources like water and nutrients leading to the suppression of decomposition (Fernandez & Kennedy, 2016). Second, as litter inputs are transferred into more protected heavy POM, root ingrowth has the potential to both invade aggregates and increase the formation rate of new aggregates (Six, Paustian, et al., 2000). Finally, roots can enhance new MAOM formation by increasing the efficiency of microbial litter decomposition, resulting in greater microbial biomass production and the formation of microbial necromass (Liang et al., 2017). This necromass can associate with mineral surfaces and is the main precursor to MAOM in grassland ecosystems (Angst et al., 2021). However, roots may also deplete new, litter-derived MAOM as recent evidence suggests that roots can actively mine MAOM for nutrients (Jilling et al., 2021) and that root exudate compounds can displace MAOM from soil minerals (Keiluweit et al., 2015). As such, predicting whether roots will drive a net gain or loss of soil C is hindered by uncertainty in how roots impact SOM formation in these different pools.

The extent to which roots and mycorrhizal fungi facilitate SOM formation or loss in agricultural ecosystems may be modulated by fertilization. For example, some N-limited plants

can dynamically shift C allocation belowground to root exudation and mycorrhizal symbionts to stimulate microbial decomposition in the rhizosphere and increase N acquisition (Brzostek et al., 2014; Kane et al., 2022). When N limitation is alleviated by fertilization, plants can also reduce belowground C allocation, suppressing SOM decomposition (Eastman et al., 2021; Frey et al., 2014). The degree to which fertilization alters SOM cycling also depends upon the activity of saprotrophic soil microbial decomposers. In contrast to plants, soil microbes are primarily understood to be energy, or carbon, limited (Soong et al., 2020). As such, organic fertilizer that contains C and N can prime microbial activity and decomposition relative to inorganic N fertilizer (Cui et al., 2022; Ndung'u et al., 2021). However, uncertainty remains in the extent to which the priming of microbial activity leads to net soil C losses by enhancing decomposition or net C gains by promoting the production of microbial necromass that can form MAOM. Collectively, the effect of fertilization on SOM formation depends upon the strength of plant-microbe interactions and the form of fertilizer applied, but the magnitude of this effect is uncertain.

Given the uncertainty above, our objectives were to: **1) determine how living roots and symbiotic fungi influence litter decomposition and SOM formation in distinct SOM pools and 2) assess how microbially-driven SOM formation is altered by fertilization.** For the first objective, we assayed the net effect of the opposing hypotheses illustrated in Figure 3.1. For the second objective, we tested two hypotheses: (1) the effect of living roots on SOM formation would be strongest in unfertilized soil and (2) organic fertilizer would accelerate microbial decomposition and SOM cycling to a greater extent than inorganic fertilizer (SI Figure **4**). To meet our objectives, we measured the effects of living roots and fungi on new SOM formation

from isotopically enriched litter over one growing season. We incubated litter inputs in soil cores that were open to roots and fungal ingrowth (root), that excluded roots but were open to fungal ingrowth (fungal), or that excluded both roots and fungi (none) to quantify the effect of living roots and fungi on new SOM formation (SI Fig. **5**). We installed ingrowth cores in *Miscanthus x giganteus* (herein miscanthus) plots with different nutrient treatments to investigate the effect of soil N and C availability on how roots, mycorrhizal fungi, and saprotrophic microbes drive the transfer of litter C and N into light POM, heavy POM, and MAOM. We used the bioenergy feedstock crop miscanthus as a study system because it produces extensive root systems to overcome nutrient limitation (Dohleman & Long, 2009; Heaton et al., 2008) and because miscanthus agriculture typically increases SOM levels (Harris et al., 2015). Further, because bioenergy offers the potential to become a C neutral or C negative alternative to fossil fuels, it is particularly critical to investigate what drives SOM accumulation in these ecosystems (Hanssen et al., 2020).

3.3 Materials and Methods

Site description and location selection

This experiment was performed at the West Virginia University (WVU) Animal Sciences farm in Morgantown, West Virginia (39°40'10.2"N, 79°55'53.6"W). This site is located next to the former Baker's Ridge Mine Site (National Mine Repository 304559) and is managed as a cool-season grass pasture (detailed site description available in Kane et al. 2023, *in review*). Miscanthus plots were established in 2019 using a fully randomized block design with 4 fertilization treatments replicated 8 times for a total of 32 plots (Kane et al. 2023, *in review*). Each plot is 5 m^2 and was established by planting 25 miscanthus rhizomes using 1 m^2 grid spacing (site map, SI Fig. **6a**). Plots are fertilized yearly with treatments that include no fertilization, low-level inorganic N additions (28.5 kg N/ha), high-level inorganic N additions (57 kg N/ha), and organic fertilization (local manure, ~57 kg N/ha). Due to logistical constraints for sample size, we utilized the control, high-level inorganic, and organic fertilization treatments for this experiment.

Experimental design

We incubated isotopically enriched litter in soil ingrowth cores and traced the fate of litter C and N into SOM over one growing season. Our experimental design included 3 levels of root/hyphal ingrowth: root and fungal ingrowth (root), root exclusion and fungal ingrowth (fungal), and root and fungal exclusion (none) and 3 fertilization treatments: no fertilization (control), high-level inorganic fertilization (high N), or organic fertilization (organic). We randomly selected 5 plots from each fertilization treatment from those which had successful rhizome establishment during initial plot development. Within each plot, we replicated each

ingrowth core treatment twice, where we installed ingrowth cores by 2 of the plot's 25 plants (SI Fig. **6b**). This resulted in a total of 90 experimental ingrowth cores (3 cores x 3 fertilization treatments x 5 plots x 2 locations/plot).

Ingrowth core construction and installation

Ingrowth core treatments included root and fungal ingrowth (root), root exclusion and fungal ingrowth (fungal), and root and fungal exclusion (none) (SI Fig. **5**). Each ingrowth core was constructed with 10 cm long, 4.5 cm diameter rigid plastic 5 mm mesh tubing. The top 2.5 cm of each core was inserted into 5cm long PVC collars and attached with elastic sealant. Mesh bases were sewn onto each core with 12 lb. nylon fishing line and each core was wrapped with mesh that was glued on with 100% silicon adhesive. Root and fungal ingrowth (root) cores were constructed with 1.5 mm polyacrylic mesh that allowed fine root ingrowth. Root exclusion (fungal and none) cores were constructed with 50 um nylon mesh that was too fine for root ingrowth but allowed hyphal ingrowth (Phillips et al., 2012). Root and fungal exclusion (none) cores were constructed with the same root exclusion mesh and were also twisted once or twice a week to break off hyphae and prevent significant fungal ingrowth and establishment (SI Fig. **5**).

Ingrowth cores were prepared in the lab using isotopically enriched litter amendments and soil harvested from the corresponding plot. In April 2021, soils from the top 10 cm were collected from each future ingrowth core location and were brought back to the lab where they were sieved to 2 mm and stored at 5°C when not being processed. Soils were homogenized within each nutrient treatment (control, high N, or organic) and were mixed with sand that had been acid washed and separated from particles less than 53 um diameter in a 9:1 soil:sand ratio to prevent soil compaction. 250 mg of isotopically enriched corn leaf litter, generated as

described in Ridgeway et al., 2022, was used as the substrate in each ingrowth core. This addition rate was selected to be lower than litter production at the site to limit experimental artefacts from introducing a new decomposition substrate and high enough to ensure that the ^{13}C inputs were traceable into SOM pools. This litter had a %C of 41.7% (±0.17%), C:N of 18.8 (±0.64), $\delta\,^{13}C$ of 7020 (±49), and $\delta\,^{15}N$ of 34,800 (±310) and was dried and coarsely ground. Each core was filled with corresponding soil, and the labeled litter was gently mixed in to the top 2 cm.

Within 5 days of initial soil collection, the assembled cores were transported to the field location where they were installed into the top 10 cm of soil in each corresponding treatment plot (SI Fig. **6a**). This occurred in April 2021 when miscanthus shoots were beginning to emerge. Within each plot, ingrowth cores were installed 8" north of visibly emerged miscanthus shoots (SI Fig. **6b**). After 20 weeks, the ingrowth cores were carefully cut from the soil in September 2021 and were brought back to the lab for processing. Although each treatment combination began with a planned replicate of n=10, two cores were removed from analysis due to animal interference. Additionally, five cores intended for the root exclusion fungal ingrowth treatment (fungal) were invaded by roots. After determining that these cores did not significantly vary from the rest of the root ingrowth (root) cores, these were also analyzed as root ingrowth (root) cores. Given these adjustments, the total replication ranged from 5-15 for each treatment (provided in SI table 2).

Soil fractionation

Ingrowth cores were destructively harvested in September and litter C and N inputs were traced into SOM pools (Ridgeway et al., 2022). A 5 g subsample of dry soil from each core was

separated into light POM, heavy POM, and MAOM by density and size fractionation as described in Lavallee et al. (2020). In brief, the light POM was separated through density floatation in 1.85 g/mL sodium polytungstate salt solution. The remaining soil was separated into heavy POM and MAOM fractions by size separation where the MAOM fraction passes through a 53 um sieve.

Tracing litter C and N fate

To trace the fate of ^{13}C and ^{15}N litter amendments, the soil fractions were analyzed for %C, %N, $\delta\,^{13}C$, and $\delta\,^{15}N$ using a Thermo Fisher Delta V+ isotope ratio mass spectrometer interfaced with a Carlo Erba NC2500 Elemental Analyzer. First, the proportion of litter-derived C or N in each soil fraction (f_{litter}) was determined with two endmember mixing models (eq. 1) (Derrien & Amelung, 2011; Poeplau et al., 2018). Here, the C and N isotope signatures were measured from the enriched litter substrate and each of the 3 SOM fractions from control, high N, and organic soils.

eq. 3.1: $$f_{litter} = \frac{sample\ isotope\ signature - SOM\ isotope\ signature}{litter\ isotope\ signature - SOM\ isotope\ signature}$$

Next, the litter C and N recovered in each SOM pool (shown in Fig. **3.2**, Fig. **3.5**) was determined for each ingrowth core (eq. 2). Here, the mass proportion of each SOM fraction was determined from lab fractionation and the %C, %N, $\delta\,^{13}C$, and $\delta\,^{15}N$ were measured on an elemental analyzer as described above. The distribution of litter C between the SOM fractions (shown in Fig. **3.3**) was calculated as the litter mass in each SOM fraction out of the total litter mass remaining in the ingrowth core soil.

eq. 3.2: litter mass = dry soil mass in each core × SOM fraction mass proportion × SOM fraction %C/100 or %N/100 × f_{litter}

Root biomass, root colonization, and microbial biomass

All roots that were inside of the cores were separated from soils and washed in the lab. Dry root biomass was measured, and microbial biomass C was measured from a subsample of soil from each core using chloroform slurry fumigations (Witt et al., 2000) followed by persulfate digestion to CO_2 (Doyle et al., 2004; Kane et al., 2022). In brief, soils were extracted in potassium sulfate with and without chloroform for 4 hrs. Filtered supernatant was digested in persulfate solution where dissolved C was oxidized to CO_2. Total CO_2 and $\delta\,^{13}CO_2$ was measured on a Picarro G2201 (Picarro Inc). Microbial biomass C was calculated as the difference between chloroform-fumigated and non-fumigated samples scaled by 2.64 (Vance et al., 1987) and litter C-derived microbial biomass was determined using two endmember isotope mixing models.

A sample of roots was separated for root arbuscular mycorrhizal (AM) colonization measurements. To remove pigment, root samples were cleared in 10% potassium hydroxide followed with 85% ethanol to leach excess pigmentation. Roots were acidified in 5% hydrochloric acid and then stained for 5 minutes in 0.05% trypan blue (Comas et al., 2014). AM colonization was determined by suspending root samples in water on a 1x1 cm gridded petri dish and measuring how often arbuscules or hyphae were present at each root-gridline intersect (Giovannetti & Mosse, 1980).

Net mineralization and nitrification

Net N mineralization and net nitrification were measured immediately after ingrowth core harvest. These were expressed as the difference in pools of ammonium (NH_4^+) and nitrate (NO_3^-) between an initial sample that was extracted within 24 hours of collection and a sample that was incubated for 2 weeks at room temperature. Inorganic N was extracted from 5 g of soil

from each core in 10 mL of 1M KCl solution, and dissolved inorganic N was determined through phenol-hypochlorite and azo-dye colorimetric assays for NH_4^+ and NO_3^-, respectively (Finzi et al., 1998).

Statistical analysis

To determine the extent to which ingrowth core treatments and fertilization treatments altered the fate of litter C and N amendments, we performed two-way analyses of variance in R version 3.5.1 (R Core Team 2021). Model factors were ingrowth core treatment, fertilization treatment, and their interaction. Post-hoc comparisons between groups were made using the Tukey's HSD test. Differences were considered statistically significant at an alpha level of 0.05 ($p<0.05$) and marginally significant at an alpha level of 0.10 ($p<0.10$). Linear regression was used to investigate the effect of living roots or microbial decomposers on litter C incorporation into MAOM. Data was checked for normality and heteroscedasticity. Outliers, defined as samples where decomposer biomass was greater than 2 standard deviations from the mean, were omitted from linear regression.

3.4 Results

Root impacts on litter C and N transformations did not depend on fertilization

Root ingrowth core treatments and fertilization treatments both altered the fate of litter C and N in SOM, but the root effect did not depend on fertilization. All p-values for ingrowth core treatment x fertilization treatment interactions are above 0.05 (SI Table 3) and root biomass did not vary across fertilization treatment (SI Fig. 7a). As such, subsequent data shown for each factor are aggregated over the other factor.

Root ingrowth reduces litter N remaining in SOM

Root ingrowth did not significantly alter litter C in total SOM (Fig. **3.2a**, p>0.10) but reduced the litter N in total SOM by 20% relative to both root exclusion treatments (Fig. **3.2b**, p<0.001). Within the SOM fractions, root ingrowth reduced both litter C (Fig. **3.2a**, light green, p=0.001) and litter N (Fig. **3.2b**, light green, p<0.001) remaining in the unprotected light POM fraction.

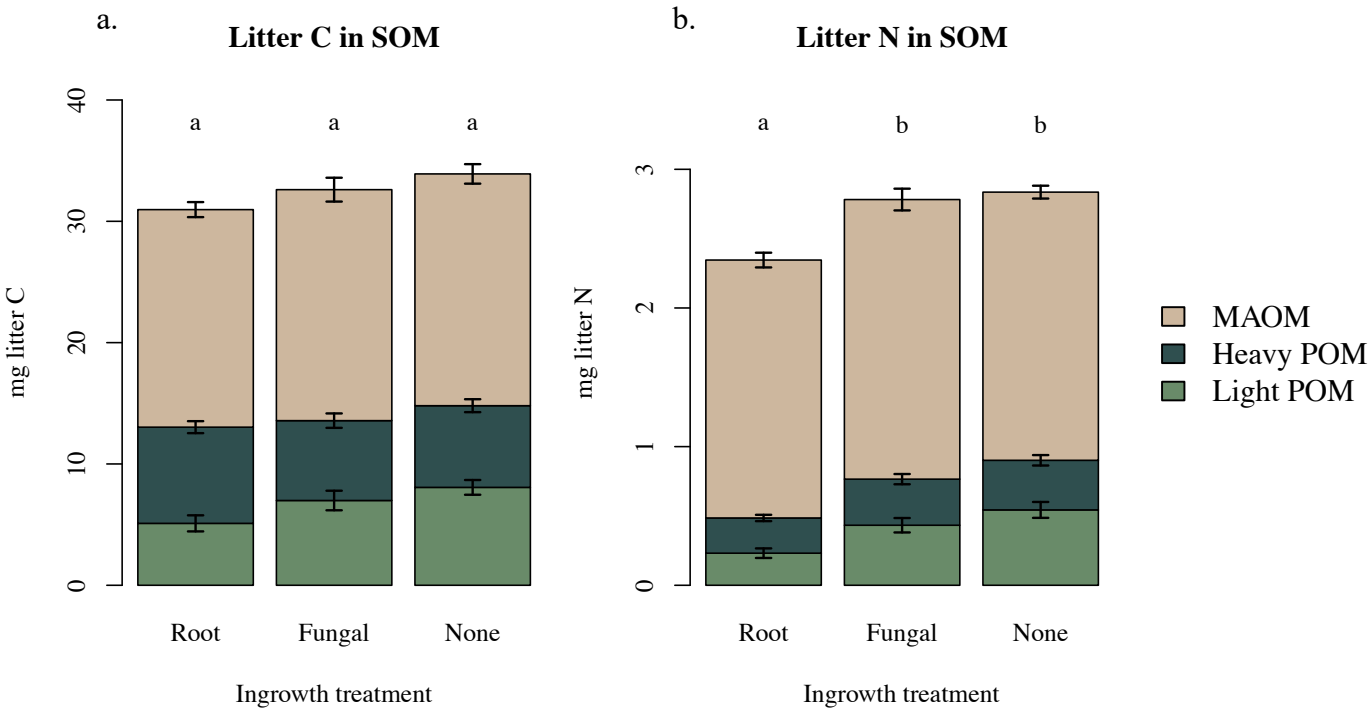

Fig. 3. 2: The total mass of litter C (left) and litter N (right) recovered in the light POM fraction (light green), heavy POM fraction (dark blue), and MAOM fraction (brown) for root and fungal ingrowth (root), root exclusion and fungal ingrowth (fungal), or root and fungal exclusion (none) soil cores. Litter mass is calculated from measurements of isotopic signature, and mean data is shown with standard error bars. Letters denote statistically significant differences between the ingrowth core treatments in total C or N recovered in all SOM pools ($p<0.05$).

Root ingrowth alters the balance of C in SOM pools

Of the litter C that remained in SOM, root ingrowth altered the balance of C between SOM pools. Root ingrowth decreased the proportion of litter C remaining in light POM by 32% (Fig. **3.3a**, $p<0.001$) and increased the proportion of litter C incorporation into protected heavy POM by 30% (Fig. **3.3b**, $p=0.001$) relative to both root exclusion treatments. Roots did not significantly alter the incorporation of litter C into MAOM (Fig. **3.3c**). There were no significant differences between fungal only and fungal exclusion treatments.

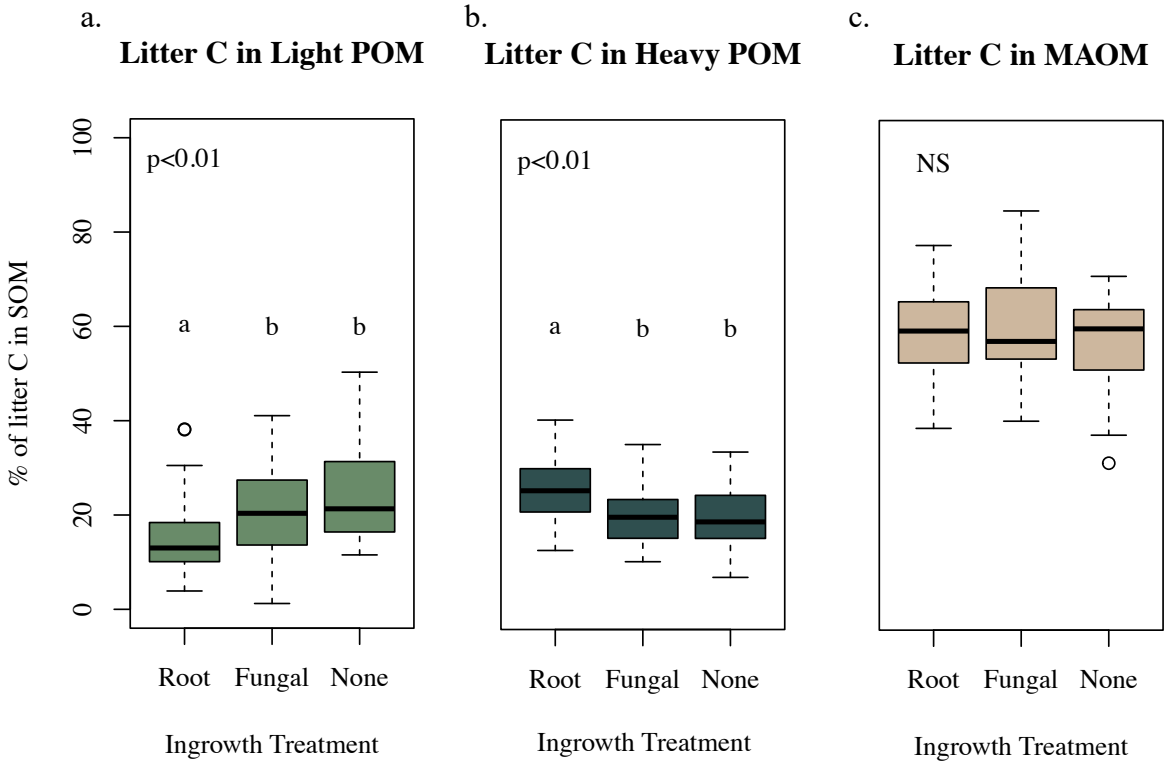

Fig. 3. 3: Distribution of litter C between light POM, heavy POM, and MAOM pools shown as the % of litter C in each pool of the litter C remaining in the soil after the field incubation for root and fungal ingrowth (root), root exclusion and fungal ingrowth (fungal), or root and fungal exclusion (none) soil cores.

Roots mine light and heavy POM for litter N

Root ingrowth selectively mined N from organic matter in both POM pools. Root ingrowth preferentially reduced the litter N remaining in light and heavy POM fractions (Fig. **3.2b**, green light POM N is 55 % lower with root ingrowth, $p<0.001$; blue heavy POM N is 26% lower with root ingrowth, $p<0.01$). In turn, root ingrowth increased the C:N ratio of litter-derived SOM in light POM (Fig. **3.4a**, $p<0.001$) and heavy POM (Fig. **3.4b**, $p<0.001$).

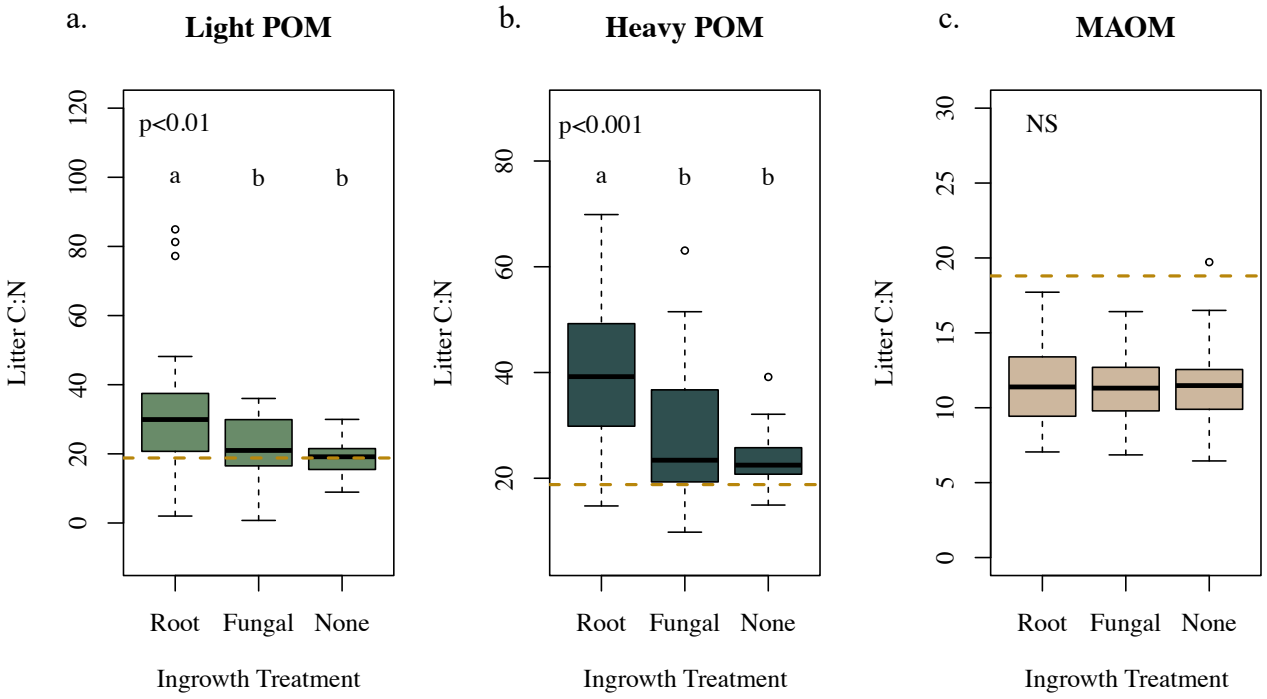

Fig. 3. 4: Litter C:Litter N in light POM(3.4a), heavy POM (3.4b), and MAOM (3.4c) fractions compared to added litter C:N (18.8, gold dashed line) for root and fungal ingrowth (root), root exclusion and fungal ingrowth (fungal), or root and fungal exclusion (none) soil cores.

Organic fertilization reduces litter retention in SOM

Organic fertilization reduced litter C and N remaining in the soil relative to control treatments, but there were no significant differences between control and high N fertilization treatments.

Net litter C remaining in SOM was reduced by 14% under the organic fertilization treatment (Fig. **3.5a**, $p<0.01$) relative to the unfertilized control treatment soils. Within the SOM fractions, the loss of litter C was driven by an 18% reduction in litter C incorporation into MAOM (Fig. **3.5a**, brown, $p=0.018$). Organic fertilization reduced litter N remaining in total SOM by 12% (Fig. **3.5b**, $p=0.020$) relative to unfertilized control treatments. Within the SOM fractions, the loss of litter N was primarily driven by a 16% reduction in litter N incorporation into MAOM (Fig. **3.5b**, brown, $p<0.001$).

Organic fertilization treatments had 25% greater microbial biomass (SI Fig. **7b**, $p=0.09$) relative to unfertilized treatments. Microbial decomposition in organic fertilization treatments was more effective with less litter C remaining in each SOM pool per gram microbial biomass compared to control fertilization (SI Fig. **8, a-c**). However, this decomposition was less effective for litter N than litter C, with no significant difference in litter N in POM pools per gram of microbial biomass across nutrient treatments (SI Fig. **8, d-e**). Litter C and N incorporation into MAOM was lower per gram of microbial biomass with organic fertilization compared to control fertilization (SI Fig. **8c, 5f**).

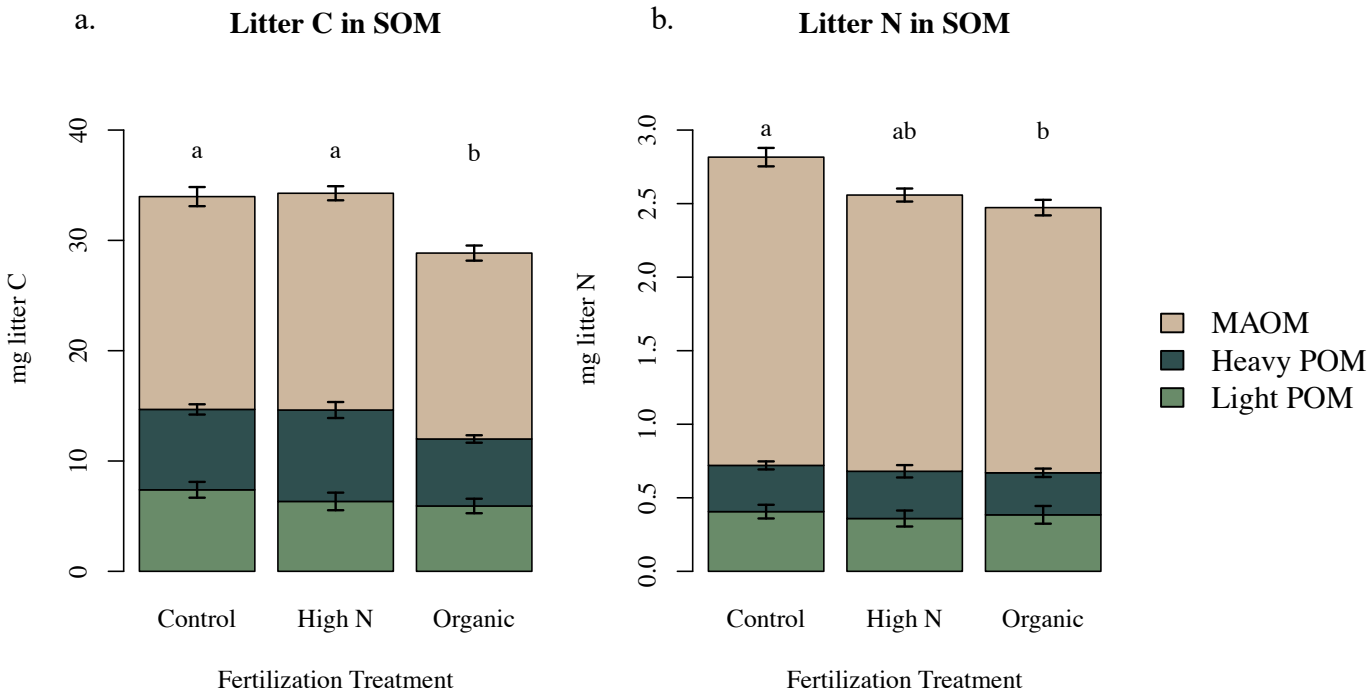

Fig. 3. 5: The total mass of litter C (left) and litter N (right) recovered in the light fraction (light green), heavy POM fraction (dark blue), and silt/clay fraction (brown) for control fertilization, high inorganic N fertilization, or organic fertilization plot treatments. Mean data is shown and error bars represent plus or minus one standard deviation. Letters denote statistically significant differences between the plot treatments in total C or N recovered in all SOM pools ($p<0.05$).

3.5 Discussion

Collectively, this work identifies how roots and soil microbes drive SOM loss and formation in miscanthus systems that can promote soil C sequestration and support plant productivity. Root ingrowth did not promote a net litter C loss from soil (Fig. **3.2**) despite increased light POM decomposition due to the enhanced transfer of C into heavy POM (Fig. **3.3**). Notably, we document the potential for roots to mobilize litter-derived N from POM without priming litter C loss (Fig. **3.2**, Fig. **3.4**). We also identified that microbial nutrient or carbon limitation may alter how microbes grow and decompose litter-derived SOM, with more litter decomposition and less MAOM formation from litter in organically fertilized soils (Fig. **3.5**).

It appears that miscanthus roots can mine N from litter without stimulating corresponding litter C losses (Fig. **3.2**) and can increase the C:N of litter-derived light and heavy POM (Fig. **3.4**). This raises the question of how miscanthus accesses N from decomposing litter without priming C losses that are commonly observed in other ecosystems (Cheng et al., 2014; Zhu et al., 2014). One plausible mechanism may be that miscanthus roots engineer their rhizosphere microbiome composition or function to preferentially decompose N-rich litter compounds like proteins, potentially by stimulating proteolytic enzyme production (Brzostek & Finzi, 2011). While the specific mechanism remains uncertain, preferential N mining from litter has important implications for miscanthus sustainability (e.g.,, the propensity of miscanthus to be high yielding and build soil C). The resulting increase in remaining litter C:N may make new litter-derived SOM even more resistant to further decomposition. In addition, there has been a long-standing question of how miscanthus can maintain relatively high yields with limited N inputs (Cadoux et

al., 2012). Previous research has posited that high nutrient use efficiency (Beale & Long, 1997) or the promotion of N-fixing symbionts (Davis et al., 2010) sustains N nutrition by miscanthus. Overall, our results suggest that miscanthus may also meet its N nutrition by effectively mining N from litter and SOM.

Our research suggests that roots can actively support the transfer of litter derived C into more protected forms. We observed that the priming of litter decomposition from light POM was balanced by litter C incorporation in heavy POM (Fig. **3.3**). The composition of heavy POM is not as well-characterized as light POM or MAOM, but this pool is commonly assumed to be composed of stable soil macro- or micro-aggregates (Lavallee et al., 2020). Aggregate-occluded SOM is largely formed through root and mycorrhizal symbiont activity (Rillig & Mummey, 2006) and often consists of partially decomposed plant and microbial organic matter fragments. This pool has a higher activation energy for decomposition than low C:N compounds like those in MAOM (Williams et al., 2018) and is more protected from decomposers than free light POM (Keiluweit et al., 2017; Kögel-Knabner et al., 2008). As such, there is an opportunity to build soil carbon in high C:N, heavy POM rather than lower C:N MAOM. The N requirements of low C:N SOM retention have often been cited as a criticism to efforts to use soil C management to mitigate global change (Schlesinger & Amundson, 2019). Future research efforts that investigate how roots can build new, persistent, and high C:N SOM could help realize the potential of soil C sequestration to combat climate change.

We found that the organic fertilizer treatments had the greatest microbial biomass and litter-derived light POM decomposition, in support of our second fertilization hypothesis, but

less litter C and N were incorporated into MAOM (Fig. **3.5**, SI Figs. **7, 8**). On one hand, differences between fertilization treatments could arise from a shift in the microbial community structure or function with organic fertilization (Pan et al., 2014). However, other research at the site has found no significant effects of nutrient treatment on microbial diversity or mycorrhizal abundance between treatments (Kane et al. 2023, *in review*). On the other hand, C vs. N limitation over microbial decomposition can regulate the rate and efficiency of SOM cycling (Averill & Waring, 2018; Schimel & Weintraub, 2003). As organic fertilization deposits both C and N, our observations could be explained by the alleviation of C limitation and induction of N limitation. In support, we observed a reduction in nitrification rates with organic fertilization relative to unfertilized plots (SI Fig. **9**) and other research found that organic fertilization increases plot-scale microbial respiration (Kane et al., 2023, *in review*). Here, microbial decomposers could increase decomposition and growth while respiring excess C and immobilizing N in living biomass rather than forming more microbially-derived MAOM (Schimel & Weintraub, 2003).

While our experiment identified several important ways living roots and soil microbes control litter decomposition and SOM formation, some mechanisms may not have been fully captured. Our experiment was designed to separate the effects of roots vs. mycorrhizal fungi on litter C and N transformations, but our data only identifies a root effect despite the presence of mycorrhizal fungal symbionts (SI Fig. **10**). The lack of differences between fungal ingrowth and total exclusion cores could be linked to the greater dependence of AM plants on root than hyphal foraging for nutrient uptake (Chen et al., 2016). As such, our experiment may not have isolated fungal effects on litter decomposition and SOM formation. Future efforts should quantify

mycorrhizal fungal ingrowth to better investigate the contribution of symbiotic fungi to root-driven SOM transformations. In addition, our observations that fertilization did not impact root biomass (SI Fig 7**a**) and that there was no significant interaction between fertilization and ingrowth treatments (SI Table **3**) do not support our first fertilization hypothesis that roots would have the greatest effect in unfertilized soils. While miscanthus root systems do not always respond to fertilization treatments (Amougou et al., 2011), this pattern may have been driven by the stand age of miscanthus in our experiment. These plots were in the third year of growth whereas older, more nutrient limited stands exhibit greater differences in root C allocation and N acquisition (Kantola et al., 2022). As such, future efforts to investigate how nutrient availability alters living root impacts on SOM formation should leverage ecosystems with longer-term fertilization history. Despite these limitations, our data has identified several important mechanisms of SOM formation *in situ* and provides the foundation for future efforts to study how living roots and fungi alter SOM dynamics with more sophisticated measurements, under different environmental conditions, or across different ecosystems and plant-microbe interactions.

This work has expanded our mechanistic understanding of how living roots shape ecosystem processes in agricultural systems. Our finding that miscanthus roots can simultaneously prime N release from litter without an additional C release and transfer C into a more persistent form of SOM has important implications for the sustainability of bioenergy production as well as the viability of restorative agricultural to offset carbon emissions. Overall, our work suggests that living roots can selectively mine N while sequestering soil C. This knowledge can help improve the predictive understanding of SOM cycling that is critical to meeting the goals of restorative agriculture.

3.6 Literature Cited

Amougou, N., Bertrand, I., Machet, J.-M., & Recous, S. (2011). Quality and decomposition in soil of rhizome, root and senescent leaf from *Miscanthus x giganteus*, as affected by harvest date and N fertilization. *Plant and Soil*, *338*(1), 83–97. https://doi.org/10.1007/s11104-010-0443-x

Angst, G., Mueller, K. E., Nierop, K. G. J., & Simpson, M. J. (2021). Plant- or microbial-derived? A review on the molecular composition of stabilized soil organic matter. *Soil Biology and Biochemistry*, *156*, 108189. https://doi.org/10.1016/j.soilbio.2021.108189

Averill, C., & Waring, B. (2018). Nitrogen limitation of decomposition and decay: How can it occur? *Global Change Biology*, *24*(4), 1417–1427. https://doi.org/10.1111/gcb.13980

Bais, H. P., Weir, T. L., Perry, L. G., Gilroy, S., & Vivanco, J. M. (2006). The Role of Root Exudates in Rhizosphere Interactions with Plants and Other Organisms. *Annual Review of Plant Biology*, *57*(1), 233–266. https://doi.org/10.1146/annurev.arplant.57.032905.105159

Beale, C. V., & Long, S. P. (1997). Seasonal dynamics of nutrient accumulation and partitioning in the perennial C4-grasses *Miscanthus* × *giganteus* and *Spartina cynosuroides*. *Biomass and Bioenergy*, *12*(6), 419–428. https://doi.org/10.1016/S0961-9534(97)00016-0

Benbi, D. K., Boparai, A. K., & Brar, K. (2014). Decomposition of particulate organic matter is more sensitive to temperature than the mineral associated organic matter. *Soil Biology and Biochemistry*, *70*, 183–192. https://doi.org/10.1016/j.soilbio.2013.12.032

Bronick, C. J., & Lal, R. (2005). Soil structure and management: A review. *Geoderma*, *124*(1), 3–22. https://doi.org/10.1016/j.geoderma.2004.03.005

Brzostek, E. R., & Finzi, A. C. (2011). Substrate supply, fine roots, and temperature control proteolytic enzyme activity in temperate forest soils. *Ecology*, *92*(4), 892–902.

Brzostek, E. R., Fisher, J. B., & Phillips, R. P. (2014). Modeling the carbon cost of plant nitrogen acquisition: Mycorrhizal trade-offs and multipath resistance uptake improve predictions of retranslocation. *Journal of Geophysical Research: Biogeosciences*, *119*(8), 1684–1697. https://doi.org/10.1002/2014JG002660

Cadoux, S., Riche, A. B., Yates, N. E., & Machet, J.-M. (2012). Nutrient requirements of *Miscanthus x giganteus*: Conclusions from a review of published studies. *Biomass and Bioenergy*, *38*, 14–22. https://doi.org/10.1016/j.biombioe.2011.01.015

Chen, W., Koide, R. T., Adams, T. S., DeForest, J. L., Cheng, L., & Eissenstat, D. M. (2016). Root morphology and mycorrhizal symbioses together shape nutrient foraging strategies of temperate trees. *Proceedings of the National Academy of Sciences*, *113*(31), 8741–8746. https://doi.org/10.1073/pnas.1601006113

Cheng, W., Parton, W. J., Gonzalez-Meler, M. A., Phillips, R., Asao, S., McNickle, G. G., Brzostek, E., & Jastrow, J. D. (2014). Synthesis and modeling perspectives of rhizosphere priming. *New Phytologist*, *201*(1), 31–44. https://doi.org/10.1111/nph.12440

Comas, L. H., Callahan, H. S., & Midford, P. E. (2014). Patterns in root traits of woody species hosting arbuscular and ectomycorrhizas: Implications for the evolution of belowground strategies. *Ecology and Evolution*, *4*(15), 2979–2990. https://doi.org/10.1002/ece3.1147

Cotrufo, M. F., Ranalli, M. G., Haddix, M. L., Six, J., & Lugato, E. (2019). Soil carbon storage informed by particulate and mineral-associated organic matter. *Nature Geoscience*, *12*(12), Article 12. https://doi.org/10.1038/s41561-019-0484-6

Cotrufo, M. F., Wallenstein, M. D., Boot, C. M., Denef, K., & Paul, E. (2013). The Microbial Efficiency-Matrix Stabilization (MEMS) framework integrates plant litter decomposition

with soil organic matter stabilization: Do labile plant inputs form stable soil organic matter? *Global Change Biology*, *19*(4), 988–995. https://doi.org/10.1111/gcb.12113

Cui, J., Zhu, R., Wang, X., Xu, X., Ai, C., He, P., Liang, G., Zhou, W., & Zhu, P. (2022). Effect of high soil C/N ratio and nitrogen limitation caused by the long-term combined organic-inorganic fertilization on the soil microbial community structure and its dominated SOC decomposition. *Journal of Environmental Management*, *303*, 114155. https://doi.org/10.1016/j.jenvman.2021.114155

Davis, S. C., Parton, W. J., Dohleman, F. G., Smith, C. M., Grosso, S. D., Kent, A. D., & DeLucia, E. H. (2010). Comparative biogeochemical cycles of bioenergy crops reveal nitrogen-fixation and low greenhouse gas emissions in a *Miscanthus* × *giganteus* agro-ecosystem. *Ecosystems*, *13*(1), 144–156. https://doi.org/10.1007/s10021-009-9306-9

Derrien, D., & Amelung, W. (2011). Computing the mean residence time of soil carbon fractions using stable isotopes: Impacts of the model framework. *European Journal of Soil Science*, *62*(2), 237–252. https://doi.org/10.1111/j.1365-2389.2010.01333.x

Dohleman, F. G., & Long, S. P. (2009). More Productive Than Maize in the Midwest: How Does Miscanthus Do It? *Plant Physiology*, *150*(4), 2104–2115. https://doi.org/10.1104/pp.109.139162

Doyle, A., Weintraub, M. N., & Schimel, J. P. (2004). Persulfate Digestion and Simultaneous Colorimetric Analysis of Carbon and Nitrogen in Soil Extracts. *Soil Science Society of America Journal*, *68*(2), 669–676. https://doi.org/10.2136/sssaj2004.6690

Eastman, B. A., Adams, M. B., Brzostek, E. R., Burnham, M. B., Carrara, J. E., Kelly, C., McNeil, B. E., Walter, C. A., & Peterjohn, W. T. (2021). Altered plant carbon partitioning enhanced

forest ecosystem carbon storage after 25 years of nitrogen additions. *New Phytologist*, *230*(4), 1435–1448. https://doi.org/10.1111/nph.17256

Fernandez, C. W., & Kennedy, P. G. (2016). Revisiting the "Gadgil effect": Do interguild fungal interactions control carbon cycling in forest soils? *New Phytologist*, *209*(4), 1382–1394. https://doi.org/10.1111/nph.13648

Finzi, A. C., Van Breemen, N., & Canham, C. D. (1998). Canopy Tree–Soil Interactions Within Temperate Forests: Species Effects on Soil Carbon and Nitrogen. *Ecological Applications*, *8*(2), 440–446. https://doi.org/10.1890/1051-0761(1998)008[0440:CTSIWT]2.0.CO;2

Frey, S. D., Ollinger, S., Nadelhoffer, K. ea, Bowden, R., Brzostek, E., Burton, A., Caldwell, B. A., Crow, S., Goodale, C. L., & Grandy, A. S. (2014). Chronic nitrogen additions suppress decomposition and sequester soil carbon in temperate forests. *Biogeochemistry*, *121*(2), 305–316.

Georgiou, K., Jackson, R. B., Vindušková, O., Abramoff, R. Z., Ahlström, A., Feng, W., Harden, J. W., Pellegrini, A. F. A., Polley, H. W., Soong, J. L., Riley, W. J., & Torn, M. S. (2022). Global stocks and capacity of mineral-associated soil organic carbon. *Nature Communications*, *13*(1), Article 1. https://doi.org/10.1038/s41467-022-31540-9

Giovannetti, M., & Mosse, B. (1980). An Evaluation of Techniques for Measuring Vesicular Arbuscular Mycorrhizal Infection in Roots. *The New Phytologist*, *84*(3), 489–500.

Grayston, S. J., Vaughan, D., & Jones, D. (1997). Rhizosphere carbon flow in trees, in comparison with annual plants: The importance of root exudation and its impact on microbial activity and nutrient availability. *Applied Soil Ecology*, *5*(1), 29–56. https://doi.org/10.1016/S0929-1393(96)00126-6

Hanssen, S. V., Daioglou, V., Steinmann, Z. J. N., Doelman, J. C., Van Vuuren, D. P., & Huijbregts, M. a. J. (2020). The climate change mitigation potential of bioenergy with carbon capture and storage. *Nature Climate Change*, *10*(11), Article 11. https://doi.org/10.1038/s41558-020-0885-y

Harris, Z. M., Spake, R., & Taylor, G. (2015). Land use change to bioenergy: A meta-analysis of soil carbon and GHG emissions. *Biomass and Bioenergy*, *82*, 27–39. https://doi.org/10.1016/j.biombioe.2015.05.008

Heaton, E. A., Dohleman, F. G., & Long, S. P. (2008). Meeting US biofuel goals with less land: The potential of Miscanthus. *Global Change Biology*, *14*(9), 2000–2014. https://doi.org/10.1111/j.1365-2486.2008.01662.x

Jilling, A., Keiluweit, M., Gutknecht, J. L., & Grandy, A. S. (2021). Priming mechanisms providing plants and microbes access to mineral-associated organic matter. *Soil Biology and Biochemistry*, *158*, 108265.

Kane, J. L., Robinson, M. C., Schartiger, R. G., Freedman, Z. B., McDonald, L. M., Skousen, J. G., & Morrissey, E. M. (2022). Nutrient management and bioaugmentation interactively shape plant–microbe interactions in Miscanthus × giganteus. *GCB Bioenergy*, *14*(11), 1235–1249. https://doi.org/10.1111/gcbb.13000

Kantola, I. B., Masters, M. D., Blanc-Betes, E., Gomez-Casanovas, N., & DeLucia, E. H. (2022). Long-term yields in annual and perennial bioenergy crops in the Midwestern United States. *GCB Bioenergy*, *14*(6), 694–706. https://doi.org/10.1111/gcbb.12940

Keiluweit, M., Bougoure, J. J., Nico, P. S., Pett-Ridge, J., Weber, P. K., & Kleber, M. (2015). Mineral protection of soil carbon counteracted by root exudates. *Nature Climate Change*, *5*(6), 588–595. https://doi.org/10.1038/nclimate2580

Keiluweit, M., Wanzek, T., Kleber, M., Nico, P., & Fendorf, S. (2017). Anaerobic microsites have an unaccounted role in soil carbon stabilization. *Nature Communications*, *8*(1), 1–10.

Kögel-Knabner, I., Guggenberger, G., Kleber, M., Kandeler, E., Kalbitz, K., Scheu, S., Eusterhues, K., & Leinweber, P. (2008). Organo-mineral associations in temperate soils: Integrating biology, mineralogy, and organic matter chemistry. *Journal of Plant Nutrition and Soil Science*, *171*(1), 61–82. https://doi.org/10.1002/jpln.200700048

Lal, R. (2004). Soil Carbon Sequestration Impacts on Global Climate Change and Food Security. *Science*, *304*(5677), 1623–1627. https://doi.org/10.1126/science.1097396

Lavallee, J. M., Soong, J. L., & Cotrufo, M. F. (2020). Conceptualizing soil organic matter into particulate and mineral-associated forms to address global change in the 21st century. *Global Change Biology*, *26*(1), 261–273. https://doi.org/10.1111/gcb.14859

Lehmann, J., & Kleber, M. (2015). The contentious nature of soil organic matter. *Nature*, *528*(7580), Article 7580. https://doi.org/10.1038/nature16069

Liang, C., Schimel, J. P., & Jastrow, J. D. (2017). The importance of anabolism in microbial control over soil carbon storage. *Nature Microbiology*, *2*(8), Article 8. https://doi.org/10.1038/nmicrobiol.2017.105

Minasny, B., Malone, B. P., McBratney, A. B., Angers, D. A., Arrouays, D., Chambers, A., Chaplot, V., Chen, Z.-S., Cheng, K., Das, B. S., Field, D. J., Gimona, A., Hedley, C. B., Hong, S. Y., Mandal, B., Marchant, B. P., Martin, M., McConkey, B. G., Mulder, V. L., … Winowiecki, L. (2017). Soil carbon 4 per mille. *Geoderma*, *292*, 59–86. https://doi.org/10.1016/j.geoderma.2017.01.002

Ndung'u, M., Ngatia, L. W., Onwonga, R. N., Mucheru-Muna, M. W., Fu, R., Moriasi, D. N., & Ngetich, K. F. (2021). The influence of organic and inorganic nutrient inputs on soil

organic carbon functional groups content and maize yields. *Heliyon*, *7*(8), e07881. https://doi.org/10.1016/j.heliyon.2021.e07881

Pan, Y., Cassman, N., de Hollander, M., Mendes, L. W., Korevaar, H., Geerts, R. H. E. M., van Veen, J. A., & Kuramae, E. E. (2014). Impact of long-term N, P, K, and NPK fertilization on the composition and potential functions of the bacterial community in grassland soil. *FEMS Microbiology Ecology*, *90*(1), 195–205. https://doi.org/10.1111/1574-6941.12384

Paustian, K., Lehmann, J., Ogle, S., Reay, D., Robertson, G. P., & Smith, P. (2016). Climate-smart soils. *Nature*, *532*(7597), Article 7597. https://doi.org/10.1038/nature17174

Phillips, R. P., Meier, I. C., Bernhardt, E. S., Grandy, A. S., Wickings, K., & Finzi, A. C. (2012). Roots and fungi accelerate carbon and nitrogen cycling in forests exposed to elevated CO2. *Ecology Letters*, *15*(9), 1042–1049. https://doi.org/10.1111/j.1461-0248.2012.01827.x

Poeplau, C., Don, A., Six, J., Kaiser, M., Benbi, D., Chenu, C., Cotrufo, M. F., Derrien, D., Gioacchini, P., Grand, S., Gregorich, E., Griepentrog, M., Gunina, A., Haddix, M., Kuzyakov, Y., Kühnel, A., Macdonald, L. M., Soong, J., Trigalet, S., … Nieder, R. (2018). Isolating organic carbon fractions with varying turnover rates in temperate agricultural soils – A comprehensive method comparison. *Soil Biology and Biochemistry*, *125*, 10–26. https://doi.org/10.1016/j.soilbio.2018.06.025

Ridgeway, J. R., Morrissey, E. M., & Brzostek, E. R. (2022). Plant litter traits control microbial decomposition and drive soil carbon stabilization. *Soil Biology and Biochemistry*, *175*, 108857. https://doi.org/10.1016/j.soilbio.2022.108857

Rillig, M. C., & Mummey, D. L. (2006). Mycorrhizas and soil structure. *New Phytologist*, *171*(1), 41–53. https://doi.org/10.1111/j.1469-8137.2006.01750.x

Schimel, J. P., & Weintraub, M. N. (2003). The implications of exoenzyme activity on microbial carbon and nitrogen limitation in soil: A theoretical model. *Soil Biology and Biochemistry*, *35*(4), 549–563. https://doi.org/10.1016/S0038-0717(03)00015-4

Schlesinger, W. H., & Amundson, R. (2019). Managing for soil carbon sequestration: Let's get realistic. *Global Change Biology*, *25*(2), 386–389. https://doi.org/10.1111/gcb.14478

Six, J., Paustian, K., Elliott, E. T., & Combrink, C. (2000). Soil Structure and Organic Matter I. Distribution of Aggregate-Size Classes and Aggregate-Associated Carbon. *Soil Science Society of America Journal*, *64*(2), 681–689. https://doi.org/10.2136/sssaj2000.642681x

Soong, J. L., Fuchslueger, L., Maranon-Jimenez, S., Torn, M. S., Janssens, I. A., Penuelas, J., & Richter, A. (2020). Microbial carbon limitation: The need for integrating microorganisms into our understanding of ecosystem carbon cycling. *Global Change Biology*, *26*(4), 1953–1961. https://doi.org/10.1111/gcb.14962

Stockmann, U., Padarian, J., McBratney, A., Minasny, B., de Brogniez, D., Montanarella, L., Hong, S. Y., Rawlins, B. G., & Field, D. J. (2015). Global soil organic carbon assessment. *Global Food Security*, *6*, 9–16. https://doi.org/10.1016/j.gfs.2015.07.001

Sulman, B. N., Moore, J. A., Abramoff, R., Averill, C., Kivlin, S., Georgiou, K., Sridhar, B., Hartman, M. D., Wang, G., & Wieder, W. R. (2018). Multiple models and experiments underscore large uncertainty in soil carbon dynamics. *Biogeochemistry*, *141*(2), 109–123.

Vance, E. D., Brookes, P. C., & Jenkinson, D. S. (1987). An extraction method for measuring soil microbial biomass C. *Soil Biology and Biochemistry*, *19*(6), 703–707. https://doi.org/10.1016/0038-0717(87)90052-6

Williams, E. K., Fogel, M. L., Berhe, A. A., & Plante, A. F. (2018). Distinct bioenergetic signatures in particulate versus mineral-associated soil organic matter. *Geoderma*, *330*, 107–116. https://doi.org/10.1016/j.geoderma.2018.05.024

Witt, C., Gaunt, J. L., Galicia, C. C., Ottow, J. C. G., & Neue, H.-U. (2000). A rapid chloroform-fumigation extraction method for measuring soil microbial biomass carbon and nitrogen in flooded rice soils. *Biology and Fertility of Soils*, *30*(5), 510–519. https://doi.org/10.1007/s003740050030

Zhu, B., Gutknecht, J. L. M., Herman, D. J., Keck, D. C., Firestone, M. K., & Cheng, W. (2014). Rhizosphere priming effects on soil carbon and nitrogen mineralization. *Soil Biology and Biochemistry*, *76*, 183–192. https://doi.org/10.1016/j.soilbio.2014.04.033

Chapter 4: Modelling plant-microbe interactions improves predictions of how forest carbon and nitrogen cycles respond to declining nitrogen deposition

4.1 Abstract

As anthropogenic nitrogen (N) deposition declines across the eastern US, uncertainty remains in whether temperate forests will continue to provide a critically important carbon (C) sink. This uncertainty is amplified by the inability of ecosystem models to accurately capture the microbial mechanisms that drive greater soil C sequestration and N loss under enhanced N availability. To address this limitation, we leveraged decades of C and N cycling data from a whole-watershed N fertilization experiment at the Fernow Experimental Forest in Parsons, WV to run the microbially-explicit plant-microbe interactions model FUN-CORPSE (Fixation and Uptake of Nitrogen- Carbon, Organisms, Rhizosphere, and Protection in the Soil Environment). We had three objectives, including: 1) Reproducing key ecosystem responses to N fertilization, 2) Modeling microbially-explicit inorganic N cycling, and 3) Assessing how modeled soil C and N retention respond to shifts in N deposition and other future climate drivers.

FUN-CORPSE accurately represents overarching ecosystem C and N cycling at the Fernow (e.g., soil C pools, streamwater N losses) and captures key responses to experimental N deposition, including the 25% decline in plant C cost of N acquisition that reduces root-primed decomposition and increases soil C. We validated our newly integrated inorganic N cycling in FUN-CORPSE against measured inorganic N pools, nitrification rates, and the relative abundance of nitrifying microbes. With microbially-explicit inorganic N cycling, FUN-CORPSE captures the 100% increase in nitrification rates and the 50% increase in streamwater nitrate loss under N fertilization. When we ran the model forward under projected declining N deposition, FUN-CORPSE predicted that N losses recovered more quickly than soil C pools. However, the eventual return of soil C to pre-fertilized levels indicates that additional C sequestered due to N deposition may be vulnerable to future loss, particularly with global changes like warming.

4.2 Introduction

Human activities like fossil fuel burning, fertilizer synthesis, and planting N-fixing crops have increased the global production rate of bioavailable nitrogen by approximately an order of magnitude since the industrial revolution (Galloway et al., 2004). This effect has been particularly apparent in the temperate forests of the Eastern US, a historical hot spot for atmospheric N deposition from fossil fuel combustion (Gilliam et al., 2019). Among other deleterious impacts, elevated N deposition has acidified forest ecosystems, shifted tree community composition, and exacerbated streamwater N leaching and aquatic eutrophication (Bobbink et al., 2010; Clark et al., 2013; Gundersen et al., 2006). However, N deposition has also stimulated forest uptake of excess atmospheric CO_2, facilitating the globally-critical terrestrial C sink (Pan et al., 2011; Schimel, 1995). In recent decades, the institution of the Clean Air Act (CAA) and its successive amendments has limited reactive N emissions and drastically reduced N deposition across the eastern US (NADP https://nadp.slh.wisc.edu). As such, predictions of the continuing ability of these forests to sequester C remain highly uncertain.

Much of the uncertainty in predicting C cycling responses to N deposition results from ecosystem models lacking robust representations of plant-microbe interactions (Sulman et al., 2018). Specifically, most models do not represent the central role of belowground C investment by trees in driving soil C and N cycling. Decades of empirical research has shown that the allocation of C belowground by trees to roots, symbiotic fungi, and soil microbes in the rhizosphere, or zone of soil surrounding plant roots, stimulates SOM decomposition and enhances plant N uptake (Cheng et al., 2014). Under elevated N availability, however, this mechanism appears to weaken. Research from a 30-year, whole-watershed N fertilization experiment at the Fernow Experimental Forest has shown that excess inorganic N availability

drove trees to reduce belowground C allocation (Eastman et al., 2021). In turn, this decline in belowground C allocation suppressed microbial decomposition potential, extracellular enzyme activity, and SOM decomposition (Carrara et al., 2018; Eastman et al., 2022; Moore et al., 2020) (Fig. 4.1a). Because they do not represent these processes, most terrestrial biogeochemical models simulate the opposite response. For example, in the Community Land Model (CLM), N deposition removes N limitation controls on photosynthesis, stimulating both leaf and root production and litter inputs. However, because CLM simulates SOM cycling with first-order rate kinetics, enhanced litter inputs stimulate decomposition (Lawrence et al., 2019). It is imperative for models to better capture the mechanisms driving observed ecosystem responses to N deposition to capture C and N cycling in a changing world.

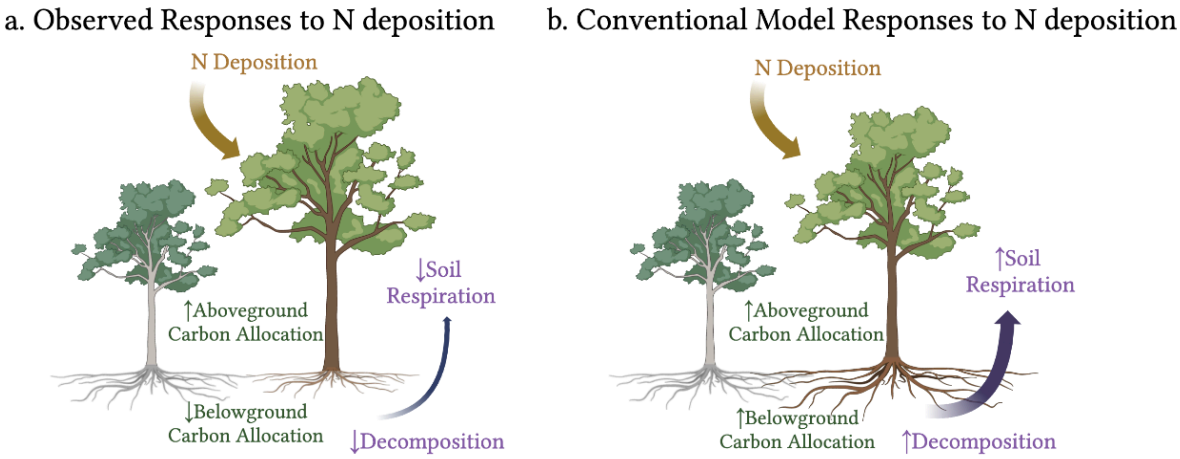

Fig. 4. 1a: Observations show that N deposition reduces tree C allocation belowground, suppresses microbial decomposition, and enhances the retention of unprotected SOM. 4.1b: Conventional ecosystem process models predict that N deposition alleviates tree N limitation, enhancing belowground C allocation and priming SOM decomposition.

While microbially-explicit decomposition models can capture ecosystem C cycling, model predictions of ecosystem N losses are hindered by a simplification of soil N transformations where N transformations are not microbially mediated. N transformations (e.g.,,

nitrification, denitrification, N leaching) are commonly modeled with simple rate constant equations (Berardi et al., 2020; Kyker-Snowman et al., 2020; Saifuddin et al., 2021; Sulman et al., 2017). Here, N losses from a pool of size *S* are controlled through a rate constant *k*, where the N losses are modeled as $S * k$. These simple rate constant equations are unlikely to capture how rates of N transformation are impacted by the physiological traits, biomass, and environmental responses of microbes that drive them. Given that N availability constrains ecosystem C uptake, the lack of microbially-mediated N transformations in these models may limit model representations of N availability and C uptake under N deposition.

However, robust theoretical and empirical understandings of microbial N cycling offer the potential to incorporate data-based microbial N cycling in models. In terrestrial ecosystems, functionally and often phylogenetically distinct microbes perform key inorganic N cycling processes like nitrification, denitrification, and N fixation (Kuypers et al., 2018). Of these, nitrification is the best starting point for improving modeled N cycling through explicit microbial representation. Nitrification, or the conversion of inorganic N from ammonium to nitrate, is one of the most critical N transformations that is second in magnitude only to N mineralization from SOM (Kuypers et al., 2018). Nitrification is typically performed by microbes who can use the energy gained from the oxidation to fix inorganic C into biomass (Norton & Ouyang, 2019). Nitrification controls bioavailable N and regulates the potential for inorganic soil N to be lost through pathways like nitrate leaching to streamwater that can harm aquatic ecosystems or gaseous losses that enhance greenhouse gas accumulation (Lehmann & Schroth, 2002). As such, the potential exists to model microbially-explicit, empirically-constrained, and more mechanistic N cycling to improve predictions of soil C and N retention.

Improving model representations of forest responses to N deposition is imperative to projecting the response of eastern temperate forests to future shifts in N availability. At a broader scale, this work is critical because of the potential for inorganic N cycling and N availability to interact with other projected environmental changes like altered precipitation patterns and elevated temperatures to drive how ecosystems feedback to global change (Thornton et al., 2009). As a result, models that lack N cycling mechanisms and dynamic plant-microbe interactions may exacerbate the high degree of uncertainty in predictions of the future of the globally important land C sink (Meirholt et al., 2020). To address this uncertainty, the overarching objectives of this research were to: **1) Reproduce key ecosystem responses to N fertilization in a plant-microbe interactions model; 2) Model microbially-explicit inorganic N cycling; and 3) Assess how modeled soil C and N retention respond to declining N deposition and a warming climate.**

To meet these objectives, we leveraged decades of C and N cycling data from the Fernow Experimental Forest, located in Parsons, WV, to develop, constrain, and validate modeled ecosystem responses to N deposition and fertilization using the FUN-CORPSE (Fixation and Uptake of Nitrogen: Carbon, Organisms, Rhizosphere, and Protection in the Soil Environment) model (Sulman et al., 2017). First, we tested whether FUN-CORPSE could capture key C cycling responses to N deposition by modelling how trees invest C belowground to prime microbial decomposition and mineralize N. Next, we incorporated microbially-explicit nitrification to investigate if this process could facilitate model projections of N cycling responses to N deposition. Finally, we ran the model forward to look at how future changes in climate could alter forest N and C retention.

4.2 Methods

Site Description

The Fernow Experimental Forest (herein, the Fernow) is located near Parsons, WV, USA (39.03N, 79.67W). A long-term, whole-watershed N fertilization experiment was perfomed at the Fernow from 1989-2019. Here, N additions in the form of ammonium sulfate were aerially applied to an entire watershed at a rate of 35.4kg N/ha/yr, which was roughly double ambient N deposition in 1989. A similar, adjacent watershed was maintained with only ambient N deposition to serve as an unfertilized reference. A more detailed site description is published by Adams et al., 2006. Briefly, the Fernow is dominated by broadleaf deciduous trees, and the soils are predominantly loams and silt loams. Both watersheds have similar tree species, including *Betula lenta, Prunus serotina, Acer rubrum, Liriodendron tulipifera* (more dominant in the fertilized watershed), and *Quercus rubra* (more dominant in the reference watershed) (Eastman et al., 2021). Forest stands were roughly two decades old at the beginning of the fertilization experiment, where the reference watershed was clearcut and maintained barren with herbicide prior to 1969 and the fertilized watershed was clearcut prior to 1972 (Adams et al., 2006).

A wealth of long-term, ecosystem C and N cycling data exists for both the fertilized (watershed 3) and reference (watershed 7) watersheds at the Fernow, much of which is summarized in Eastman et al., 2021. Below, we detail how data from the Fernow was used to drive the model, constrain model parameters, and validate model predictions.

The main C and N cycling data from the Fernow used as inputs to drive the model include tree aboveground net primary productivity (ANPP), leaf litter inputs, fine root biomass and turnover, and atmospheric and applied N deposition. ANPP was estimated at the Fernow using measurements of leaf litterfall mass data collected from 25 plots in each watershed from

1989-2015 and tree growth measured from changes in tree diameter at breast height (DBH) and species-specific allometric equations at 25 plots in each watershed from 1990 (WS3) or 1991 (WS7) through 2018 (M.B. Adams, unpublished data; Eastman et al., 2021). Leaf litterfall mass data was scaled by litter C and N content data collected from 2015-2017 to estimate litter C and N inputs (Eastman et al., 2021). Fine root biomass was estimated from measurements made at varying depths and time points from 1991-2018 and was scaled by the C and N content of fine roots measured in 2012, 2013, and 2016 (Eastman et al., 2021). Fine root production and turnover were estimated using ingrowth core data collected from 2016-2018 (Eastman et al., 2021). Ambient atmospheric N deposition data inputs were estimated from measurements of wet deposition and modeled estimates of historical N deposition (Adams et al., 2006)

New model N cycling parameters were constrained by observations from the Fernow, including soil nitrification rates, microbial nitrifier relative abundance, and nitrate leaching losses pre-fertilization. Soil nitrification parameters were selected to allow the model to reflect measured nitrification rates and ammonium vs. nitrate soil N pool (Carrara et al., 2018). Nitrifier growth efficiency and turnover rates were selected such that model representations of nitrifiers vs. decomposer microbes reflected measurements of relative abundance of microbial nitrifiers from 2019 and 2020 (Chansotheary Dang, unpublished data). First-order nitrate loss rate constants were selected to reflect measurements of streamwater nitrate leaching losses from before fertilization began. Streamwater nitrate leaching since 1983 or earlier has been monitored through continuous streamflow measurements and weekly or biweekly streamwater chemistry measurements at weirs at the base of each watershed (Edwards & Wood, 2011).

Model representations of Fernow C and N cycling responses to fertilization were validated against data from the Fernow, including streamwater nitrate losses as well as soil C and

N pools and tree C cost of N acquisition both with and without N fertilization. Mineral soil C and N pools were measured from soil C and N concentrations measured to 45cm depth for 15 soil pits in each watershed in 2016 and measurements of soil bulk density from each watershed and a nearby reference site (Gilliam et al., 2018). Tree C cost of N acquisition was calculated in Eastman et al. (2021) as the ratio of total belowground carbon flux (approximated as soil respiration – leaf litter C inputs) to tree N acquisition for the unfertilized and fertilized watersheds.

FUN-CORPSE Model Description

The FUN-CORPSE (Fixation and Uptake of Nitrogen-Carbon, Organisms, Rhizosphere, and Protection in the Soil Environment) model (Sulman et al., 2017) was used to simulate how N deposition shifted ecosystem C and N cycling. A detailed description of the core model equations is available in Sulman et al. (2017). This model couples FUN, a tree C allocation model, with CORPSE, a SOM decomposition model, to mechanistically represent critical plant-microbe interactions that traditional first-order models broadly lack. To meet plant N demand, the FUN model (Brzostek et al., 2014) uses a resistance framework to optimally allocate C belowground to the rhizosphere where the microbes represented in the CORPSE model (Sulman et al., 2014) can use it to prime SOM decomposition and enhance N availability (Fig. 4.2). As such, FUN-CORPSE is uniquely equipped to capture how shifts in plant-microbe interactions may drive observed ecosystem responses to N deposition.

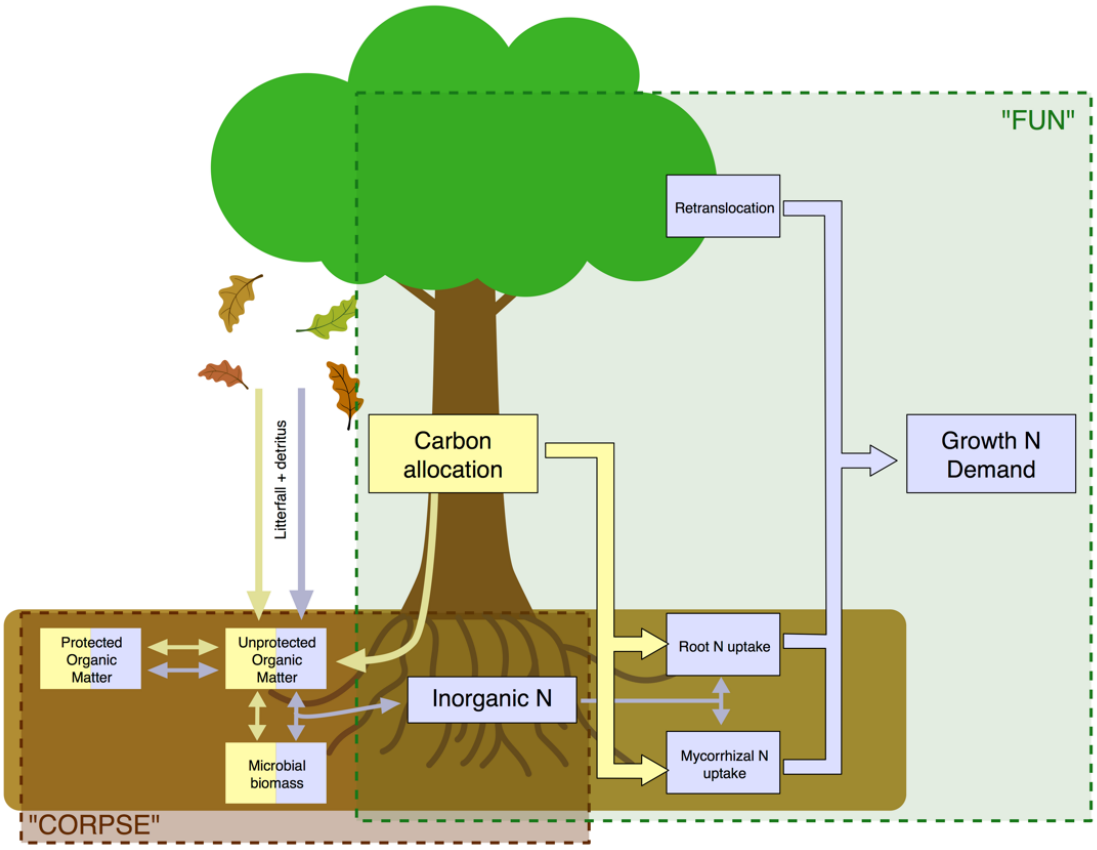

Fig. 4. 2: FUN-CORPSE Model Diagram from Sulman et al. (2017). This model couples FUN, a plant C allocation model highlighted in green, with CORPSE, a SOM cycling model highlighted in brown.

The FUN model (Brzostek et al., 2014) determines N demand to meet growth requirements and dynamically allocates C to different pathways of N acquisition: biological N fixation, retranslocation, non-mycorrhizal root uptake, mycorrhizal uptake, or N from storage. This model uses a resistance framework where a C cost associated with each pathway determines the uptake rate to optimize N uptake per C allocated.

The CORPSE model (Sulman et al., 2014) simulates soil C and N cycling through microbially-explicit SOM decomposition. CORPSE has litter, rhizosphere, and bulk compartments that each have three SOM chemical types representing fast (easily decomposable), slow (decomposition-resistant), and microbial necromass organic matter. Further, this organic matter can be incorporated into protected SOM pools in the bulk and rhizosphere soil compartments, with the highest protection rate for microbial necromass. Microbial biomass in each compartment controls the decomposition and transfer of C and N between SOM pools through reverse Michaelis-Menten kinetics (eq. 1). Here, SOM decomposition is scaled by a temperature-dependent maximum enzymatic conversion rate (Vmax) and soil moisture scalar (θ). Decomposition is limited by the size of the microbial biomass pool (M), a proxy for the decomposition enzymes in Schimel and Weintraub (2003) and scales linearly with the substrate (S) when the ratio of microbial biomass to unprotected C (uC) is constant.

$$\textbf{eq. 4. 1:} \qquad \text{Decomposition rate} = \text{Vmax} \times \theta \times \text{S} \times \frac{\frac{\text{M}}{\text{uC}}}{\frac{\text{M}}{\text{uC}} + \text{k}}$$

Like most terrestrial biogeochemical models, FUN-CORPSE implicitly represents the microbes responsible for driving N cycling. FUN-CORPSE has a single inorganic N pool that is shared across the soil compartments. Inorganic N is supplemented through external N inputs or through excess microbial N mineralization, taken up to meet plant or microbial N demand, and drained through a first-order rate loss equation to capture nitrate leaching (Fig. 4.3a).

Running FUN-CORPSE at the Fernow

FUN-CORPSE was run with plant productivity and litter input files reflected Fernow data as described above. Default parameters were used as published in Juice et al. (2021), the majority

of which were calibrated using ecosystem C and N cycling measurements from temperate broadleaf deciduous forest plots in Indiana (Sulman et al., 2017). FUN-CORPSE was spun up at the Fernow under pre-industrial estimates of ambient N deposition (0.25g $N/m^2/yr$) until soil C and N pools equilibrated. Following spinup, forest C and N cycling was simulated with estimates of anthropogenic N deposition from 1900-2100 and inorganic N inputs reflecting the 30-year N fertilization experiment at the Fernow. Disturbance legacies (e.g., clear-cutting) prior to the fertilization experiment were not simulated. The fertilized and reference watersheds were run with the same input data despite some differences between the sites including lower wood production and ANPP in the reference watershed to better identify mechanistic differences in how N availability alters soil C and N cycling alone rather than with an interaction with tree N demand. FUN-CORPSE runs at a daily timestep and a scale of 1x1m area and simulates the top 30cm of soil. Model results are validated against data from the Fernow that has been scaled to per m^2 (Eastman et al., 2021) and measured or corrected to estimate to 30cm depth.

Incorporating Microbially-Explicit Nitrification in FUN-CORPSE:

Nitrification splits soil inorganic N between ammonium and nitrate, which is more mobile in the soil. To incorporate this process, the model shared inorganic N pool was parsed into 4 pools where each soil compartment (litter, bulk, and rhizosphere) has a distinct ammonium pool and the combined soil shares a nitrate pool (Fig. 4.3b). Microbial nitrifiers in each compartment drive the transfer of inorganic N from ammonium to nitrate. Decomposer microbes in each compartment can immobilize N from both their corresponding ammonium pool and from the shared nitrate pool. Microbially-mineralized N and the proportion of microbial biomass turnover that forms inorganic N joins the corresponding ammonium pool for each compartment.

Tree roots can access ammonium in the mineral soil (bulk and rhizosphere) compartments and the shared nitrate pool. Inorganic ammonium inputs to the soil join the litter inorganic N pool. Nitrate is available to be lost through first-order rate constant loss flux that simulates nitrate leaching.

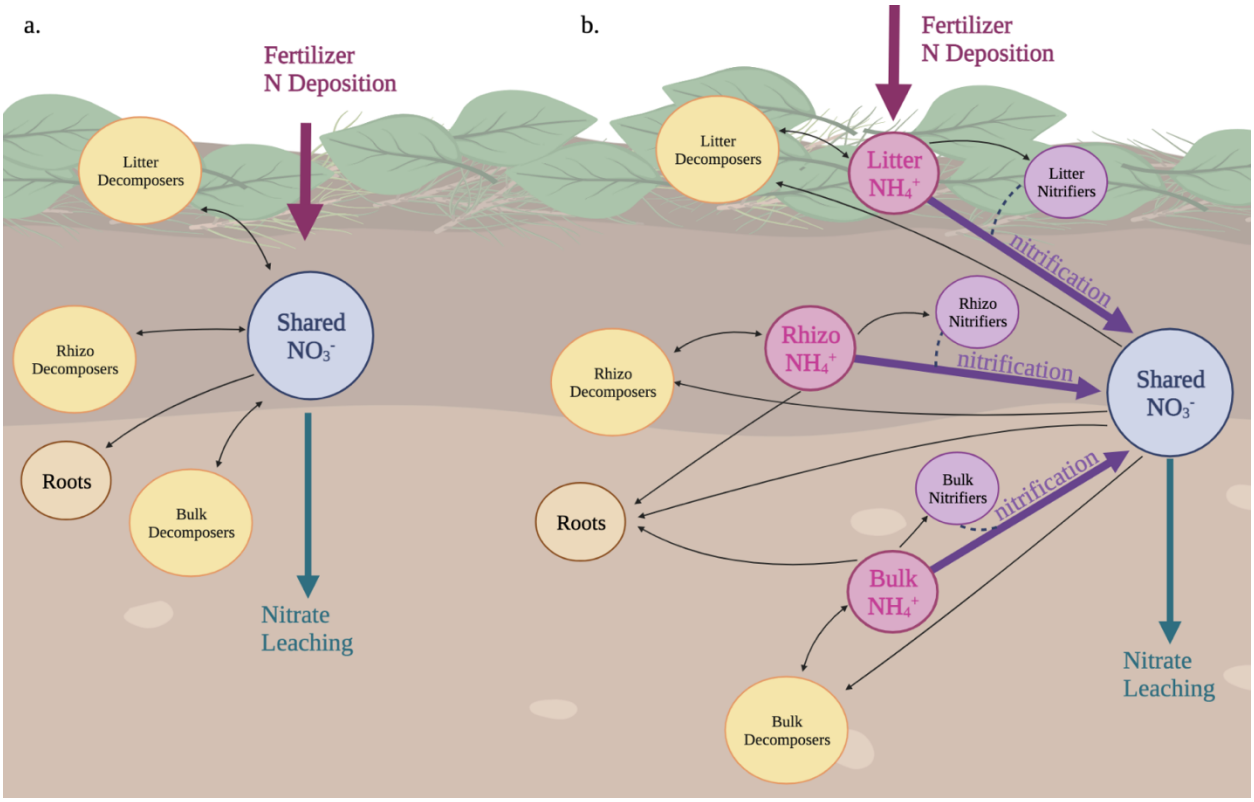

Fig. 4. 3a: Simple inorganic N cycling in FUN-CORPSE is modeled with a single shared inorganic N pool. Decomposers in each compartment can mineralize inorganic N from SOM decomposition and roots and decomposers can take up inorganic N. N is externally amended through fertilization and ambient N deposition, and N is lost through first-order kinetics. 4.3b: FUN-CORPSE inorganic N cycling was modified to incorporate the microbial nitrifiers that transform inorganic N from ammonium inputs into more mobile nitrate that can be lost from the soil. Each soil compartment (litter, rhizosphere, and bulk) has an ammonium pool that can be built through inorganic N mineralization from SOM decomposition. This ammonium can be nitrified by nitrifiers in each soil compartment to a single nitrate pool, which is shared across all soil compartments as nitrate is highly mobile in soil. Roots and microbes in each compartment can take up ammonium and nitrate. N inputs can be added to the corresponding inorganic N pool and are added to the top compartment of soil (e.g., ammonium fertilization is initially added to the litter compartment ammonium pool). Nitrate leaching is lost from the nitrate pool through first-order kinetics.

Nitrification rates were modeled using Michaelis-Menten enzyme kinetics as in equation 2, where nitrification rates are a function of the maximum nitrification enzyme conversion rate ($Vmax_N$), soil moisture scalar (θ), the biomass of microbial nitrifiers (MIC_N), ammonium substrate (NH_4), and the half-saturation constant (k_N).

$$\textbf{eq. 4. 2:} \qquad \text{Nitrification} = Vmax_N \times \theta \times MIC_N \times \frac{NH_4}{NH_4 + k_N}$$

Model nitrifiers are chemoautotrophic and fix C to grow biomass at an assumed rate of 1 C fixed per 10 N transformed (Berg et al., 2015; Sharma & Ahlert, 1977). Beyond this, microbial nitrifiers use the same processes and parameters as the decomposer microbes (described in Sulman et al., 2017) to control growth, death, and necromass transfers into inorganic and organic soil C and N pools.

The model with microbial nitrifiers was calibrated with data from the Fernow such that the model roughly captured measurements of nitrification rates and the distribution of inorganic N between ammonium and nitrate made by J Carrara (2015), unpublished data. Modeled nitrate leaching losses were tuned to match pre-fertilization (year 1980) N leaching losses from the microbially-implicit model. Model representations of microbial nitrifiers relative to microbial decomposers were validated against microbial biomass data and the relative abundance of nitrifiers as measured by Chansotheary Dang (2020), unpublished data.

Predictions of Future Forest Ecosystem Services in Response to Declining N Deposition and Elevated Temperatures

Whether forest ecosystem can maintain productivity and sequester C under reduced N deposition and future climate change remains uncertain. In particular, temperatures are predicted to rise as N deposition declines in the eastern US (Sixth Assessment Report of the IPCC, 2021).

Elevated temperatures stimulate microbial decomposition, N mineralization, and the loss of soil C in FUN-CORPSE. As such, the potential for soils to sequester C and retain N to fuel plant productivity may depend on an interaction between N inputs and soil temperature. This model was run forward to predict Fernow soil C and N retention until year 2100 from fertilized and unfertilized watersheds. Following modeled trajectories of rainwater nitrate concentrations (Adams et al., 2006), ambient N deposition was projected to decline at the same rate as it increased in the 20th century. A +2^{o} C increase in soil T was also modeled beginning in 2025 to investigate how elevated temperature could impact soil N losses and C retention.

4.3 Results:

Objective 1: Model ecosystem responses to N fertilization

FUN-CORPSE accurately represents the Fernow's soils and captures key responses to N deposition. Model representations of soil carbon captured both the total soil C pool (Fig. 4.4a) and the proportion of this pool that was observed to be in unprotected particulate SOM vs. MAOM (Fig. 4.4b) were within observed ranges at the Fernow. Fertilization increased soil C in the topsoil at the Fernow (Eastman et al., 2021), which is captured by a modeled increase in soil C (Fig. 4.4a).

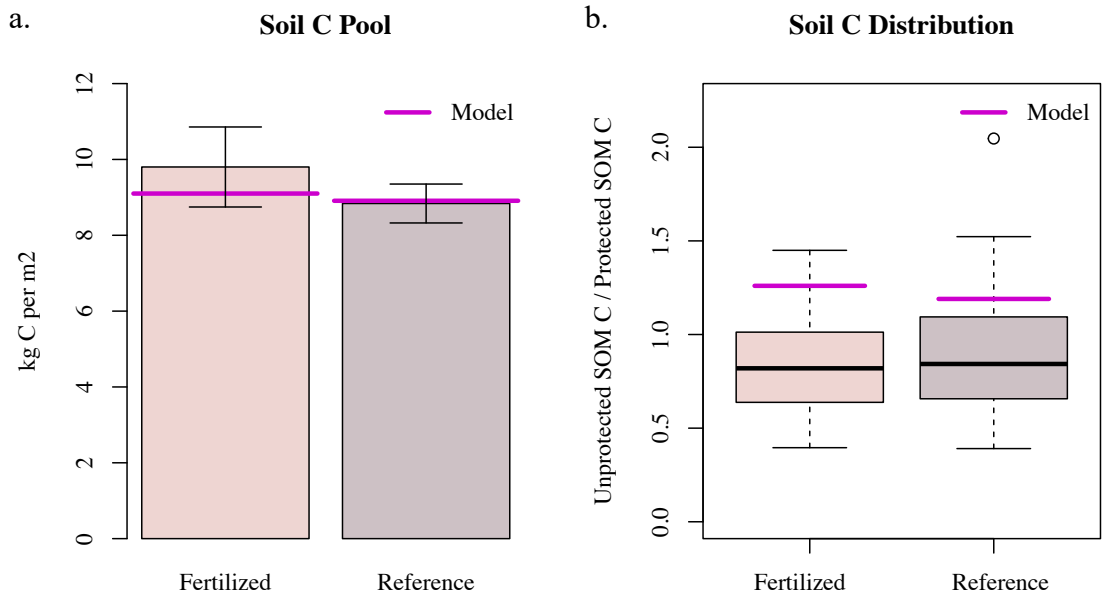

Fig. 4. 4a: Soil C pools at the fertilized (pale red barplot) and reference (purple barplot) Fernow watersheds compared to model projections of soil C (magenta lines) 4.4b: Soil C distribution as the ratio of unprotected to protected SOM-C from the Fernow fertilized (pale red) and reference (purple) watersheds (Eastman et al., 2022) compared with model projections of unprotected to protected SOM-C (magenta lines).

Further, a key response of the Fernow ecosystem to elevated N deposition includes the decoupling of plant-microbe interactions through a 25% reduction in tree C allocation belowground in exchange for N acquisition, as calculated in Eastman et al. (2021). By dynamically shifting tree C allocation in response to soil N availability, FUN-CORPSE predicts a similar 21% decrease in the C trees allocate to the rhizosphere per N acquired (Fig. 4.5a). This decoupling of tree-stimulated SOM mineralization is linked with observations of a 56% reduction in arbuscular mycorrhizal root colonization from roots in the mineral soil (Carrara et al., 2022) and a 30% reduction in microbial biomass in the mineral soil (Chansotheary Dang, unpublished data). The model predicts similar patterns of a reduction in C allocated to symbiotic fungal decomposers (80%, Fig. 4.5b) and mineral soil microbial biomass (11%, Fig. 4.5c).

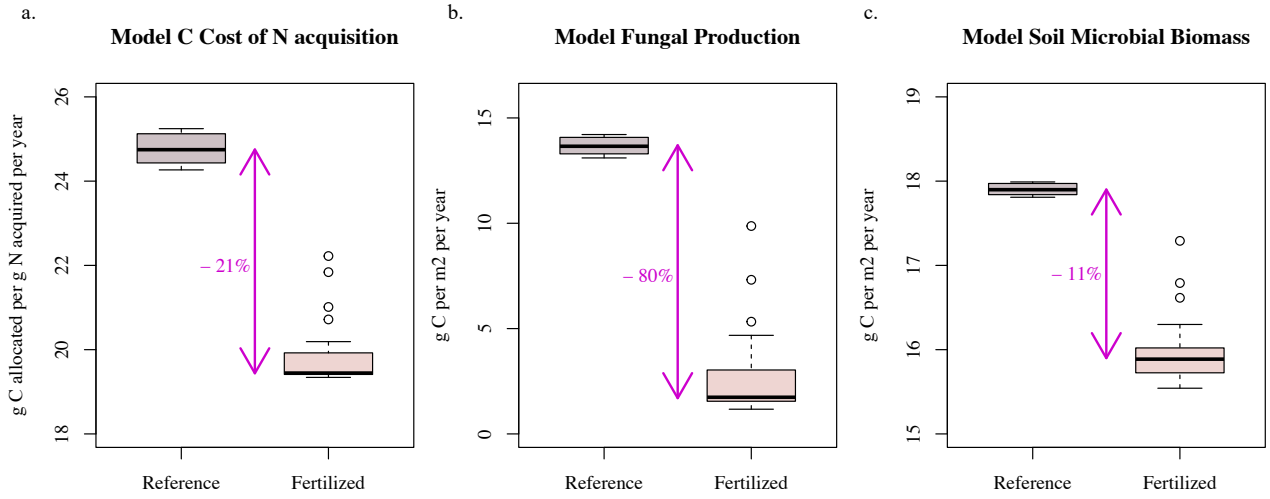

Fig. 4. 5: Model values for the reference (light purple) and fertilized (light red) watersheds from 1989-2019. (a) average yearly C allocated belowground to fine roots, mycorrhizae, and exudates per average yearly N acquired by trees; (b) average yearly fungal C production from FUN; (c) average yearly mineral soil microbial decomposer biomass in CORPSE.

Objective 2: Incorporate microbially-explicit inorganic N cycling:

While FUN-CORPSE captures key C cycling responses to N deposition, the model does not accurately represent soil N retention. In particular, due to its simplistic representation of soil N cycling (Fig. 4.3a), when N is deposited to the shared inorganic N pool, nitrate leaching linearly increases and leads to greater N losses than observed at the Fernow. At the Fernow, N fertilization led to 5x greater N inputs (roughly 100 g N/m^2 over 30 years) in the fertilized than reference watershed, but only increased cumulative stream N export by roughly 12 g N/m^2 over 30 years (Fig. 4.6e,f).

Incorporating the microbial nitrifiers responsible for transforming inorganic N inputs into nitrate (Nitrification Model, purple) improved model representations of seasonal inorganic N leaching relative to the model without N microbes (Baseline Model, blue) for both the fertilized watershed in red (Fig. 4.6a) and the unfertilized watershed in gray (Fig. 4.6b). When averaged for each year during the fertilization period from 1989-2019, the Baseline Model (blue) simulated roughly double the yearly nitrogen loss as the Nitrification Model (purple) during fertilization (Fig. 4.6c). The N loss rates for each model were tuned to capture yearly nitrate loss rates pre-fertilization, so the models performed similarly when nitrate losses were averaged over each year for the unfertilized watershed (Fig. 4.6d).

Over the fertilization period from 1989-2019, the observed cumulative N loss for the fertilized watershed was roughly 42 g N/m^2 (Fig. 4.6e, red) while the reference watershed was roughly 27 g N/m^2 (Fig. 4.6f, gray). The model with microbial nitrifiers slightly underestimated observed N losses during fertilization at roughly 38 g N/m^2, as the lag in microbial nitrification led to an increase in the ammonium available for trees to take up (Fig. 4.6e, purple). The model without explicit nitrifiers increased N losses linearly with total inorganic N availability and as

such overestimated cumulative N losses at roughly 55 g N/m^2 (Fig. 4.6e, blue).

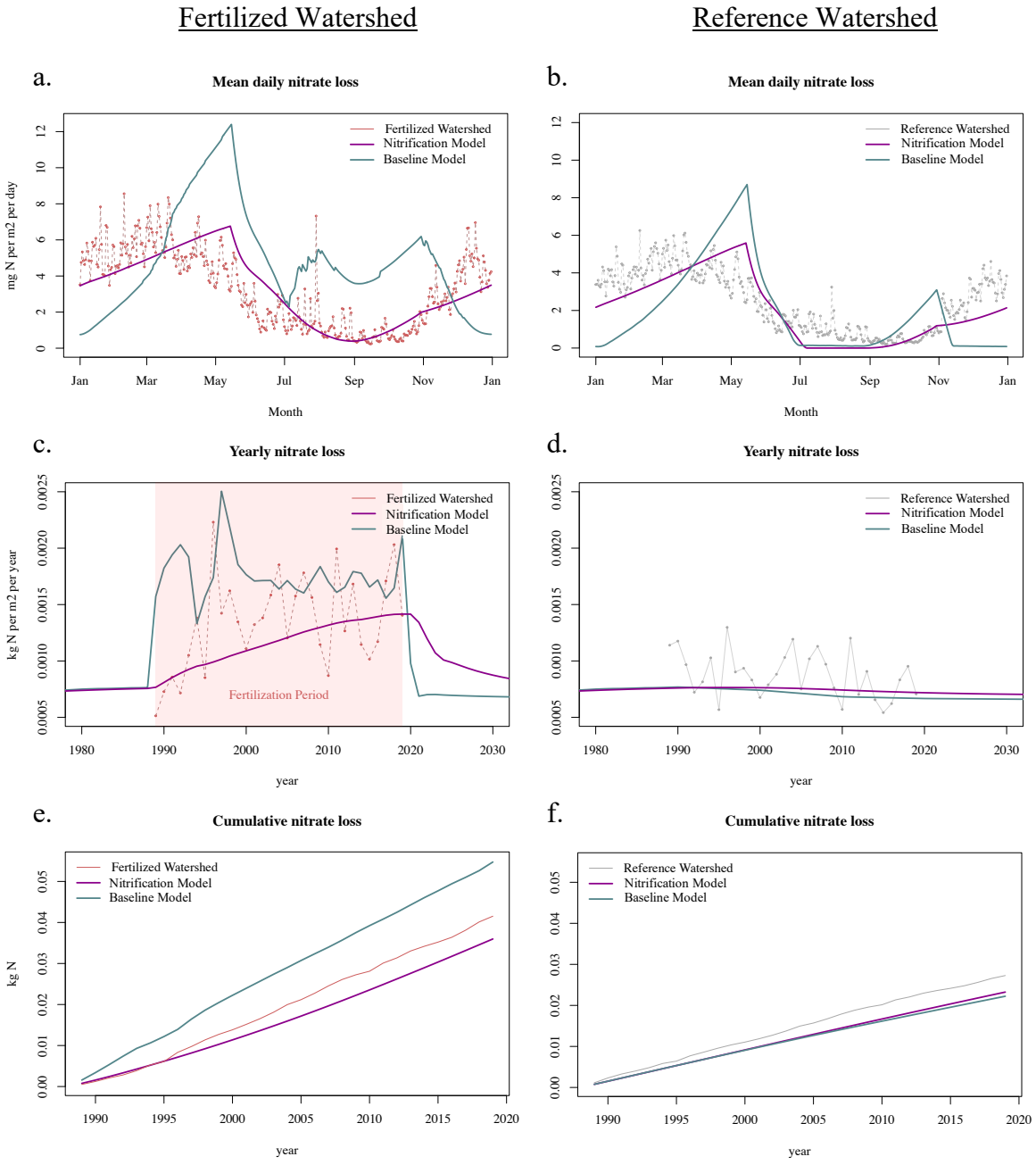

Fig. 4. 6: Modeled nitrate losses for the explicit Nitrification Model (purple) and implicit Baseline Model (blue) compared with data from the fertilized watershed (left panels, pale red) and reference watershed (right panels, gray). 4.6a,b: Mean daily streamwater nitrate loss from years 1989-2019 (USDA Forest Service, https://www.fs.usda.gov/rds/efrdata/efr/2) compared to daily model N losses. 4.6c,d: Yearly patterns of streamwater nitrate losses from 1989-2019 compared with yearly model N losses. 4.6e,f: Cumulative streamwater nitrate losses from 1989-2019 compared with cumulative model N losses.

Objective 3: Model Projections of recovery from N fertilization and elevated temperature:

FUN-CORPSE predicts that the soil C gained during N fertilization declines more gradually during recovery than streamwater nitrate leaching. When running the model with N microbes forward under recovery from N fertilization, it takes more than 150 years for 95% of the soil C gained from fertilization to be lost (Fig. 4.7a, the fertilized watershed soil C shown in solid red remains elevated compared to the reference in solid purple). The model predicted that soil C accumulated during the 30 years of fertilization at an average rate of 9 g C/m^2/yr and lost soil C at an average rate of 2.5 g C/m^2/yr in 30 years post-fertilization. However, streamwater nitrate leaching recovers to pre-fertilization levels in roughly 30 years (Fig. 4.7b, nitrate leaching from the fertilized watershed shown in solid red more rapidly returns to reference levels in solid purple). While the Fernow has only been in recovery from N fertilization for 3-4 years, nitrate leaching from the fertilized watershed is still higher than from the reference watershed (USDA Forest Service, https://www.fs.usda.gov/rds/efrdata/*efr/2*), which better aligns with the model projections of a decades-scale return in streamwater nitrate leaching as modeled with N microbes compared to the elastic response of nitrate leaching to fertilization in the model without N microbes (Fig. 4.7c, Nitrification Model in purple vs. Baseline Model in blue).

FUN-CORPSE predicts that increased temperatures accelerate soil C losses to a greater degree than streamwater nitrate leaching. Elevated temperatures reduce temperature constraints on unprotected SOM decomposition by model decomposer microbes, which leads to a greater loss of unprotected SOM C (Fig. 4.7a) and a smaller subsequent increase in organic N mineralization, nitrification, and streamwater N losses (Fig. 4.7b). N fertilization history had a minor impact on predictions of soil C losses, where the model predicted that soil C was lost at an average rate of 21 g C/m^2/yr in the fertilized watershed and 17 g C/m^2/yr in the unfertilized

watershed (Fig. 4.7a). The model predicts that elevated temperatures had a similar impact on nitrate leaching regardless of fertilization history (Fig. 4.7b).

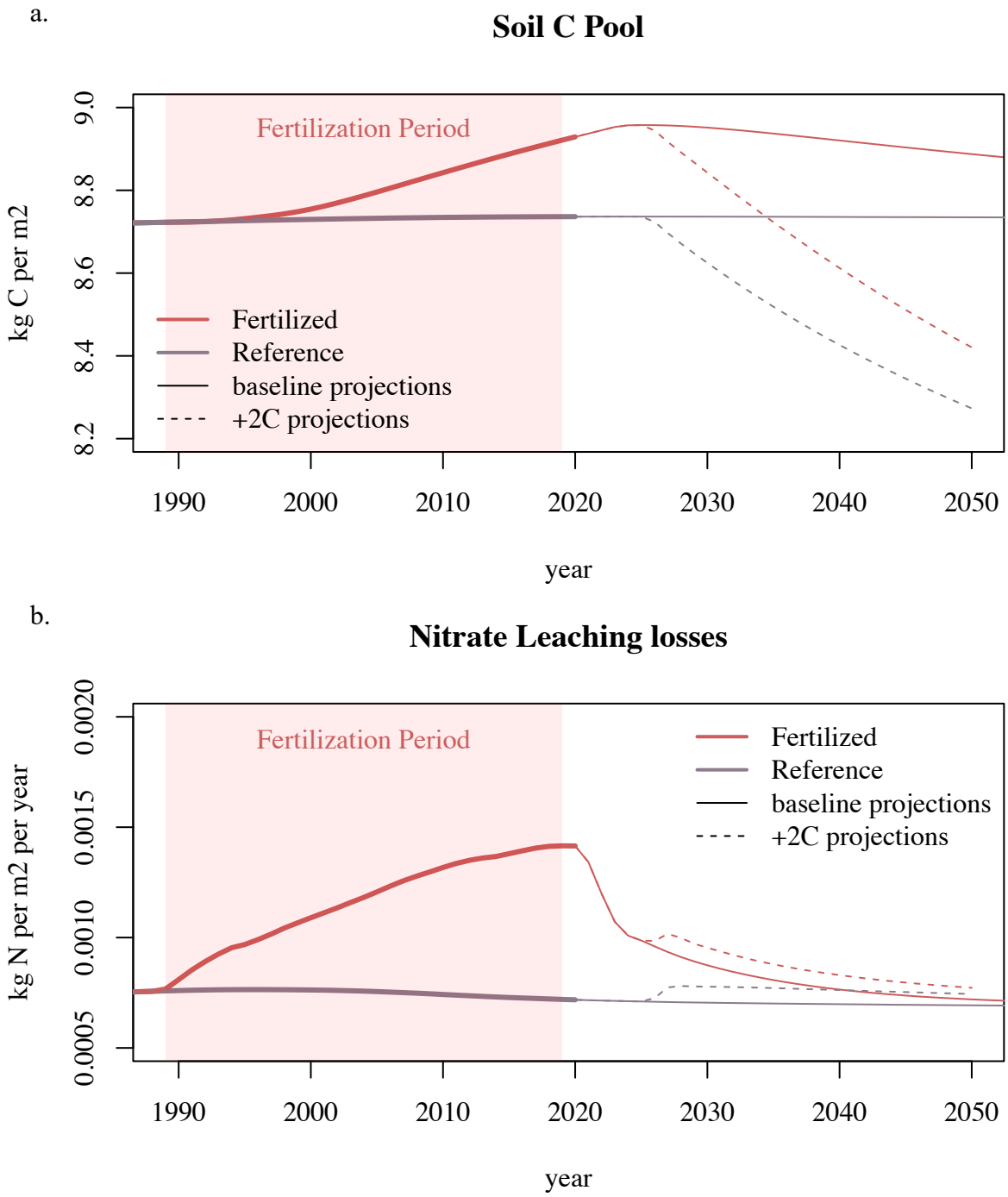

Fig. 4. 7a: Model representations of soil carbon projected past 2020 (thin lines) for the fertilized (red) and unfertilized (purple) watersheds. Soil C under a 2°C stepped temperature increase

beginning in year 2025 is shown in dashed lines. 4.7b: Model representations of nitrate leaching projected past 2020 (thin lines) for the fertilized (red) and unfertilized (purple) watersheds. Streamwater nitrate leaching under a 2°C stepped temperature increase beginning in year 2025 is shown in dashed lines.

4.5 Discussion:

The ability of FUN-CORPSE to capture key C cycling responses of forest ecosystems to increased N availability depended on how the model simulates plant-microbe interactions in the rhizosphere. In FUN-CORPSE, fertilization allows the FUN model to acquire N with a lower root C allocation to exudates and symbiotic fungi (Fig. 4.5a,b). When FUN sends less of this C belowground during fertilization, decomposition of unprotected SOM is slowed in the CORPSE model. As a result, modeled soil C increases due to an increase in unprotected SOM remaining in the soil (Fig. 4.4). This mechanism aligns well with observations from the Fernow and from other N deposition experiments at the Harvard Forest and in Michigan where N fertilization leads to an increase in particulate SOM through the suppression of microbial SOM decomposition (Eastman et al., 2022; Frey et al., 2014; Zak et al., 2008). Further, the model captures observations that drive reduced decomposition under increased N availability, like a reduction in mycorrhizal symbionts and reduced microbial decomposer enzyme activity (Argiroff et al., 2019; Carrara et al., 2018; Treseder, 2004). As such, inorganic N availability plays a key role in regulating plant-microbe interactions and driving model C cycling.

However, in contrast to the explicit plant-microbe interactions governing decomposition in FUN-CORPSE, the model (herein, baseline model) lacks microbially-explicit N cycling (Sulman et al., 2017). As a result, the baseline model simulates an elastic response of N leaching losses to N inputs, where streamwater N losses immediately triple in magnitude at the onset of N fertilization and return to ambient levels within one year of ending fertilization (Fig. 4.6c). At the Fernow, N fertilization inputs are added as ammonium, which is less mobile in the soil than nitrate. By separating inorganic N and using microbially-driven nitrification to transfer N inputs from ammonium into more mobile nitrate, the microbial nitrification model simulates an

attenuated response of nitrate production and streamwater N loss to N fertilization. This gradual increase in nitrate losses following N inputs better reflects observations of the seasonality (Fig. 4.6a,b) and pattern of streamwater nitrate losses during fertilization (Fig. 4.6c).

Explicitly representing nitrifiers and nitrification in the microbial nitrification model improves seasonal model nitrate production and leaching in both the fertilized and reference watersheds (Fig. 4.6a,b). Over the growing season (May-October), the microbial nitrification model simulates that trees are highly competitive for inorganic N uptake. As a result, less ammonium remains in the soil to fuel nitrification, which reduces nitrifier growth, nitrate production, and nitrate leaching in the summer months. This modeled pattern reflects observations from the Fernow and other ecosystem experiments where streamwater nitrate losses decline sharply during the summer (Edwards & Williard, 2006; Rusjan & Mikoš, 2010; White et al., 1983). By contrast, after new litter inputs are added to the soil in the fall, the microbial nitrification model simulates that decomposer microbes can begin to mineralize N from SOM to ammonium. This substrate fuels microbial nitrification, leading to greater nitrate production and predicted streamwater nitrate losses in the early spring when temperatures increase but before the trees start growing and taking up inorganic N. Overall, incorporating these microbial mechanisms allows the microbial nitrification model to capture a similar nitrate leaching pattern as observed at the Fernow, where nitrate leaching peaks around March and declines during the growing season in both fertilized and reference watersheds (Fig. 4.6c,d).

The more accurate seasonal representation of nitrate production improves the microbial nitrification model's representation of nitrate leaching over multiple years (Fig 4.6c,d). Here, the microbial nitrification model projects that ammonium inputs from fertilization more slowly move through the soil and increase nitrate leaching more gradually as soil N levels increase to

surpass tree N uptake, reflecting the gradual increase in streamwater nitrate leaching observed from 1989-2019 at the Fernow (Gilliam et al., 2020). Further, the microbial nitrification model simulates a more gradual decline in N losses post-fertilization than the baseline model (Fig. 4.6c). This model projection is supported by observations from other older reference watersheds at the Fernow as well as Hubbard Brook, NH, which show that reductions in ambient N deposition due to the Clean Air Act lead to gradual declines in streamwater nitrate over several years (Aber et al., 2002; Adams et al., 2006; Campbell et al., 2007). Overall, the ability of the microbial nitrification model to capture seasonal and annual patterns in streamwater N losses at the Fernow suggests that explicit representations of microbial nitrifiers could enable ecosystem and larger terrestrial biosphere models to capture coupled C-N cycling responses to shifts in N deposition and global change.

The microbial nitrification model supports the hypothesis that soil N retention accounts for the missing sink of N observed in the fertilization experiment at the Fernow (Eastman et al., 2021). Field measurements of N cycling are difficult to mass balance due to uncertainty in using limited spatial and temporal measurements of ecosystem N pools and fluxes. This difficulty is apparent at the Fernow, where a missing N sink in the fertilized watershed accounts for more than ¾ of the N inputs to the fertilized watershed (Eastman et al., 2021). This missing sink was posited to be accounted for by an increase in soil N in the top layer of soil during fertilization. The microbial nitrification model supports this hypothesis because it predicts an increase in soil N from the accumulation of inorganic N and organic N in undecomposed plant litter during fertilization. This model prediction aligns with other observations of a soil N sink with N deposition (Gundersen et al., 1998; Nadelhoffer et al., 1999; Templer et al., 2012). While there have been other hypotheses that have focused on abiotically driven sinks (Compton & Boone,

2002; Davidson et al., 2003), the observations and microbial nitrification model results at the Fernow suggest that microbes may be an equal or more important driver of N retention in temperate forest ecosystems.

Although FUN-CORPSE captured several key forest responses to N fertilization, there remain gaps in the model's representation of empirically-derived mechanisms of biogeochemical cycling at the Fernow. For example, fertilization may alter ecosystem C and N cycling by shifting microbial community composition and function (Carrara et al., 2018; Frey et al., 2004; Levy-Booth et al., 2014). On the C side, FUN-CORPSE predicts that N fertilization reduces plant C transfers to soil microbes, but the model cannot capture commonly observed shifts in bacterial and fungal community composition that have been implicated as a driver of declines in overall microbial decomposition and lignin-degrading enzyme activity with N fertilization (Carrara et al., 2021; Morrison et al., 2016; Zak et al., 2008). On the N side, while the microbial nitrification model represents an important advance, the model lacks microbially explicit representations of other processes like N fixation and denitrification that also impact plant N availability and drive gaseous losses of N. To address these gaps in microbial representations of C and N cycling in FUN-CORPSE as well as other plant-microbial interactions models, our efforts to model microbial nitrifiers may provide an important roadmap for using long-term ecosystem experiments to parameterize and validate future efforts.

The microbial nitrification model predictions that streamwater nitrate losses return to ambient levels faster than soil C after N fertilization ends (Fig. 4.7a,b) have important implications for our understanding of the recovery of eastern temperate forests from elevated N deposition. While there is empirical evidence supporting the model's trajectory of declining streamwater N losses (Adams et al., 2006; Campbell et al., 2007), there are few observations of

how declines in external N inputs will alter soil C, especially given concurrent environmental changes (Gilliam et al., 2019). Following first order principles, the most parsimonious hypothesis is that the soil C accumulated over 30 years of N fertilization will decrease at a similar rate. By contrast, the model predicts that previously fertilized soil C declines roughly 4 times more slowly than the rate it accumulated, remaining elevated above the unfertilized reference for over a century (Fig. 4.7a). However, there is the potential for the stability of the N-induced soil C gains to be threatened by future increases in soil temperature. In response to a 2^{o} C increase in soil temperature, the microbial nitrification model predicts that soil C remains higher in the previously fertilized watershed after 30 years, but it also predicts a 23.5% higher rate of carbon loss from the previously fertilized than the reference watershed. This greater temperature sensitivity of the N-induced soil C gains in the model is due to an increase in unprotected C pools that mirrors empirical evidence of an increase in particulate organic matter at the Fernow (Eastman et al., 2021). Collectively, across both ambient and elevated temperatures, these model results suggest that the good effects of N deposition may be more stable than the bad effects.

Overall, this work demonstrates the importance of explicitly modelling microbial controls over soil C and N transformations to predicting how ecosystem C and N cycling respond to anthropogenic perturbations. First, we show that key ecosystem responses to N deposition could be captured by modelling the potential for trees to dynamically reduce belowground C allocation, limiting microbially-driven SOM mineralization. Next, by incorporating nitrifiers and more realistic N cycling, we show that the model is better able to represent seasonal and multi-year changes in streamwater nitrate losses. Finally, in recovery from N fertilization, streamwater N leaching rapidly declines while the soil C gained under N fertilization is more persistent and

remains elevated. However, this soil C is vulnerable to future losses, particularly under warming. Collectively, we show that model efforts should prioritize the role of dynamic plant-microbe interactions and microbially mediated C and N cycling to predict forest ecosystem services and feedbacks on global change.

4.6 Literature Cited

Aber, J. D., Ollinger, S. V., Driscoll, C. T., Likens, G. E., Holmes, R. T., Freuder, R. J., & Goodale, C. L. (2002). Inorganic nitrogen losses from a forested ecosystem in response to physical, chemical, biotic, and climatic perturbations. *Ecosystems*, *5*(7), 0648–0658. https://doi.org/10.1007/s10021-002-0203-8

Adams, M. B., DeWalle, D. R., & Hom, J. L. (Eds.). (2006). *The Fernow watershed acidification study*. Springer.

Argiroff, W. A., Zak, D. R., Upchurch, R. A., Salley, S. O., & Grandy, A. S. (2019). Anthropogenic N deposition alters soil organic matter biochemistry and microbial communities on decaying fine roots. *Global Change Biology*, *25*(12), 4369–4382.

Berardi, D., Brzostek, E., Blanc-Betes, E., Davison, B., DeLucia, E. H., Hartman, M. D., Kent, J., Parton, W. J., Saha, D., & Hudiburg, T. W. (2020). 21st-century biogeochemical modeling: Challenges for Century-based models and where do we go from here? *GCB Bioenergy*, *12*(10), 774–788. https://doi.org/10.1111/gcbb.12730

Berg, C., Listmann, L., Vandieken, V., Vogts, A., & Jürgens, K. (2015). Chemoautotrophic growth of ammonia-oxidizing Thaumarchaeota enriched from a pelagic redox gradient in the Baltic Sea. *Frontiers in Microbiology*, *5*. https://www.frontiersin.org/articles/10.3389/fmicb.2014.00786

Bobbink, R., Hicks, K., Galloway, J., Spranger, T., Alkemade, R., Ashmore, M., Bustamante, M., Cinderby, S., Davidson, E., & Dentener, F. (2010). Global assessment of nitrogen deposition effects on terrestrial plant diversity: A synthesis. *Ecological Applications*, *20*(1), 30–59.

Brzostek, E. R., Fisher, J. B., & Phillips, R. P. (2014). Modeling the carbon cost of plant nitrogen acquisition: Mycorrhizal trade-offs and multipath resistance uptake improve predictions of retranslocation. *Journal of Geophysical Research: Biogeosciences*, *119*(8), 1684–1697. https://doi.org/10.1002/2014JG002660

Campbell, J. L., Driscoll, C. T., Eagar, C., Likens, G. E., Siccama, T. G., Johnson, C. E., Fahey, T. J., Hamburg, S. P., Holmes, R. T., Bailey, A. S., & Buso, D. C. (2007). *Long-term trends from ecosystem research at the Hubbard Brook Experimental Forest* (NRS-GTR-17; p. NRS-GTR-17). U.S. Department of Agriculture, Forest Service, Northern Research Station. https://doi.org/10.2737/NRS-GTR-17

Carrara, J. E., Fernandez, I. J., & Brzostek, E. R. (2022). Mycorrhizal type determines root–microbial responses to nitrogen fertilization and recovery. *Biogeochemistry*, *157*(2), 245–258. https://doi.org/10.1007/s10533-021-00871-y

Carrara, J. E., Walter, C. A., Freedman, Z. B., Hostetler, A. N., Hawkins, J. S., Fernandez, I. J., & Brzostek, E. R. (2021). Differences in microbial community response to nitrogen fertilization result in unique enzyme shifts between arbuscular and ectomycorrhizal-dominated soils. *Global Change Biology*, *27*(10), 2049–2060. https://doi.org/10.1111/gcb.15523

Carrara, J. E., Walter, C. A., Hawkins, J. S., Peterjohn, W. T., Averill, C., & Brzostek, E. R. (2018). Interactions among plants, bacteria, and fungi reduce extracellular enzyme activities under long-term N fertilization. *Global Change Biology*, *24*(6), 2721–2734. https://doi.org/10.1111/gcb.14081

Cheng, W., Parton, W. J., Gonzalez-Meler, M. A., Phillips, R., Asao, S., McNickle, G. G., Brzostek, E., & Jastrow, J. D. (2014). Synthesis and modeling perspectives of rhizosphere priming. *New Phytologist*, *201*(1), 31–44. https://doi.org/10.1111/nph.12440

Clark, C. M., Morefield, P. E., Gilliam, F. S., & Pardo, L. H. (2013). Estimated losses of plant biodiversity in the United States from historical N deposition (1985–2010). *Ecology*, *94*(7), 1441–1448. https://doi.org/10.1890/12-2016.1

Compton, J. E., & Boone, R. D. (2002). Soil nitrogen transformations and the role of light fraction organic matter in forest soils. *Soil Biology and Biochemistry*, *34*(7), 933–943. https://doi.org/10.1016/S0038-0717(02)00025-1

Davidson, E. A., Chorover, J., & Dail, D. B. (2003). A mechanism of abiotic immobilization of nitrate in forest ecosystems: The ferrous wheel hypothesis. *Global Change Biology*, *9*(2), 228–236. https://doi.org/10.1046/j.1365-2486.2003.00592.x

Eastman, B. A., Adams, M. B., Brzostek, E. R., Burnham, M. B., Carrara, J. E., Kelly, C., McNeil, B. E., Walter, C. A., & Peterjohn, W. T. (2021). Altered plant carbon partitioning enhanced forest ecosystem carbon storage after 25 years of nitrogen additions. *New Phytologist*, *230*(4), 1435–1448. https://doi.org/10.1111/nph.17256

Eastman, B. A., Adams, M. B., & Peterjohn, W. T. (2022). The path less taken: Long-term N additions slow leaf litter decomposition and favor the physical transfer pathway of soil organic matter formation. *Soil Biology and Biochemistry*, *166*, 108567. https://doi.org/10.1016/j.soilbio.2022.108567

Edwards, P. J., & Williard, K. W. (2006). Declines in soil-water nitrate in nitrogen-saturated watersheds. *Canadian Journal of Forest Research*, *36*(8), 1931–1942. https://doi.org/10.1139/x06-085

Edwards, P. J., & Wood, F. (2011). *Fernow Experimental Forest stream chemistry* [dataset]. Forest Service Research Data Archive. https://doi.org/10.2737/RDS-2011-0017

Frey, S. D., Knorr, M., Parrent, J. L., & Simpson, R. T. (2004). Chronic nitrogen enrichment affects the structure and function of the soil microbial community in temperate hardwood and pine forests. *Forest Ecology and Management*, *196*(1), 159–171. https://doi.org/10.1016/j.foreco.2004.03.018

Frey, S. D., Ollinger, S., Nadelhoffer, K. ea, Bowden, R., Brzostek, E., Burton, A., Caldwell, B. A., Crow, S., Goodale, C. L., & Grandy, A. S. (2014). Chronic nitrogen additions suppress decomposition and sequester soil carbon in temperate forests. *Biogeochemistry*, *121*(2), 305–316.

Galloway, J. N., Dentener, F. J., Capone, D. G., Boyer, E. W., Howarth, R. W., Seitzinger, S. P., Asner, G. P., Cleveland, C. C., Green, P. A., Holland, E. A., Karl, D. M., Michaels, A. F., Porter, J. H., Townsend, A. R., & Vöosmarty, C. J. (2004). Nitrogen Cycles: Past, Present, and Future. *Biogeochemistry*, *70*(2), 153–226. https://doi.org/10.1007/s10533-004-0370-0

Gilliam, F. S., Adams, M. B., & Peterjohn, W. T. (2020). Response of soil fertility to 25 years of experimental acidification in a temperate hardwood forest. *Journal of Environmental Quality*, *49*(4), 961–972. https://doi.org/10.1002/jeq2.20113

Gilliam, F. S., Burns, D. A., Driscoll, C. T., Frey, S. D., Lovett, G. M., & Watmough, S. A. (2019). Decreased atmospheric nitrogen deposition in eastern North America: Predicted responses of forest ecosystems. *Environmental Pollution*, *244*, 560–574. https://doi.org/10.1016/j.envpol.2018.09.135

Gilliam, F. S., Walter, C. A., Adams, M. B., & Peterjohn, W. T. (2018). Nitrogen (N) dynamics in the mineral soil of a Central Appalachian hardwood forest during a quarter century of whole-watershed N additions. *Ecosystems*, *21*(8), 1489–1504.

Gundersen, P., Emmett, B. A., Kjønaas, O. J., Koopmans, C. J., & Tietema, A. (1998). Impact of nitrogen deposition on nitrogen cycling in forests: A synthesis of NITREX data. *Forest Ecology and Management*, *101*(1), 37–55. https://doi.org/10.1016/S0378-1127(97)00124-2

Gundersen, P., Schmidt, I. K., & Raulund-Rasmussen, K. (2006). Leaching of nitrate from temperate forests effects of air pollution and forest management. *Environmental Reviews*, *14*(1), 1–57. https://doi.org/10.1139/a05-015

Juice, S. M., Walter, C. A., Allen, K. E., Berardi, D. M., Hudiburg, T. W., Sulman, B. N., & Brzostek, E. R. (2022). A new bioenergy model that simulates the impacts of plant-microbial interactions, soil carbon protection, and mechanistic tillage on soil carbon cycling. *GCB Bioenergy*, *n/a*(n/a). https://doi.org/10.1111/gcbb.12914

Kuypers, M. M. M., Marchant, H. K., & Kartal, B. (2018). The microbial nitrogen-cycling network. *Nature Reviews Microbiology*, *16*(5), Article 5. https://doi.org/10.1038/nrmicro.2018.9

Kyker-Snowman, E., Wieder, W. R., Frey, S. D., & Grandy, A. S. (2020). Stoichiometrically coupled carbon and nitrogen cycling in the MIcrobial-MIneral Carbon Stabilization model version 1.0 (MIMICS-CN v1.0). *Geoscientific Model Development*, *13*(9), 4413–4434. https://doi.org/10.5194/gmd-13-4413-2020

Lawrence, D. M., Fisher, R. A., Koven, C. D., Oleson, K. W., Swenson, S. C., Bonan, G., Collier, N., Ghimire, B., van Kampenhout, L., & Kennedy, D. (2019). The Community

Land Model version 5: Description of new features, benchmarking, and impact of forcing uncertainty. *Journal of Advances in Modeling Earth Systems*, *11*(12), 4245–4287.

Lehmann, J., & Schroth, G. (2002). Nutrient leaching. *Trees, Crops and Soil Fertility: Concepts and Research Methods*, 151–166. https://doi.org/10.1079/9780851995939.0151

Levy-Booth, D. J., Prescott, C. E., & Grayston, S. J. (2014). Microbial functional genes involved in nitrogen fixation, nitrification and denitrification in forest ecosystems. *Soil Biology and Biochemistry*, *75*, 11–25. https://doi.org/10.1016/j.soilbio.2014.03.021

Moore, J. A. M., Sulman, B. N., Mayes, M. A., Patterson, C. M., & Classen, A. T. (2020). Plant roots stimulate the decomposition of complex, but not simple, soil carbon. *Functional Ecology*, *34*(4), 899–910. https://doi.org/10.1111/1365-2435.13510

Morrison, E. W., Frey, S. D., Sadowsky, J. J., van Diepen, L. T. A., Thomas, W. K., & Pringle, A. (2016). Chronic nitrogen additions fundamentally restructure the soil fungal community in a temperate forest. *Fungal Ecology*, *23*, 48–57. https://doi.org/10.1016/j.funeco.2016.05.011

Nadelhoffer, K. J., Emmett, B. A., Gundersen, P., Kjønaas, O. J., Koopmans, C. J., Schleppi, P., Tietema, A., & Wright, R. F. (1999). Nitrogen deposition makes a minor contribution to carbon sequestration in temperate forests. *Nature*, *398*(6723), Article 6723. https://doi.org/10.1038/18205

Norton, J., & Ouyang, Y. (2019). Controls and Adaptive Management of Nitrification in Agricultural Soils. *Frontiers in Microbiology*, *10*. https://www.frontiersin.org/articles/10.3389/fmicb.2019.01931

Pan, Y., Birdsey, R. A., Fang, J., Houghton, R., Kauppi, P. E., Kurz, W. A., Phillips, O. L., Shvidenko, A., Lewis, S. L., Canadell, J. G., Ciais, P., Jackson, R. B., Pacala, S. W.,

McGuire, A. D., Piao, S., Rautiainen, A., Sitch, S., & Hayes, D. (2011). A Large and Persistent Carbon Sink in the World's Forests. *Science*, *333*(6045), 988–993. https://doi.org/10.1126/science.1201609

Rusjan, S., & Mikoš, M. (2010). Seasonal variability of diurnal in-stream nitrate concentration oscillations under hydrologically stable conditions. *Biogeochemistry*, *97*(2), 123–140. https://doi.org/10.1007/s10533-009-9361-5

Saifuddin, M., Abramoff, R. Z., Davidson, E. A., Dietze, M. C., & Finzi, A. C. (2021). Identifying Data Needed to Reduce Parameter Uncertainty in a Coupled Microbial Soil C and N Decomposition Model. *Journal of Geophysical Research: Biogeosciences*, *126*(12), e2021JG006593. https://doi.org/10.1029/2021JG006593

Schimel, D. (1995). Terrestrial Ecosystems and the Carbon-Cycle. *Global Change Biology*, *1*(1), 77–91. https://doi.org/10.1111/j.1365-2486.1995.tb00008.x

Sharma, B., & Ahlert, R. C. (1977). Nitrification and nitrogen removal. *Water Research*, *11*(10), 897–925. https://doi.org/10.1016/0043-1354(77)90078-1

Sulman, B. N., Brzostek, E. R., Medici, C., Shevliakova, E., Menge, D. N. L., & Phillips, R. P. (2017). Feedbacks between plant N demand and rhizosphere priming depend on type of mycorrhizal association. *Ecology Letters*, *20*(8), 1043–1053. https://doi.org/10.1111/ele.12802

Sulman, B. N., Moore, J. A., Abramoff, R., Averill, C., Kivlin, S., Georgiou, K., Sridhar, B., Hartman, M. D., Wang, G., & Wieder, W. R. (2018). Multiple models and experiments underscore large uncertainty in soil carbon dynamics. *Biogeochemistry*, *141*(2), 109–123.

Sulman, B. N., Phillips, R. P., Oishi, A. C., Shevliakova, E., & Pacala, S. W. (2014). Microbe-driven turnover offsets mineral-mediated storage of soil carbon under elevated CO2. *Nature Climate Change*, *4*(12), Article 12. https://doi.org/10.1038/nclimate2436

Templer, P. H., Mack, M. C., Iii, F. S. C., Christenson, L. M., Compton, J. E., Crook, H. D., Currie, W. S., Curtis, C. J., Dail, D. B., D'Antonio, C. M., Emmett, B. A., Epstein, H. E., Goodale, C. L., Gundersen, P., Hobbie, S. E., Holland, K., Hooper, D. U., Hungate, B. A., Lamontagne, S., … Zak, D. R. (2012). Sinks for nitrogen inputs in terrestrial ecosystems: A meta-analysis of 15N tracer field studies. *Ecology*, *93*(8), 1816–1829. https://doi.org/10.1890/11-1146.1

Thornton, P. E., Doney, S. C., Lindsay, K., Moore, J. K., Mahowald, N., Randerson, J. T., Fung, I., Lamarque, J.-F., Feddema, J. J., & Lee, Y.-H. (2009). Carbon-nitrogen interactions regulate climate-carbon cycle feedbacks: Results from an atmosphere-ocean general circulation model. *Biogeosciences*, *6*(10), 2099–2120. https://doi.org/10.5194/bg-6-2099-2009

Treseder, K. K. (2004). A meta-analysis of mycorrhizal responses to nitrogen, phosphorus, and atmospheric CO2 in field studies. *New Phytologist*, *164*(2), 347–355. https://doi.org/10.1111/j.1469-8137.2004.01159.x

White, R. E., Wellings, S. R., & Bell, J. P. (1983). Seasonal variations in nitrate leaching in structured clay soils under mixed land use. *Agricultural Water Management*, *7*(4), 391–410. https://doi.org/10.1016/0378-3774(83)90030-6

Zak, D. R., Holmes, W. E., Burton, A. J., Pregitzer, K. S., & Talhelm, A. F. (2008). Simulated atmospheric NO3- deposition increases soil organic matter by slowing decomposition. *Ecological Applications*, *18*(8), 2016–2027.

Chapter 5: Conclusions

Summary of results:

This dissertation explored how plant-microbe interactions drive soil C and N cycling in managed and unmanaged ecosystems. To do this, I performed experiments in the lab, in situ, and in silico to address key uncertainties limiting our understanding of how ecosystems can retain soil C and N to answer three broad questions: 1) How do plant-microbe interactions between plant litter and microbial decomposition traits influence the formation of new soil C for different bioenergy crop litters in the lab?; 2) How do rhizosphere plant-microbe interactions influence soil organic matter stabilization and destabilization depending on nutrient levels in-situ?; and 3) Can empirical measurements help constrain, parameterize, and validate modeled plant-microbe interactions to improve representations of forest ecosystem responses to global change?

Overall, I found strong evidence that vital ecosystem services like soil C sequestration to combat climate change and soil N retention to fuel plant productivity depend on microbially-mediated processes that are regulated by interactions between plants and soil microbes. First, I found that plant litter quality controls the efficiency of microbial decomposers, which in turn drives the potential for C in litter inputs to form persistent, mineral-associated SOM. Additionally, I found that using measurements of microbial carbon use efficiency to constrain model microbial decomposition parameters enabled the model to capture how bioenergy crops differ in new SOM formation. In the field, I found that living roots stimulated microbial litter decomposition but balanced this C loss through building more persistent aggregate-associated SOM. Further, roots selectively mobilized nitrogen from litter without additional carbon release, suggesting that roots prime their rhizosphere microbes to efficiently mine nitrogen while building persistent soil carbon. Finally, I found that modelling how trees stimulate microbial

decomposition to mineralize N in the rhizosphere and modelling microbially-explicit N cycling processes were integral to capturing key ecosystem C and N cycling responses to elevated soil N availability.

Collectively, the findings of this dissertation underscore the important role of plant-microbe interactions and microbial processes in driving soil C and N retention in both managed and unmanaged ecosystems. Below, I provide further detail on how each dissertation chapter answers one of the broad research questions above.

Chapter 2: How do plant-microbe interactions between plant litter and microbial decomposition traits influence the formation of new soil C for different bioenergy crop litters in the lab?

Understanding how new soil C is formed is imperative for evaluating the potential sustainability of bioenergy agricultural systems through soil C retention. In Chapter 2, I examined the extent to which litter differences in two bioenergy crops, corn and miscanthus, altered microbial decomposition and formed new soil C. To do this, I performed a soil microcosm experiment where I added ^{13}C enriched aboveground and belowground litters to soils and traced the fate of the ^{13}C into microbial respiration and soil C pools. I then used measurements of microbial carbon use efficiency (CUE) from this experiment to constrain model parameters and investigate if the model could represent how these crops differentially form soil C.

In this experiment, I found that corn litters promoted higher microbial CUE (0.37) than miscanthus litters (0.24) (Fig. 2.4). In turn, corn litter formed approximately 50% more mineral associated soil C than miscanthus litters (Fig. 2.3). Similarly, structurally complex root litters promoted a lower CUE and formed less mineral associated soil C than leaf and shoot litters for

both crops (Fig. 2.3). When I used the CUE data to parameterize the SOC model, we found that modelling microbial trait differences uniquely allowed the model to capture the fate of litter C (Fig. 2.5). Collectively, we found a robust link between litter quality, microbial efficiency, and soil C formation. This link bridges the empirical uncertainty in how different crops can form new soil C and provides an empirical basis for modelling soil C cycling.

Chapter 3: How do rhizosphere plant-microbe interactions influence soil organic matter stabilization and destabilization depending on nutrient levels in-situ?

Results from Chapter 2 suggest that plant traits like litter quality interact with soil microbes to alter soil C cycling. However, this experiment was unable to capture how living roots actively engineer soil microbes to drive soil C and N cycling. There is a great deal of conflicting evidence and theory on whether root-microbe interactions lead to soil C and N retention. In Chapter 3, I build upon my work in Chapter 2 to examine the role of living roots on microbial decomposition and the transfer of litter C and N between SOM pools. To do this, I incubated ^{13}C and ^{15}N enriched plant litter for one growing season in the field. I added litter to soil cores that were open to roots and fungal ingrowth, excluded roots but allowed fungal ingrowth, or excluded both roots and fungal ingrowth. I installed these cores in miscanthus plots with different nutrient treatments to investigate the effect of soil C and N availability on root-altered decomposition and SOM formation.

In this experiment, I found that roots primed litter decomposition and led to a 32% loss in litter C remaining in the soil C pool associated with undecomposed plant litter fragments compared with root exclusion treatments (Fig. 3.3). However, roots balanced this C loss with a 30% increase in litter C incorporation into more persistent, aggregate-associated SOM (Fig. 3.3).

Notably, root ingrowth reduced litter N in both of these pools, suggesting that roots prime rhizosphere microbes to preferentially mine N from litter without net C losses (Fig. 3.4). As a result, these plant-microbe interactions may increase the potential for litter C to persist in higher C:N, aggregate-protected SOM.

Chapter 4: Can empirical measurements help constrain, parameterize, and validate modeled plant-microbe interactions to improve representations of forest ecosystem responses to global change?

In Chapters 2 and 3, I studied how plant-microbe interactions alter soil C and N cycling in managed bioenergy agricultural ecosystems. This work is critical because optimizing ecosystem services like C sequestration could help actively combat climate change. However, it is also vital to understand how unmanaged ecosystems like temperate forests have contributed to the globally important terrestrial C sink (Pan et al., 2011) and predict whether we can continue to rely on this ecosystem service in the future. In Chapter 4, I studied whether modelling explicit plant-microbe interactions could facilitate model representations of how N deposition and soil N availability has facilitated the forest soil C sink. I leveraged decades of C and N cycling data from a whole-watershed N fertilization experiment at the Fernow Experimental Forest in Parsons, WV to run the microbially-explicit plant-microbe interactions model FUN-CORPSE (Fixation and Uptake of Nitrogen- Carbon, Organisms, Rhizosphere, and Protection in the Soil Environment). The three objectives of this work included 1) Reproducing key ecosystem responses to N fertilization, 2) Modeling microbially-explicit inorganic N cycling, and 3) Assessing how modeled soil C and N retention respond to shifts in N deposition and other future climate drivers.

By simulating rhizosphere priming, FUN-CORPSE was able to capture key ecosystem responses to N fertilization, including a 25% decline in the tree C cost of soil N acquisition that reduces root-primed decomposition and increases soil C (Fig. 4.4; Fig. 4.5). I used data from the Fernow to build and constrain a new model component where nitrifying microbes control inorganic N transformations. After incorporating these N microbes, FUN-CORPSE captured the seasonality of nitrate production and the 50% increase in streamwater nitrate loss under N fertilization (Fig. 4.6). Finally, the model predicts that declining N deposition will lead to a gradual loss of the soil C gained during fertilization, particularly under elevated temperatures (Fig. 4.7). This indicates the potential for a weakening forest C sink under projections of future climate change.

Future directions:

In this dissertation, I studied how plant-microbe interactions drive the potential for ecosystem soil C retention to combat climate change. I have employed a broad range of approaches to tackle uncertainties that limit our predictive understanding of how C and N cycle in soils. My research has helped to lay the foundation for several ongoing projects in my lab, including 1) studying how tree roots alter SOM formation and retention from litter and root exudates (DeHetre and Ridgeway et al., in progress); 2) studying how fungal necromass is incorporated into SOM (DeHetre et al., in progress); 3) studying how different bioenergy crop roots impact new SOM formation (Brzostek et al., in progress); and 4) investigating how a legacy of N deposition has impacted SOM decomposition and temperature sensitivity (Kangi et al., in progress).

I will build upon the skills and experience I have gained in my graduate research to tackle new projects as a post-doctoral researcher in the Department of Biological Sciences at Dartmouth College. Here, I will help establish a winter climate change experiment that investigates how snowmelt alters forest biogeochemical cycling. This experiment simulates changes in winter climate characterized by intermittent snow events punctuated by regular winter 'heat waves' that melt snowfall. As winters are warming three times faster than summers, this research addresses important uncertainties in how climate change will impact forest ecosystem function in the northeastern US.

Finally, I hope to expand upon my experience using empirical measurements to inform model representations of soil processes in my future research career. I believe that the potential remains to manage or protect ecosystems to address climate change and environmental degradation, and that leveraging data to improve model projections is vital to these efforts.

Appendix: Supplementary Tables and Figures

SI Table 1: Model parameters from Chapter 2

Parameter	Baseline CORPSE values	Microcosm CORPSE values	CUE CORPSE values
Protection rate: protected carbon formation rate ($year^{-1}$)	protection_rate_Fast 0.6 protection_rate_Slow 0.001 protection_rate_Necro 4	protection_rate_Fast 2.4 protection_rate_Slow 0.004 protection_rate_Necro 16	protection_rate_Fast 2.4 protection_rate_Slow 0.004 protection_rate_Necro 16
Turnover rate: protected carbon turnover time (year)	Tmic 0.25 (approx. 3 months)	Tmic 7/365 (1 week)	Tmic 7/365 (1 week)
Maximum CUE: carbon uptake efficiency	eup_Fast 0.6 eup_Slow 0.001 eup_Necro 0.6	eup_Fast 0.6 eup_Slow 0.001 eup_Necro 0.6	eup_Fast Corn AG = .79 Miscanthus AG = 0.60 Corn BG = 0.66 Miscanthus BG = 0.34 eup_Slow 0.001 eup_Necro Corn AG = .79 Miscanthus AG = 0.60 Corn BG = 0.66 Miscanthus BG = 0.34

SI Table 2: replication for each treatment

	Control	High N	Organic	Total
Root	9	13	15	37
Fungal	10	7	5	22
Twist	9	10	10	29
Total	28	30	30	88

SI Table 3: Two-way ANOVA p-values for selected dependent variables for ingrowth core treatments, fertilization treatments, and ingrowth core x fertilization interaction.

Dependent variable	Ingrowth core treatment	Fertilization treatment	Ingrowth core × fertilization
Litter C in SOM	0.11	**<0.01**	0.29
Litter N in SOM	**<0.001**	0.054	0.19
mg litter C in light POM	**<0.01**	0.48	0.10
mg litter C in heavy POM	0.16	**<0.01**	0.64
mg litter C in MAOM	0.40	**<0.05**	0.54
litter C % in light POM	**<0.001**	0.47	0.06
litter C % in heavy POM	**<0.01**	0.35	0.52
litter C % in MAOM	0.51	0.80	0.31
mg litter N in light POM	**<0.001**	0.82	0.14
mg litter N in heavy POM	**<0.05**	0.80	0.49
mg litter N in MAOM	0.21	**<0.01**	0.56
litter N % in light POM	**<0.001**	0.66	0.14
litter N % in heavy POM	0.48	0.67	0.52
litter N % in MAOM	**<0.001**	0.74	0.37

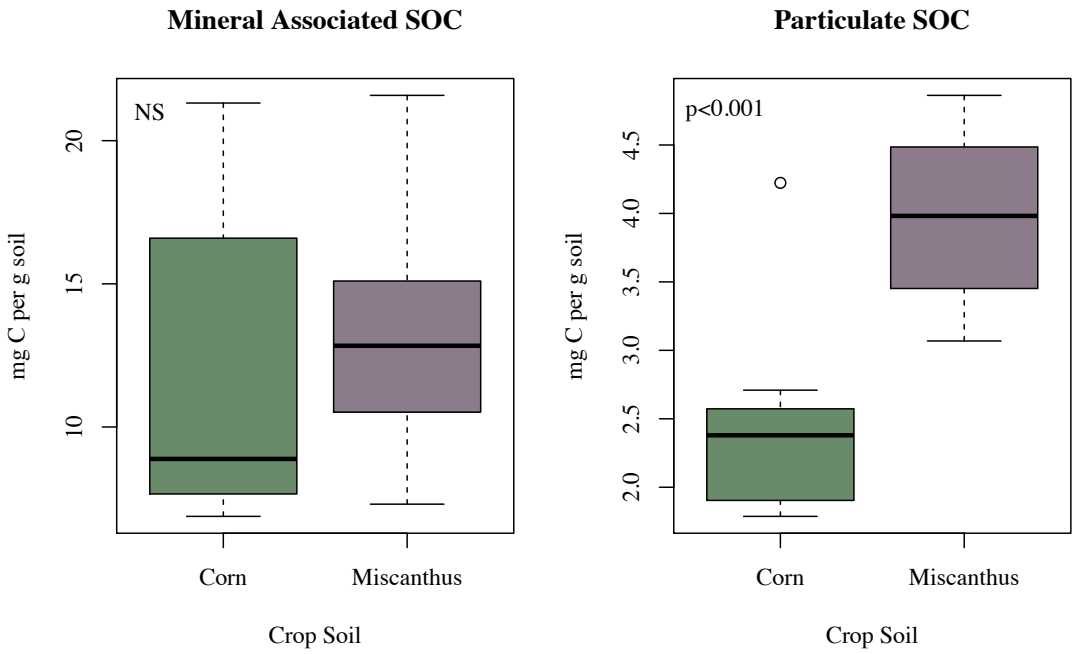

SI fig. 1: Soil organic matter pools in mineral associated SOC (left) and particulate SOC (right) for field soils from corn (green) and miscanthus (purple).

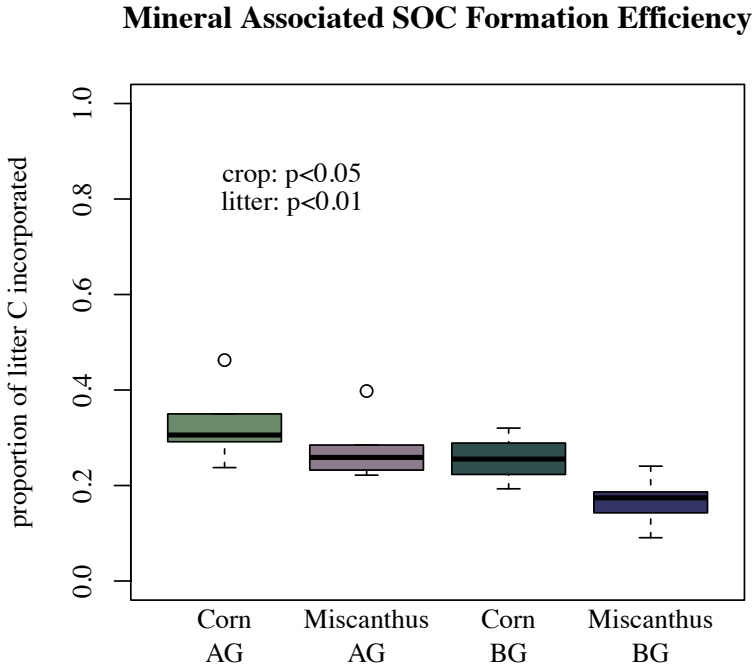

SI fig. 2: Mineral associated SOC formation efficiency: Litter C in mineral associated SOC out of litter C respired and in mineral associated SOC

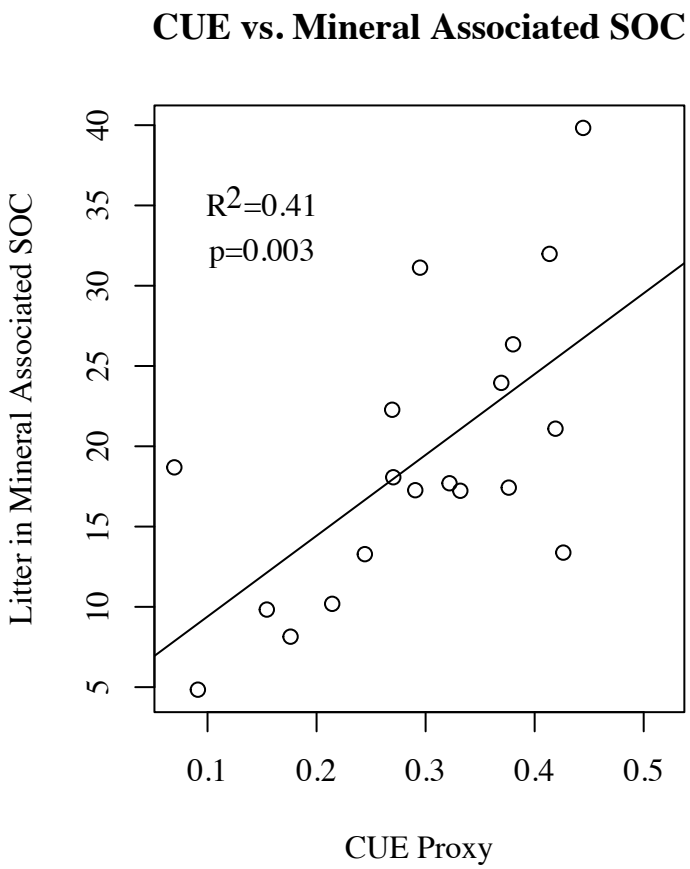

SI fig. 3: CUE vs. Mineral Associated SOC: CUE measured with endpoint microbial biomass and respiration vs. litter incorporation into mineral associated SOC

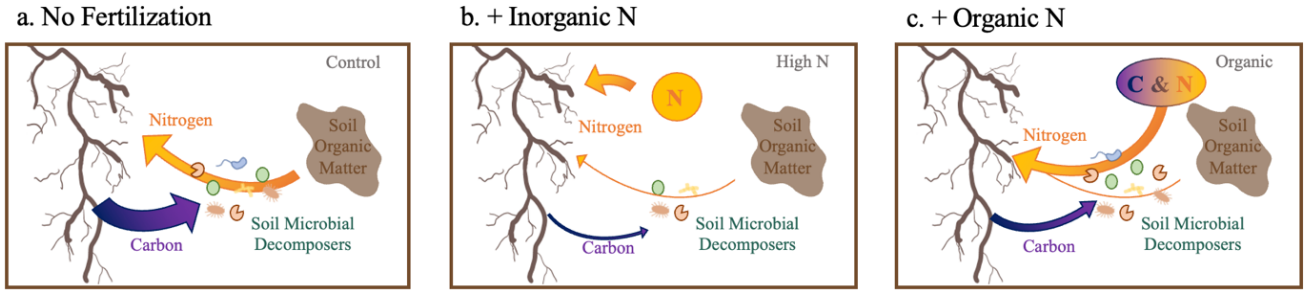

SI Figure 4a: In nutrient limited soils, roots exchange C with soil microbes in exchange for N mineralization from soil organic matter. **4b:** When fertilized with plant-available inorganic N, roots exchange less C with microbes and reduce soil organic matter decomposition. **4c:** When fertilized with organic C & N inputs, roots still rely on microbes to mineralize N from organic fertilizer and accelerate microbially-driven soil organic matter cycling

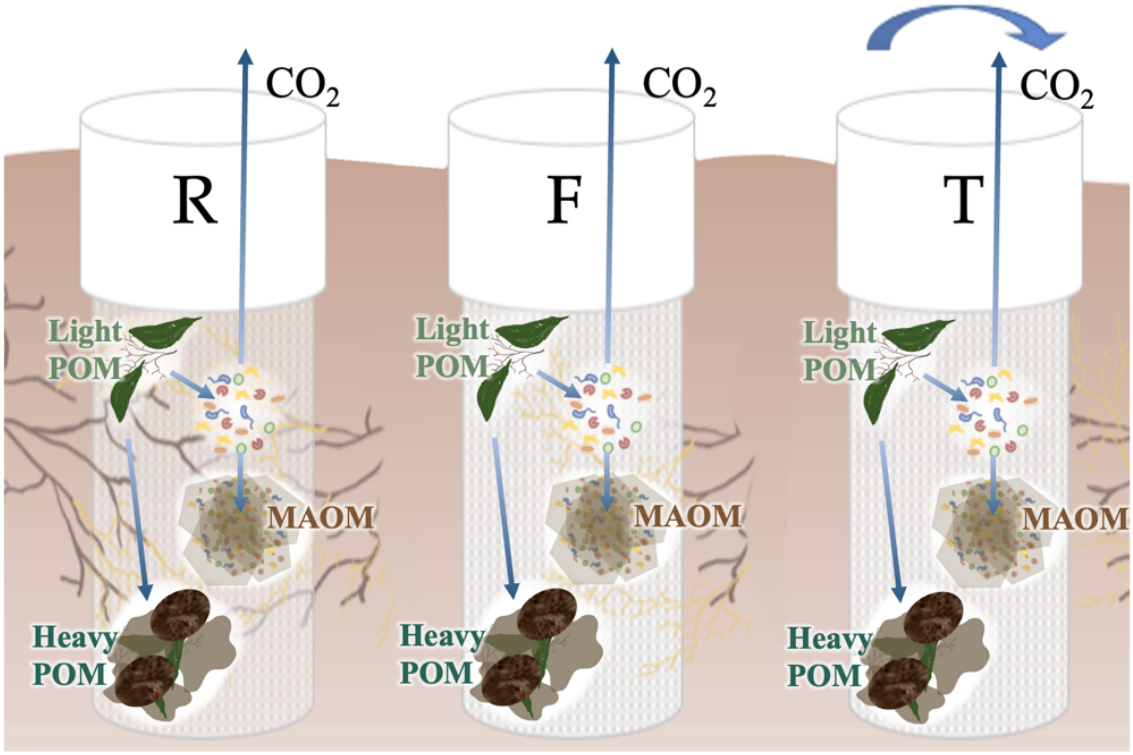

SI Figure 5: Root and fungal ingrowth (R), root exclusion and fungal ingrowth (F), and root and fungal exclusion (T) cores. R cores were constructed with 1.55mm mesh, F cores were constructed with 50um mesh, and T cores were constructed with 50um mesh and were twisted. In each core, isotopically labelled litter inputs are traced into SOM pools, microbial biomass, and respiration.

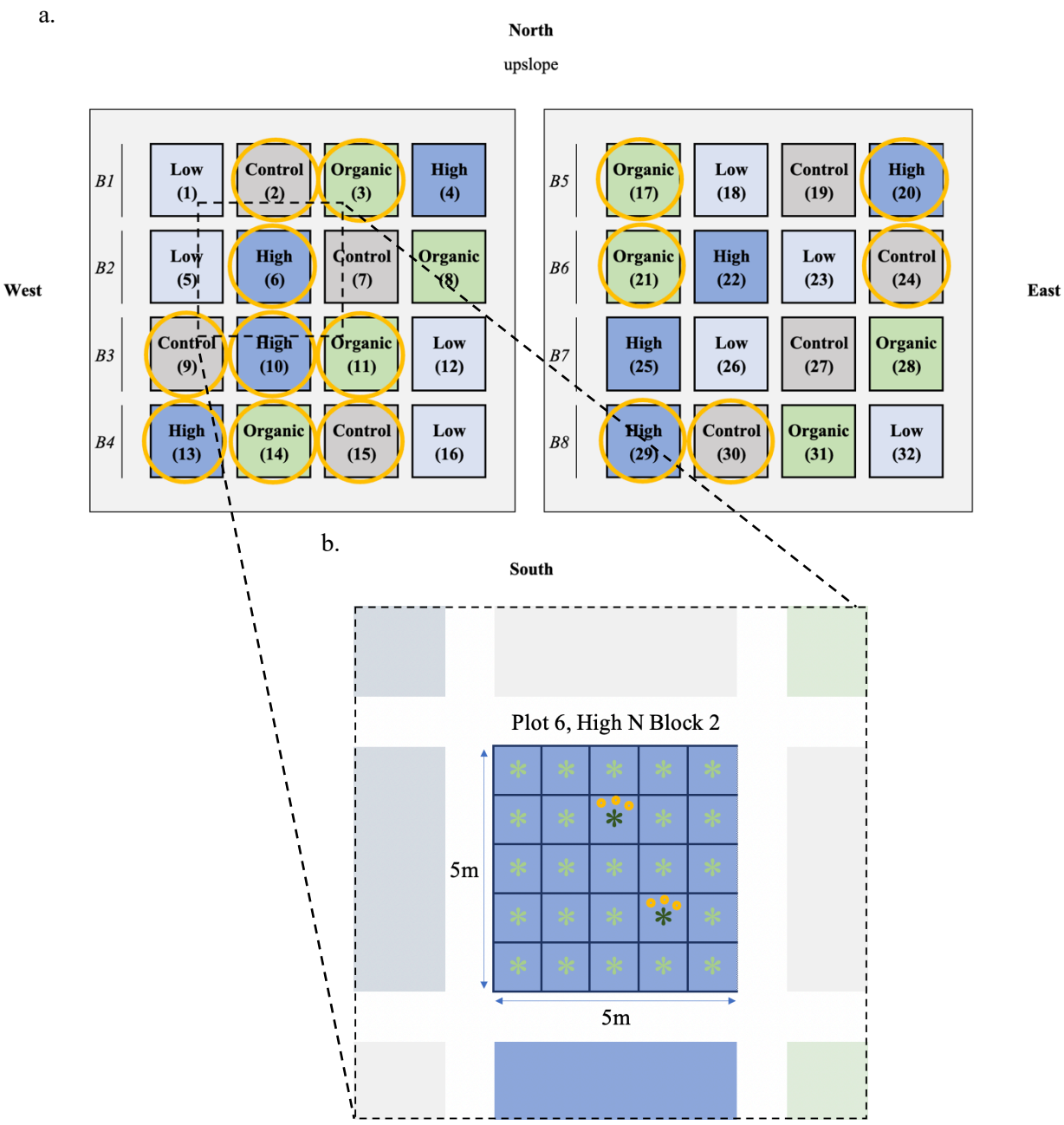

SI Figure 6a: 5x5m miscanthus plots are established in a fully randomized block design of eight blocks (B1-B8) and four nutrient treatments (Low, Control, Organic, and High). Plots selected for use in this experiment are circled in gold. **6b:** Each miscanthus plot had 25 individual plants on a 1m x 1m grid. Ingrowth cores were installed by two plants per plot. Plants were randomly selected of a subset that allowed ingrowth cores to be surrounded by established miscanthus plants. Cores were placed in random order from left to right and were installed 8" from visibly emerged miscanthus shoots in April 2021.

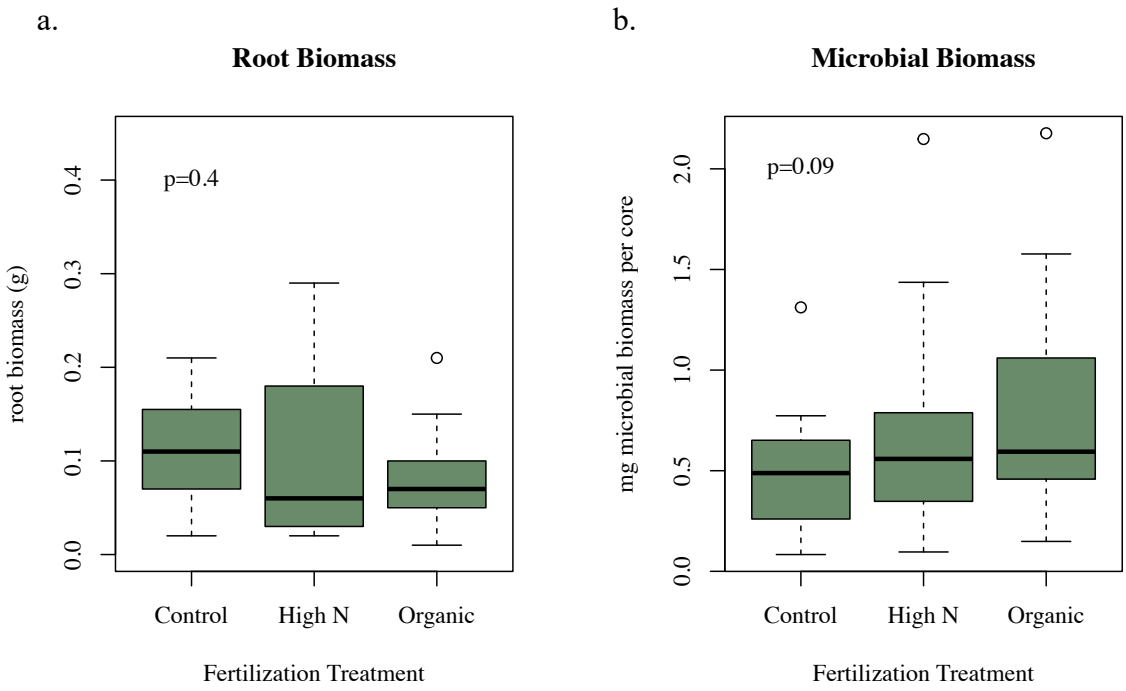

SI Fig. 7a: There were no significant differences in root biomass across the fertilization treatments (p=0.42) **Fig. 7b**: Cores in organic fertilization plots had marginally higher microbial biomass relative to cores in unfertilized control plots (p=0.09)

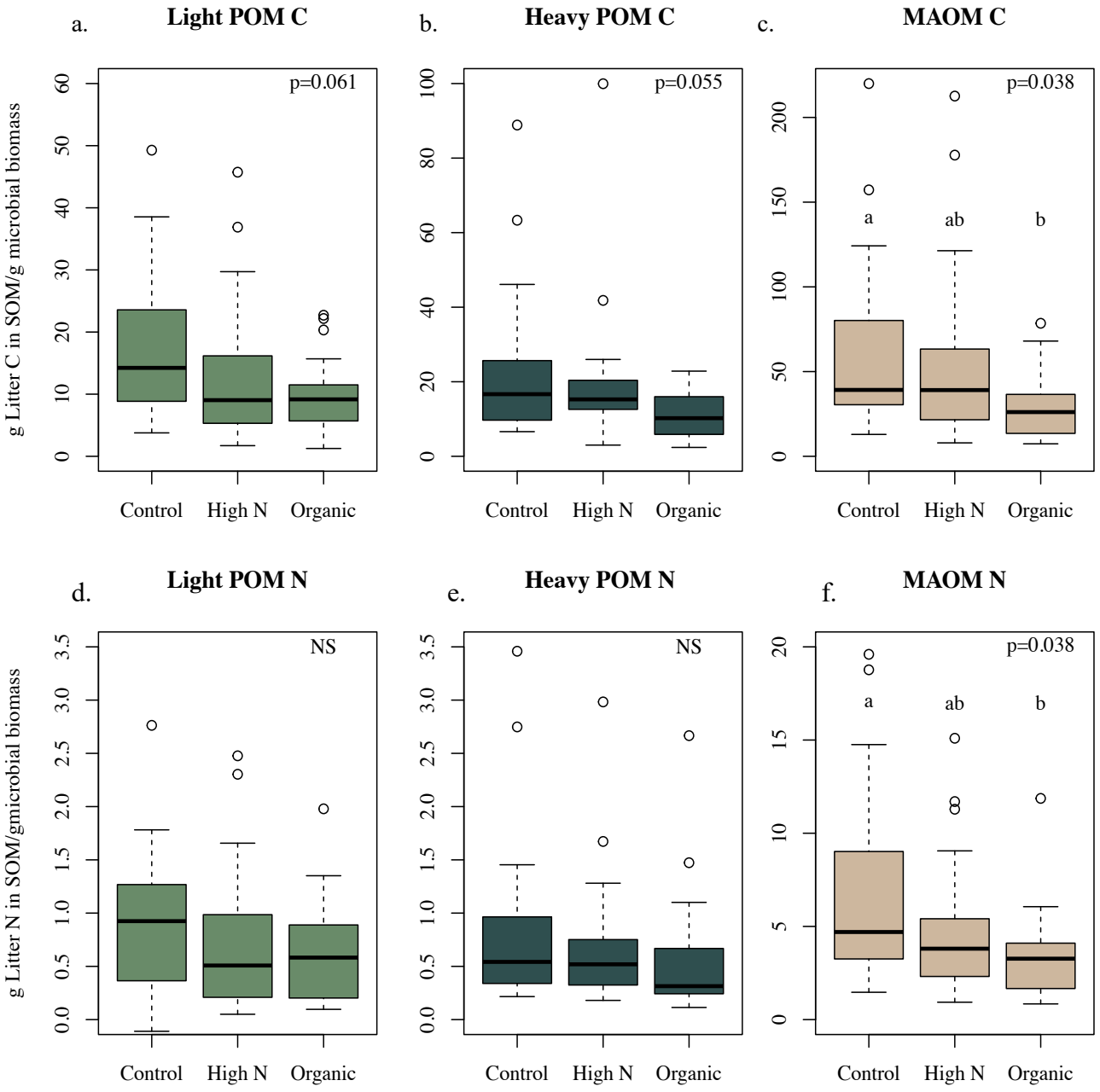

SI Figure 8: Litter C (a-c) and litter N (d-e) recovered in each SOM pool per gram of microbial biomass. More litter C was transferred from light POM per gram of microbial biomass for organic fertilization treatments (8a, p=0.064), but less litter C was incorporated into heavy POM (8b, p=0.057) and MAOM (8c, p=0.038) for organic fertilization treatments relative to control fertilization treatments. There was no difference between treatments in the transfer of litter N from light POM per gram of microbial biomass with organic fertilization treatments (8d), and the reduction in MAOM-C stabilization was mirrored with a reduction in MAOM-N stabilization per gram of microbial biomass (8f, p=0.038) relative to unfertilized control.

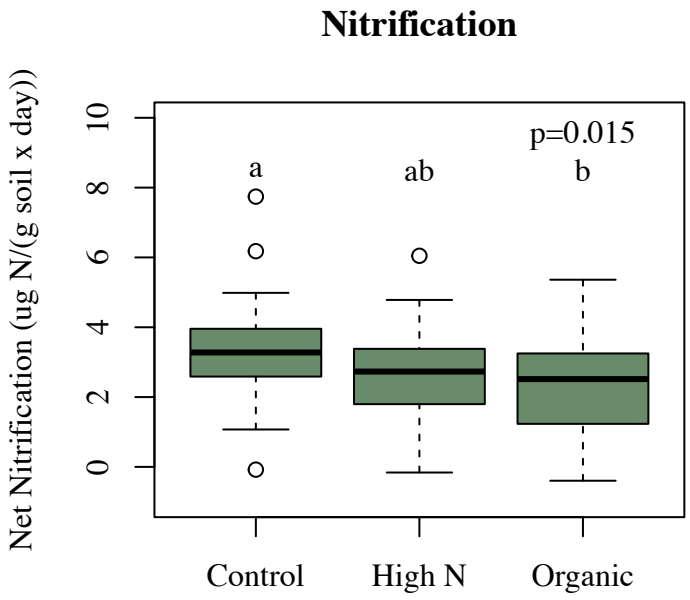

SI Figure 9: Net nitrification rates expressed as ug N of nitrate produced per gram of dry soil per day were significantly lower for organic fertilization treatments relative to unfertilized control (p=0.015).

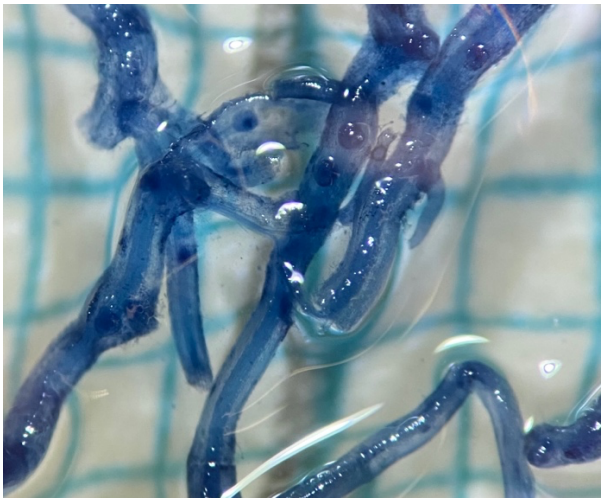

SI Figure 10: Example of a subset of roots that were cleared and stained with trypan blue to determine the presence of arbuscular mycorrhizal colonization. There were no significant differences between fertilization treatments in mycorrhizal colonization as determined by the root-gridline intersect method.